AD-A078 328 OHIO STATE UNIV COLUMBUS ELECTROSCIENCE LAB F/G 17/9
IMPROVED IDENTIFICATION OF UNDERGROUND TARGETS USING VIDEO-PULS--ETC(U)
OCT 79 I L VOLAKIS N00014-78-C-0049
UNCLASSIFIED ESL-710816-4 NL

1 OF 2
AD-
A078328

OSU

The Ohio State University

IMPROVED IDENTIFICATION OF UNDERGROUND TARGETS USING VIDEO-PULSE RADARS BY ELIMINATION OF UNDESIRED NATURAL RESONANCES

Ioannis Leonidas Yolakis

LEVEL II

The Ohio State University

ElectroScience Laboratory

Department of Electrical Engineering
Columbus, Ohio 43212

TECHNICAL REPORT 710816-4

Contract N00014-78-C-0049

October 1979

Dept. of the Navy
Office of Naval Research
800 Quincy Street
Arlington, Virginia 22217

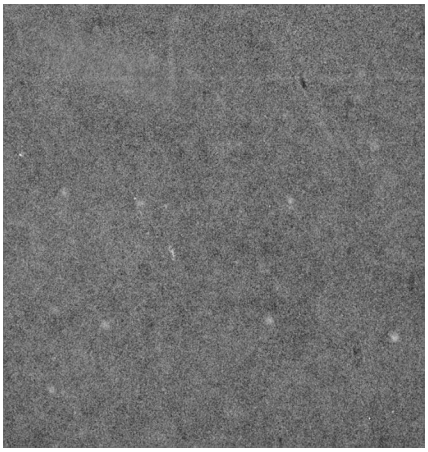

UNCLASSIFIED

SECURITY CLASSIFICATION OF THIS PAGE (When Data Entered)

REPORT DOCUMENTATION PAGE

READ INSTRUCTIONS BEFORE COMPLETING FORM

1. REPORT NUMBER	2. GOVT ACCESSION NO. (9)
3. RECIPIENT'S CATALOG NUMBER: Master's thesis	
4. TITLE (and Subtitle) (6): IMPROVED IDENTIFICATION OF UNDERGROUND TARGETS USING VIDEO-PULSE RADARS BY ELIMINATION OF UNDESIRED NATURAL RESONANCES	5. TYPE OF REPORT & PERIOD COVERED: Technical Report
	6. PERFORMING ORG. REPORT NUMBER (14): ESL-710816-4
7. AUTHOR(s) (10): Ioannis Leonidas Volakis	8. CONTRACT OR GRANT NUMBER(s) (15): Contract N00014-78-C-0049
9. PERFORMING ORGANIZATION NAME AND ADDRESS: The Ohio State University ElectroScience Laboratory, Department of Electrical Engineering, Columbus, Ohio 43212	10. PROGRAM ELEMENT, PROJECT, TASK AREA & WORK UNIT NUMBERS: Project NR 371-021/9-5-78 (427)
11. CONTROLLING OFFICE NAME AND ADDRESS: Dept. of the Navy, Office of Naval Research, 800 Quincy Street, Arlington, Virginia 22217 (11)	12. REPORT DATE: October 1979
	13. NUMBER OF PAGES: 131
14. MONITORING AGENCY NAME & ADDRESS(if different from Controlling Office): (12) 138	15. SECURITY CLASS. (of this report): Unclassified
	15a. DECLASSIFICATION/DOWNGRADING SCHEDULE

16. DISTRIBUTION STATEMENT (of this Report)

This document has been approved for public release and sale; its distribution is unlimited.

17. DISTRIBUTION STATEMENT (of the abstract entered in Block 20, if different from Report)

18. SUPPLEMENTARY NOTES

The material contained in this report is also used as a thesis submitted to the Department of Electrical Engineering, The Ohio State University as partial fulfillment for the degree Master of Science.

19. KEY WORDS (Continue on reverse side if necessary and identify by block number)

Underground video-pulse radar	Prony's method
Backscattered waveform (target echo)	Pole extraction(filtering) process
Target response waveform	Filtered waveform
Tunnel identification	Signal reconstruction process
Poles	Reconstructed waveform

20. ABSTRACT (Continue on reverse side if necessary and identify by block number)

A process for identifying and determining the structure, depth and relative position of an underground tunnel from its backscattered response is presented. Application to theoretical and measured tunnel echoes is included with very satisfactory results. Basically, the process involves the isolation of a clutter free tunnel response by effectively removing all undesired poles and clutter or noise from the original (unprocessed) echo. The results can be evaluated

DD FORM 1 JAN 73 1473 EDITION OF 1 NOV 65 IS OBSOLETE

402 251

UNCLASSIFIED

SECURITY CLASSIFICATION OF THIS PAGE (When Data Entered)

19.

Grey-Level Mapping

20.

by Grey-Level Mapping a traverse of responses over the tunnel. The employed signal-processing techniques are very general and can be used for detection of other subsurface targets.

ACKNOWLEDGMENTS

The author wishes to express gratitude to his graduate advisor Professor Leon Peters, Jr. for his guidance throughout the course of this work and to Professor David L. Moffatt for reading the manuscript. Deep appreciation is also owed to Dr. Luen C. Chan and Dr. C. W. Davis, III for their numerous consultations and suggestions. The original suggestion for the schemes developed herein was made by Professor E. M. Kennaugh.

The work reported in this thesis was supported in part by Contract N00014-78-C-0049 between Department of the Navy, Office of Naval Research, Arlington, Virginia and The Ohio State University Research Foundation.

TABLE OF CONTENTS

CHAPTER I
INTRODUCTION

A. Background and Related Research

During the past decade, efforts at the ElectroScience Laboratory have been concentrated on the detection and identification of various subsurface targets such as tunnels, mine-like targets or different kinds of pipes. In 1965 Kennaugh and Moffatt [1,2] performed a pioneering work on their first attempt to characterize backscattered transient responses (echoes). Young and Caldecott [3,4,5] later did an extensive study on the detection of pipes. Recently, Chan and Peters [5-8] have concentrated on the detection and identification of mine targets. Davis and Peters [9] give a short summary on the tunnel detection progress made thus far at the ElectroScience Laboratory. The above contributed greatly to the advances presented here.

In this thesis a new method for detecting and determining the structure (i.e., identifying), depth and relative position of underground tunnels is presented. It was applied to measured tunnel backscattered waveforms obtained at a tunnel site located at Gold Hill, Colorado. The results as compared to the actual tunnel depth and structure were reasonably accurate.

The identification process is based on the assumption that the transient response of the tunnel or generally any target can be uniquely characterized by a set of complex natural resonances (poles) [5,7,10,11]. We excite these resonances using a Video-Pulse Radar [12]. This radar consists of a pulse generator, a pair of horizontal crossed dipole antennas (one for transmitting and the other for receiving, thus isolation is maintained between the transmitted and received signals), and a sampling oscilloscope is used as a receiver. The generator produces a narrow pulse of broad spectrum ranging from the pulse repetition rate of the pulser to the lower microwave region. Although the transmitted pulse has a broad spectrum, the dipole antenna acts as a principle filter. Therefore, the natural response (or simply response) of the target must contain its resonances close to the dipole resonance for possible target detection and identification. Tribuzi and Wald [13,14] give a good description on the development of the various dipole antennas that were used in the underground radar system. It was found that the dipole antenna can be characterized by a single complex conjugate pole pair (or simply pole pair) of large real part, independent of antenna position [5-7].

The oscilloscope samples the received echo (of some finite time window) at 256 points and records it in a form compatible for computer processing [12].

B. The Tunnel Response

Figure 1(a) illustrates a simple model of the tunnel response when a pulse is incident on its surface. The incident pulse bounces back and forth in the tunnel. Every time the bouncing pulse is at the upper interface of the tunnel a pulse is also transmitted and propagates toward the antenna. This creates a multiple lobe signal structure at the receiving antenna input. Therefore, (within our system's bandwidth) the tunnel's (natural) response can be characterized in the complex frequency plane by a single complex conjugate pole pair, independent of antenna position. Figure 1(b) presents a transmission line model of the unified antenna-tunnel structure. This model will be discussed extensively in Chapter IV. A worst case study, in which the antenna is not matched to the transmission line impedance will be pursued there. In practice, when recording actual echoes our dipole antenna was closely matched to the ground impedance, thus avoiding multiple reflections from the target to facilitate the processing of the echoes, especially when dealing with shallow targets. The results of this theoretical study will prove to be very helpful in guiding tunnel identification process.

To avoid confusion in later discussions, a point of distinction is due here. It concerns the classification of the different waveforms to be encountered, and will be used consistently henceforth. When we refer to the (backscattered) original waveform, or simply echo we mean the response received by the video-pulse radar. It has not been processed yet by any identification or detection scheme, except some analog processing accomplished in the radar itself for supression of interference, clutter and noise. By tunnel or target response we refer to the natural response of the tunnel or target, respectively. For the tunnel this is just an exponentially decaying sinusoid.

C. The Identification Process

The identification process is concerned with the calculation of the tunnel resonance and the arrival time of the tunnel response. The resonance determines the tunnel's height and the arrival time indicates its depth. The problem associated with the analysis is that the received backscattered response is not only characterized by the tunnel pole pair but it also contains the antenna pole pair, possibly other false target poles, and significant portions of clutter and noise. Clutter occurrence is mainly in the early portion of

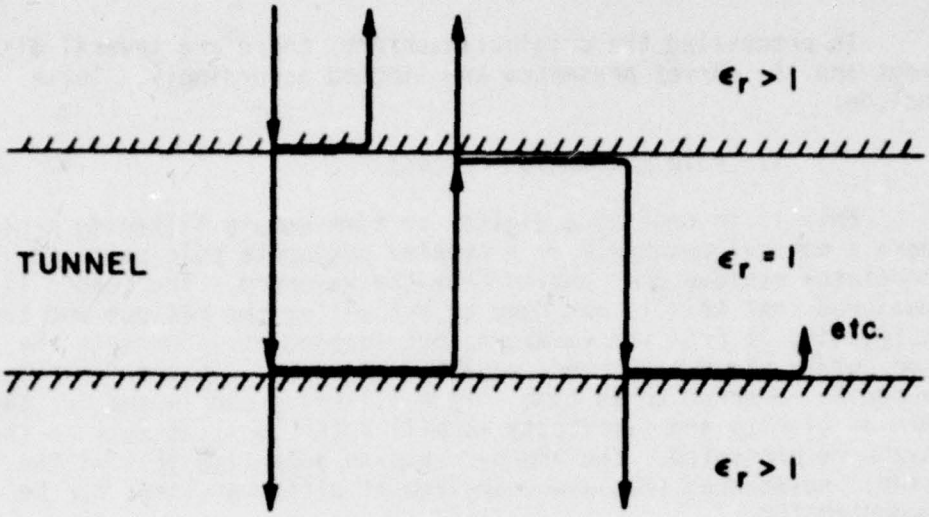

(a)

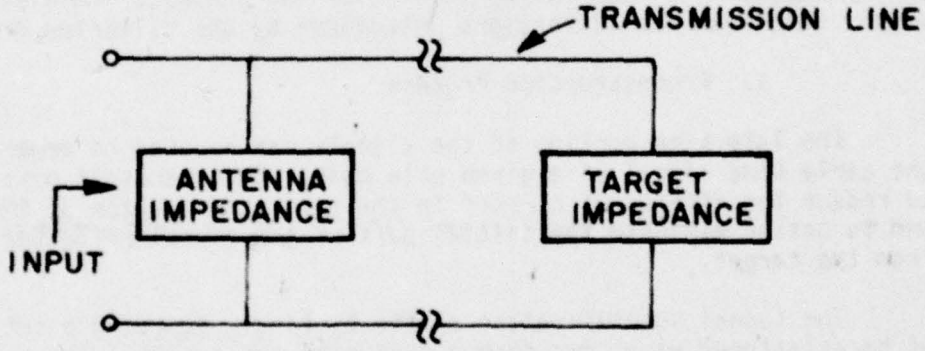

(b)

Figure 1. Simplified tunnel models.

the received echo and causes difficulty in the determination of the tunnel response arrival time. Major efforts are attempted in this study to overcome this problem.

In processing the original waveform, there are several distinct steps and the curves presented are labeled accordingly. These include:

1. Pole Extraction Process

This is in reality a digital or time domain filtering process where a natural resonance or a complex conjugate pole pair and its associated residue are removed from the waveform. The reader is cautioned that this is not done by evaluating the residue and then subtracting it from the waveform, but instead it is done in the time domain via a difference equation approach. This process could indeed be referred to as time domain filtering and indeed for the sake of clarity and simplicity we will refer to it as such on the waveforms presented. The approach has an advantage in that the natural resonances that are energized at different times can be accounted for.

2. Correction Process

In the process of extracting a natural resonance, the remainder of the waveform is modified by this filtering process. This step simply takes out the distortions introduced by the filtering process.

3. Reconstruction Process

The late time portion of the signals can be used to generate the early time signal of a given pole pair. This makes it possible to reduce the effects of clutter in the early time region of the signal and to better evaluate the initial part of the signal reflected from the target.

The tunnel identification starts by first recording a set of backscattered waveforms from a pass over the tunnel. The recorded echoes are first processed for determining the poles of each particular echo. These poles will include the antenna and tunnel pole pairs, and possibly other false target resonances. Prony's classical method [7,15-20] was used for calculating the poles. This was done as outlined in [7], by applying the method using various waveform time windows and intervals between the samples to be used for constructing Prony's difference equations. The selected time windows are characterized by their starting time and length (minimum length is dictated by the number of poles desired). According to the calculated poles from each parameter set (window starting point, window length, number of poles, and interval between samples) a theoretical waveform is constructed, and a square error is determined between

the theoretical and measured waveforms. Finally, the poles calculated by the parameter set giving the smallest error are selected. The program "Singularity Expansion by Prony" as given by Chan [7] was used. Other techniques such as the Eigenvalue method [7] or Contour Integration [21] could have been used for finding the poles.

After the pole calculation we strive to isolate the response from the tunnel alone. This is the most important step of our identification process. The accuracy of our results as compared to other attempts by Stapp [22] and GEO-CENTERS, INC. [23] is derived from this process. It is accomplished through the Pole Extraction Process and is extensively discussed. During this process, all the poles not associated with the tunnel are removed as calculated by Prony's method. Thus, ideally, we are left with the tunnel response alone.

Following the Pole Extraction Process (and correction), the Reconstruction Process is used for combating the clutter problem. It reconstructs the early portion of the tunnel response based on a predicting window of its late response. This process contributes to the estimation of the tunnel response arrival time.

Finally, the identification process can be highlighted by mapping the reconstructed set of tunnel responses, using a mapping technique extensively discussed by Stapp [22]. Such a map can indicate the relative tunnel position.

D. Structure of the Thesis

The structure of this thesis is as follows:

In Chapter II the Pole Extraction Process is discussed. It presents the derivation of the difference equation used for the extraction of undesired poles. Also, various characteristics of this process are extensively analyzed and criticized.

In Chapter III we present the Reconstruction Process. The difference equation used for accomplishing this process is derived, analyzed, and criticized. Examples on the performance of the process with measured waveforms are given.

In Chapter IV a simple transmission line model of the Radar-Tunnel structure is analyzed and tested. Application of the Pole Extraction Process and Reconstruction Process is given here for the identification of the theoretical target.

In Chapter V measured echoes from a tunnel are encountered. The effectiveness of the Pole Extraction and Reconstruction Processes is strongly indicated here as compared to other attempts.

CHAPTER II
THE POLE EXTRACTION PROCESS

A. Objectives

The objectives of this chapter are the following:

1. To give the derivation and performance of the difference equation used for extraction of all undesired poles from the raw recorded waveforms of the tunnel echo.

2. To discuss the effects of the process on the waveform associated with the remaining waveform poles and the importance of the sampling interval used in the process.

3. To derive a method for correcting the various distortions occuring on the waveform associated with the remaining poles due to the Pole Extraction Process.

B. Derivation of a Difference Equation for Extracting One Complex Conjugate Pole Pair

The Pole Extraction Process is in effect a filtering process to be used for real time calculations. It is accomplished by applying a difference equation to the recorded waveforms. As compared to classical filtering it works in the complex plane (Figure 2) for extracting (removing) particular poles from the recorded echoes as they are calculated by Prony's method. Its main advantage is simplicity and speed. It avoids convolution or frequency spectrum calculations as would be required with classical methods. Furthermore, it concentrates only on the particular poles to be extracted.

In order to understand the principle of the process let us assume an original waveform whose spectrum is $F(\omega)$ and is characterized by a set of poles. We wish to extract a set of poles characterized by a function $F_1(\omega)$. The operation of the pole extraction process is as follows:

$$F_2(\omega) = \frac{F(\omega)}{F_1(\omega)} \quad . \tag{1}$$

$F_2(\omega)$ is the spectrum of the resultant waveform. Since we divided by $F_1(\omega)$, then $F_2(\omega)$ has all the poles of $F(\omega)$ except the ones of $F_1(\omega)$.

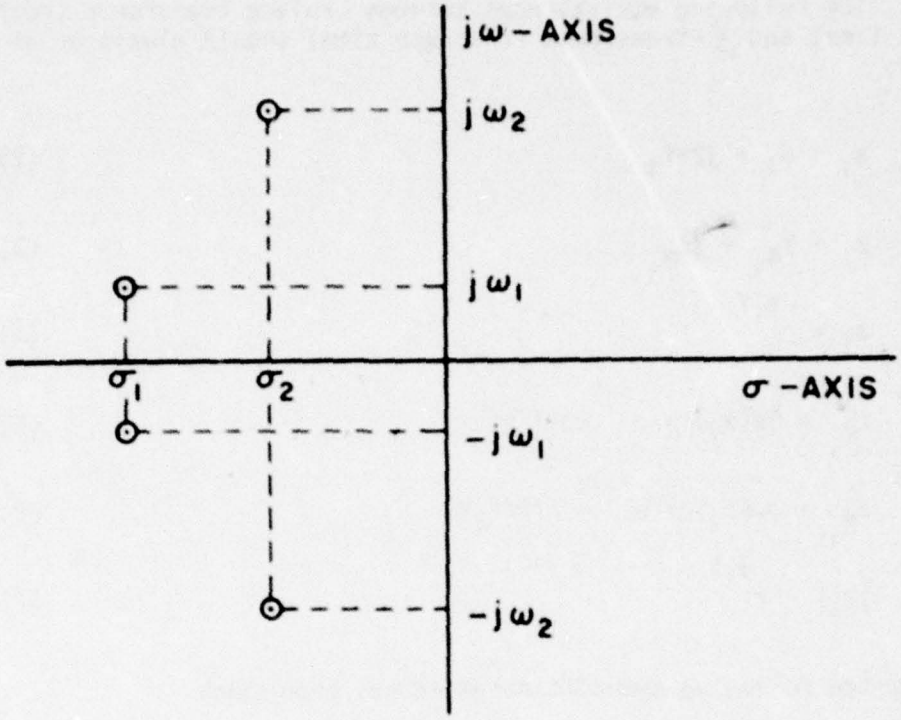

Figure 2. Complex plane.

We proceed now to generate a difference equation for implementing a process equivalent to Equation (1). The difference equation for extracting one complex pole pair (2 poles) is first derived and then generalized for extracting several poles. Since we are interested in deriving a process to be applied in the time domain and thus avoid spectrum calculations, all manipulations will be worked out in the $\mathcal{Z}$-domain. $\mathcal{Z}$-transform† representations are then easily transformed to discrete time domain [25,26]. Furthermore, we will only stress cases dealing with complex conjugate pole pairs since the antenna and all underground targets are characterized by such poles.

---

† We are referring here to one-sided $\mathcal{Z}$-transform defined as $R(z) = \sum_{n=0}^{\infty} r(nT)z^{-n}$, where $R(z)$ is the $\mathcal{Z}$-transform of $r(nT)$.

The following equivalences between Laplace transforms (continuous time) and $\mathcal{Z}$-transforms (discrete time) should always be at hand:

$$s_i = \sigma_i + j2\pi f_i \tag{2}$$

$$z_i = z_{R_i} + jz_{M_i} \tag{3}$$

$$z_i = e^{s_i T} \tag{4}$$

$$z_{R_i} = \mathrm{Re}(z_i) = e^{\sigma_i T}\cos(2\pi f_i T) \tag{5}$$

$$z_{M_i} = \mathrm{Im}(z_i) = e^{\sigma_i T}\sin(2\pi f_i T) \tag{6}$$

$$|z_i| = e^{\sigma_i T} \tag{7}$$

where the following symbolic notation has been used:

- s = Laplace transform operator
- z = $\mathcal{Z}$-transform operator
- s_i = pole in the s-domain
- z_i = pole in the z-domain, equivalent to s_i
- σ_i = real part of pole s_i
- f_i = frequency of pole s_i
- z_{R_i} = real part of pole z_i
- z_{M_i} = imaginary part of pole z_i
- T = sampling interval of the process
- $|z_i|$ = magnitude of z_i
- z_i^* = conjugate of z_i
- s_i^* = conjugate of s_i.

The above notation will be consistently used in all subsequent references.

Let us now represent our original waveform, r(t), in the $\mathcal{Z}$-domain as follows:

$$R(z) = \frac{N(z)}{(1-z^{-1}z_1)(1-z^{-1}z_1^*)D(z)} \tag{8}$$

where R(z) is the $\mathcal{Z}$-transform of r(t) ($r(t) = \mathcal{Z}^{-1}[R(z)]$). (z_1, z_1^*) is the complex pole pair to be extracted. The rest of the denominator of R(z), D(z), contains the other poles of R(z) (tunnel pole pair) to remain after the extraction of (z_1, z_1^*).

Multiplying both sides of Equation (8) by the representation of the pole pair (z_1, z_1^*), we obtain

$$R_p(z) = \frac{N(z)}{D(z)} = (1-z^{-1}z_1)(1-z^{-1}z_1^*)R(z) \quad . \tag{9}$$

$R_p(z)$ is the $\mathcal{Z}$-transform of the desired resultant waveform. Since we have multiplied R(z) by the zero,

$$R_1(z) = (1-z^{-1}z_1)(1-z^{-1}z_1^*) \tag{10}$$

the pole pair of R(z) at (z_1, z_1^*) is canceled out. Therefore, $R_p(z)$ contains only the poles of D(z). Further manipulation of Equation (9) gives

$$R_p(z) = (1-z^{-1}z_1^*-z^{-1}z_1+z^{-2}z_1z^*)R(z)$$

or

$$R_p(z) = (1-2\mathrm{Re}(z_1)z^{-1}+|z_1|^2z^{-2})R(z) \quad . \tag{11}$$

The above equation can now be easily transformed to discrete time domain, to obtain

$$r_p(nT_e)=r(nT_e)-2\mathrm{Re}(z_1)r(nT_e-T_e)+|z_1|^2r(nT_e-2T_e) \tag{12}^{\dagger}$$

---

†Its equivalent form in continuous time is derived in Appendix A.

where T_e is the sampling interval during the pole extraction process and $r_p(t) = \mathcal{Z}^{-1}[R_p(z)]$.

The sampling interval T_e is a multiple of T_B, i.e.,

$$T_e = N_e T_B$$

where T_B is the basic sampling interval of r(t). N_e must be chosen so that it satisfies Shannon's sampling theorem. This implies that

$$T_e \leq \frac{1}{2f_1} \text{ or } N_e \leq \frac{1}{2f_1 T_B} \quad . \tag{13}$$

Equation (12) as it stands can only generate points which are a multiple of T_e. In order to generate all the points within the T_e interval, spaced at the basic interval T_B, Equation (12) can be modified as follows:

$$r_p(nT_e+kT_B) = r(nT_e+kT_B) - 2\mathrm{Re}(z_1)\, r(nT_e+kT_B-T_e) + |z_1|^2\, r(nT_e+kT_B-2T_e) \quad ; \quad \begin{matrix} k=0,1,\ldots,N_e-1 \\ n=0,1,2,\ldots \end{matrix} \quad . \tag{14}$$

The above equation indicates the time domain operation required for extracting the complex conjugate pole pair (z_1,z_1^*). $r_p(t)$ is the residual or "filtered" waveform after (z_1,z_1^*) has been extracted. The choice of the proper value of T_e in Equation (14) is extremely important and the implications of this choice will be discussed later in this chapter.

It is essential to observe that the extraction of a pole pair requires only the knowledge of the pole pair itself and not any information about its residue. This is of great advantage since the values of the residues are, of course, excitation dependent. From Equation (14) it is noted that the calculation of one point of $r_p(t)$ requires three points of the discrete original waveform. The present point and two previous points spaced at intervals of T_e (or $N_e T_B$). This indicates that the first $2N_e$ points of the filtered waveform, $r_p(t)$, cannot be evaluated. In our computer implementation of Equation (14) these points were conveniently set equal to zero.

The method for implementing Equation (14) by a digital computer is shown in Figure 3. As seen Equation (14) can be very easily programmed by a field microprocessor for real time calculations by simple appropriate shifts and additions.

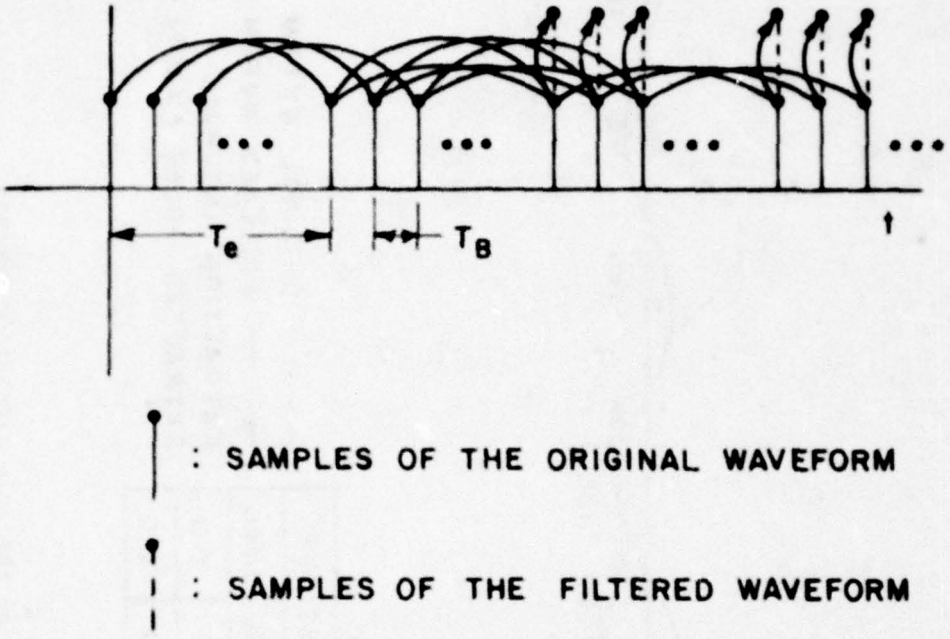

Figure 3. Computer implementation of Equation (14).

An application of Equation (14) on a theoretical waveform is shown in Figure 4. The original waveform (dotted line) is composed of two exponentially decaying sinusoids with poles at s_1, s_1^*=-3. Meganepers/sec $\pm$ j2πx15 Megarad/sec[†] and s_2, s_2^*=-6. Meganepers/sec $\pm$ j2πx20 Megarad/sec and residues at 2.0 $\pm$ j0.0 for both pole pairs. Its representation in time domain is

$$r(nT_B) = e^{-6\times10^6 nT_B}\cos(2\pi\times15\times10^6 nT_B)+e^{-3\times10^6 nT_B}\cos(2\pi\times20\times10^6 nT_B).$$

It consists of 256 points with T_B=200/255 nsec. The solid line is the result when the pole at 15 MHz is extracted. As seen, it is a decaying sinusoid corresponding to the s_2 pole pair (20 MHz). The pole extraction interval is indicated to be $10T_B$(N_e=10). Observe the early portion of the filtered waveform which is set equal to zero as was discussed previously. This time interval is measured to be $20T_B$, corresponding to 15.7 nsec.

[†] $\pm$ indicates the presence of complex conjugate poles.

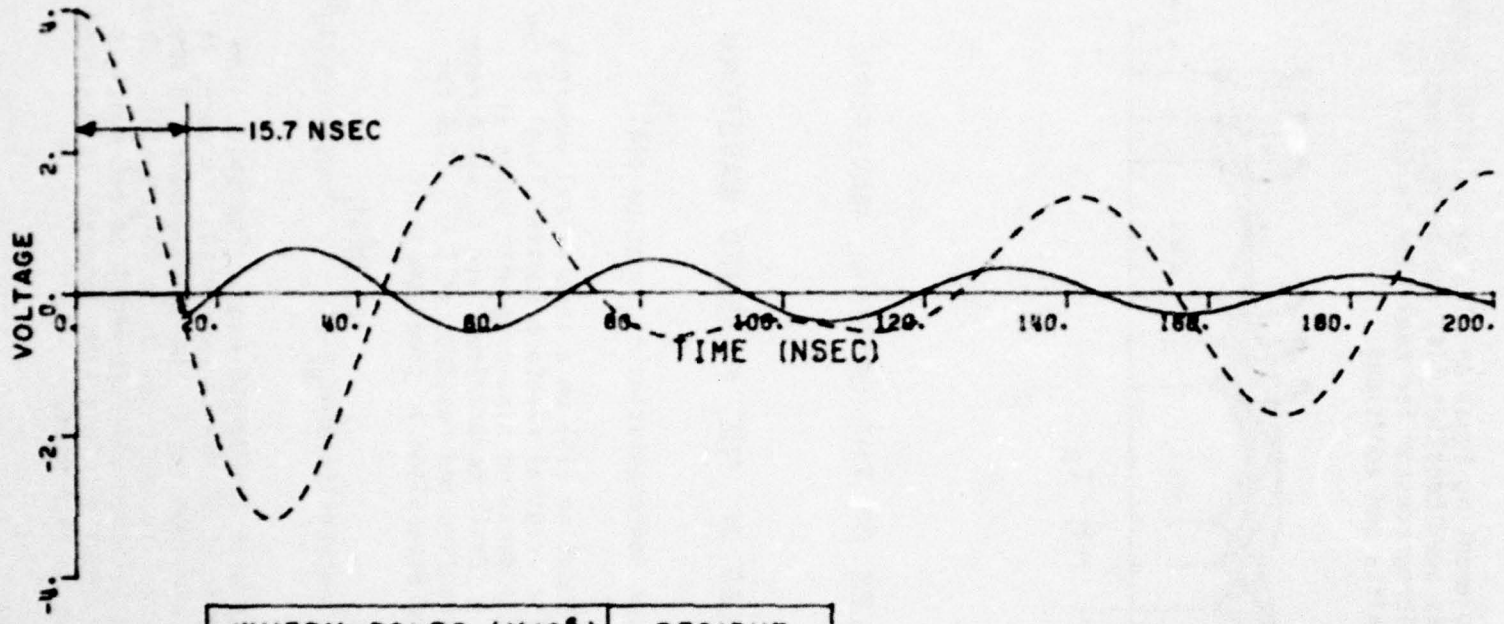

WVFRM POLES ($\times 10^6$)		RESIDUE	
σ_i	f_i	REAL	IMAG
-3.00	15.00	2.0	0.0
-6.00	20.00	2.0	0.0

---- ORIGINAL WVFRM

——— FILTERED WVFRM

EXTRACTION INTERVAL = $10T_s$

EXTRACTED POLES ($\times 10^6$): σ_i f_i

-3.0 15.0

Figure 4. Example of the pole extraction process according to Equation (14).

It is noted here that all subsequent waveforms, measured or theoretical, will consist of 256 time points.

A situation of importance occurs when the signal associated with one of the pole pairs is time delayed. This is usually the case for echoes from deep tunnels. Then, the arrival time of the tunnel response occurs after various forms of clutter, including direct coupling between transmit and receive antennas. In this case when the antenna pole pair is extracted, there will be an error region of time length $2N_eT_B$, corresponding to the initial portion of the delayed part of the echo from the tunnel. An example of such a situation is shown in Figure 5.

C. Generalization of the Pole Extraction Process to Several Poles

The application of Equation (14) can extract only one complex conjugate pole pair at a time. A similar approach to the derivation of Equation (14) can be used for deriving difference equations to extract concurrently several poles. The resulting equations will just be stated.

The difference equation for concurrent extraction of two complex conjugate pole pairs (4 poles) or less can be shown to be given by

$$r_p(nT_e+kT_B)=r(nT_e+kT_B)-c_1r(nT_e+kT_B-T_e)+c_2r(nT_e+kT_e-2T_e)$$

$$-c_3r(nT_e+kT_B-3T_e)+c_4r(nT_e+kT_B-4T_e); \qquad k=0,1,\ldots,N_e-1 \quad n=0,1,2,\ldots \tag{15}$$

where $r_p(t)$, $r(t)$, N_e, T_e and T_B are as defined previously, and the coefficients are calculated to be:

$$c_1 = 2[\mathrm{Re}(z_1)+\mathrm{Re}(z_2)]$$

$$c_2 = |z_1|^2+|z_2|^2+4\mathrm{Re}(z_1)\mathrm{Re}(z_2)$$

$$c_3 = 2[|z_1|^2\mathrm{Re}(z_3)+|z_2|^2\mathrm{Re}(z_1)]$$

$$c_4 = |z_1|^2|z_2|^2 \quad .$$

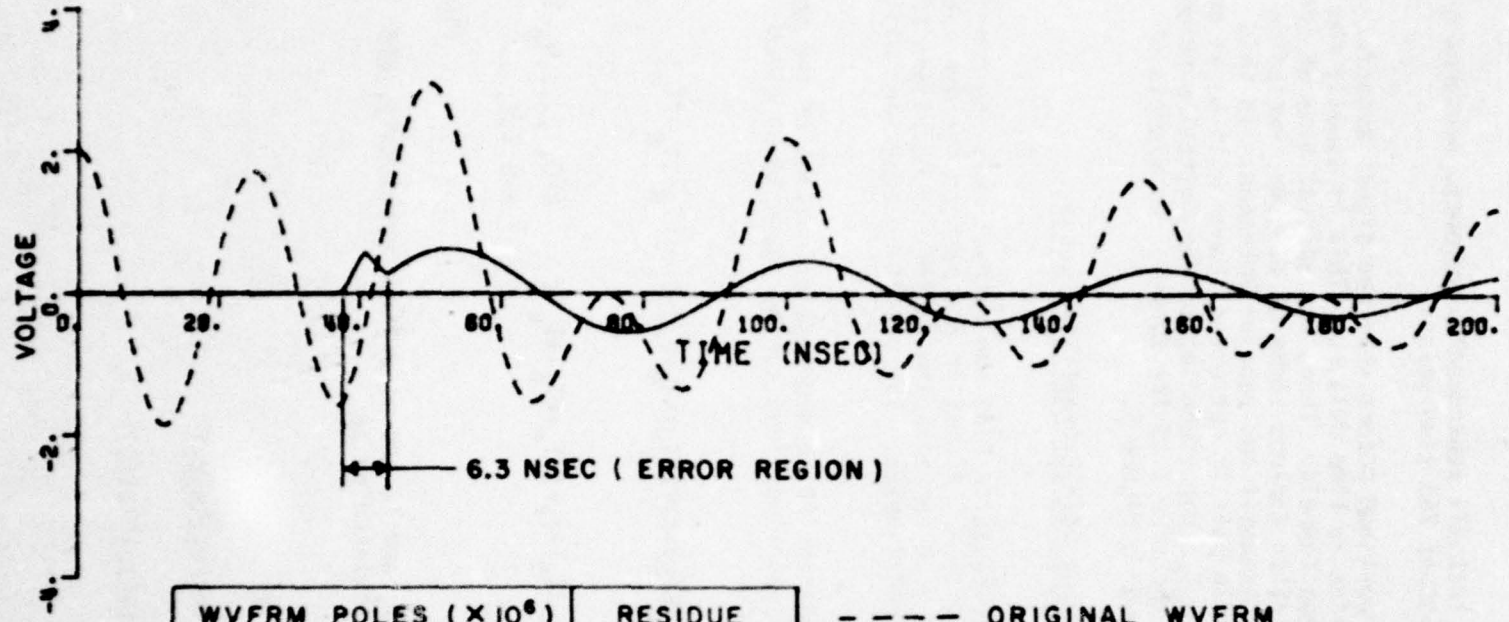

WVFRM POLES ($\times 10^6$)		RESIDUE	
σ_i	f_i	REAL	IMAG
-6.00	40.00	2.0	0.0
-6.00	20 00	2.0	0.0

---- ORIGINAL WVFRM

——— FILTERED WVFRM

LAST POLE TIME DELAY = 375

EXTRACTION INTERVAL = $4T_s$

EXTRACTED POLES ($\times 10^6$): σ_i f_i

-6.0 40.0

Figure 5. Application of the pole extraction when the signal associated with the desired (remaining) pole pair is time delayed.

(z_1, z_1^*) and (z_2, z_2^*) are the $\mathcal{Z}$-domain representation of the complex conjugate pole pairs to be extracted. Since four poles are extracted, it is seen from Equation (15) that the calculation of a single point of the filtered waveform requires four previous points of the original waveform and its present point. Therefore, the filtered waveform cannot be calculated in an initial time wondow equal to $4T_e$ by this difference equation when two complex conjugate pole pairs are extracted concurrently.

The difference equation for extracting three complex conjugate pole pairs (6 poles) or less is

$$r_p(nT_e+kT_B) = r(nT_e+kT_B) - c_1 r(nT_e+kT_B-T_e) + c_2 r(nT_e+kT_B-2T_e)$$
$$- c_3 r(nT_e+kT_B-3T_e) + c_4 r(nT_e+kT_B-4T_e)$$
$$- c_5 r(nT_e+kT_B-5T_e) + c_6 r(nT_e+kT_B-6T_e); \quad k=0,1,\ldots,N_e-1, \quad n=0,1,2,\ldots \tag{16}$$

The coefficients, c_i, of the above equation are given as follows:

$$c_1 = 2\left[\mathrm{Re}(z_1)+\mathrm{Re}(z_2)+\mathrm{Re})z_3)\right]$$

$$c_2 = |z_1|^2+|z_2|^2+|z_3|^2+4\mathrm{Re}(z_1)\mathrm{Re}(z_2)+4\mathrm{Re}(z_2)\mathrm{Re}(z_3)+4\mathrm{Re}(z_1)R_e(z_3)$$

$$c_3 = 2\left[|z_1|^2\mathrm{Re}(z_2+z_3)+|z_2|^2\mathrm{Re}(z_1+z_3)+|z_3|^2\mathrm{Re}(z_1+z_2)+ 4\mathrm{Re}(z_1)\mathrm{Re}(z_2)\mathrm{Re}(z_3)\right]$$

$$c_4 = |z_1|^2|z_2|^2+|z_1|^2|z_3|^2+|z_2|^2|z_3|^2+4|z_1|^2\mathrm{Re}(z_2)\mathrm{Re}(z_3)+ 4|z_2|^2\mathrm{Re}(z_1)\mathrm{Re}(z_3)+4|z_3|^2\mathrm{Re}(z_1)\mathrm{Re}(z_2)$$

$$c_5 = 2\left[|z_1|^2|z_2|^2\mathrm{Re}(z_3)+|z_3|^2|z_1|^2\mathrm{Re}(z_2)+|z_2|^2|z_3|^2\mathrm{Re}(z_1)\right]$$

$$c_6 = |z_1|^2|z_2|^2|z_3|^2$$

where (z_1,z_1^*), (z_2,z_2^*) and (z_3,z_3^*) are the pole pairs to be extracted. It is seen, that the coefficients of the difference equation increase to the number of poles extracted concurrently. In addition, the number of previous points required for calculation of a single point is also equal to the number of extracted poles. This necessitates the expansion of the error region of the filtered waveform, equal to $m_e T_e$, when m_e complex poles are extracted concurrently. Larger time windows of the original waveform are then required or smaller T_e if we are to use $r_p(t)$ in subsequent processings. This problem can be alleviated by use of the Reconstruction Process discussed in the next chapter.

The computer subroutine given in Appendix C implements Equation (16). An application of Equation (16) is presented in Figure 6. The results were produced by the main program given in Appendix B which also uses the pole extraction subroutine. The dotted line in Figure 6 is a theoretical waveform composed of three complex conjugate pole pairs located at s_1,s_1^*=-6. Meganepers/sec $\pm$ j2πx50. Megarad/sec, s_2,s_2^*=-6. Meganepers/sec $\pm$ j2πx40. Megarad/sec, s_3,s_3^*=-6. Meganepers/sec + j2πx20. Megarad/sec, with respective residues at 1.$\pm$j0., 1.$\pm$j0 and 2.$\pm$j0. The solid line is the result after the extraction of (s_1,s_1^*) and (s_2,s_2^*). It is simply an exponentially decaying sinusoid corresponding to (s_3,s_3^*). The coefficients are calculated to be:

$$c_1 = 2.467691$$

$$c_2 = 3.426065$$

$$c_3 = 2.376516$$

$$c_4 = .927471$$

for N_e=4. Note that the error region is equal to $4N_eT_B$=12.55 nsec.

A generalized difference equation can be found for extracting any number of poles, m_e. The $\mathcal{Z}$-transform representation of the filtered waveform after the extraction of m_e poles can be given as

$$R_p(z) = R(z) \prod_{i=1}^{m_e} (1-z_i z^{-1}) \qquad (17)$$

where z_i represents the extracted pole. If z_i is complex, then the product must also include its complex conjugate when working

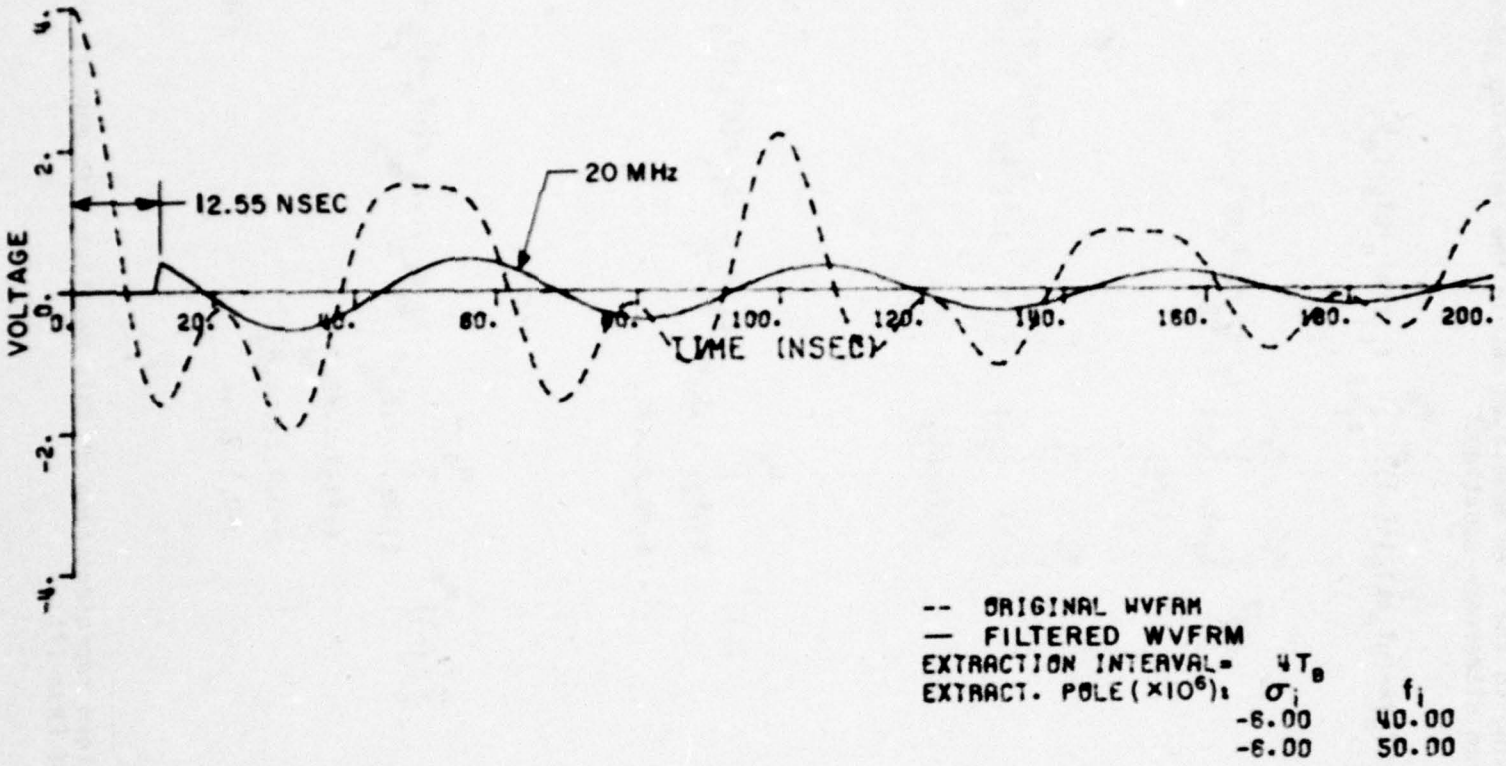

Figure 6. Application of Equation (16); concurrent extraction of two complex conjugate pole pairs.

with real waveforms. Expanding the product of Equation (17) [24] and transforming to the time domain we obtain the following general pole extraction difference equation:

$$r_p(nT_e+kT_B)=r(nT_e+kT_B)+(-1)^2 \sum_{\ell_1=1}^{m_e} z_{\ell_1} r(nT_e+kT_B-T_e)$$

$$(-1)^2 \sum_{\ell_1=1}^{m_e} \sum_{\substack{\ell_2=1 \\ \ell_1\neq\ell_2}}^{m_e} z_{\ell_1} z_{\ell_2} r(nT_e+kT_B-2T_e)$$

$$(-1)^3 \sum_{\ell_1=1}^{m_e} \sum_{\substack{\ell_2=1 \\ \ell_1\neq\ell_2}}^{m_e} \sum_{\substack{\ell_3=1 \\ \ell_1\neq\ell_2\neq\ell_3}}^{m_e} z_{\ell_1} z_{\ell_2} z_{\ell_3} r(nT_e+kT_B-3T_e)$$

$$\vdots$$

$$(-1)^i \sum_{\substack{\ell_1,\ell_2,\ldots,\ell_i=1 \\ \ell_1\neq\ell_2\neq\ldots\neq\ell_i}}^{m_e} z_{\ell_1} z_{\ell_2} \ldots z_{\ell_i} r(nT_e+kT_B-iT_e)$$

$$\vdots$$

$$(-1)^{m_e} \sum_{\substack{\ell_1,\ell_2,\ldots,\ell_{m_e}=1 \\ \ell_1\neq\ell_2\neq\ldots\neq\ell_{m_e} \\ k=0,1,2,\ldots,N_e-1 \\ n=0,1,2,\ldots}}^{m_e} z_{\ell_1} z_{\ell_2} \ldots z_{\ell_{m_e}} r(nT_e+kT_B-m_eT_e); \qquad (18)^{\dagger}$$

---

†The $\mathcal{Z}$-transform representation of this equation also appears in Chapter IV of Chan [7].

The reader can easily varify that Equation (18) can be readily reduced to Equations (14), (15) or (16).

D. Effects of the Pole Extraction Process on the Waveform Associated With the Remaining Poles

We now turn our attention to another important parameter of the pole extraction process, its sampling interval, T_e. When Equation (18) is used to extract the desired poles then the residues associated with the remainder of the waveform are changed in both magnitude and phase. These modifications will be shown to be a main function of T_e and also the natural resonances. To acquire a feeling for these effects we refer to Figures 7 and 8. The original waveform is composed of poles s_1, s_1^*=-6. Meganepers/sec $\pm$ j2πx15. Megarad/sec and s_2, s_2^*=-6. Meganepers/sec $\pm$ j2πx20. Megarad/sec with residues of 2.$\pm$j0. In both figures (s_1, s_1^*) is extracted. The extraction interval of Figure 7 is $5T_B$(T_B=500/255 nsec) and that of Figure 8 is $9T_B$. The filtered waveform is characterized by the pole pair (s_2, s_2^*), but its magnitude and phase is different for each extraction interval. In fact, none of these results correspond to the proper residue of the original signal associated with the pole pair (s_2, s_2^*) (its proper form is also shown for comparison). The case when the original waveform is composed of poles s_1, s_1^*=-6. Meganepers/sec $\pm$ j2πx30. Megarad/sec and s_2, s_2^*=-6. Meganepers/sec $\pm$j2πx20. Megarad/sec with residues of 2.+j0. is shown in Figure 9. The extraction interval is $5T_B$ (same as in Figure 7). As seen, the residue of the remaining signal does not have the same amplitude or phase as that of Figure 7. The measured amplitude and phase distortions are indicated on the respective figures.

In order to quantitatively present the effects of T_e and the extracted pole pairs on the remaining signal, a simple 2-pole pair (complex conjugate) waveform of the form

$$r(nT_B)=2|A_1|e^{\sigma_1 nT_B}\cos(\omega_1 nT_B+\alpha_1)+2|A_2|e^{\sigma_2 nT_B}\cos(\omega_2 nT_B+\alpha_2) \tag{19}$$

is first studied. We will then generalize our results to include additional poles. The $\mathcal{Z}$-transform of Equation (19) is

$$R(z) = \frac{A_1}{1-z^{-1}z_1} + \frac{A_1^*}{1-z^{-1}z_1^*} + \frac{A_2}{1-z^{-1}z_2} + \frac{A_2^*}{1-z^{-1}z_2^*} , \tag{20}$$

where $s_1, s_1^* = \sigma_1 \pm j\omega_1$, $s_2, s_2^* = \sigma_2 \pm j\omega_2$, $A_1 = |A_1|e^{j\alpha_1}$ and $A_2 = |A_2|e^{j\alpha_2}$.

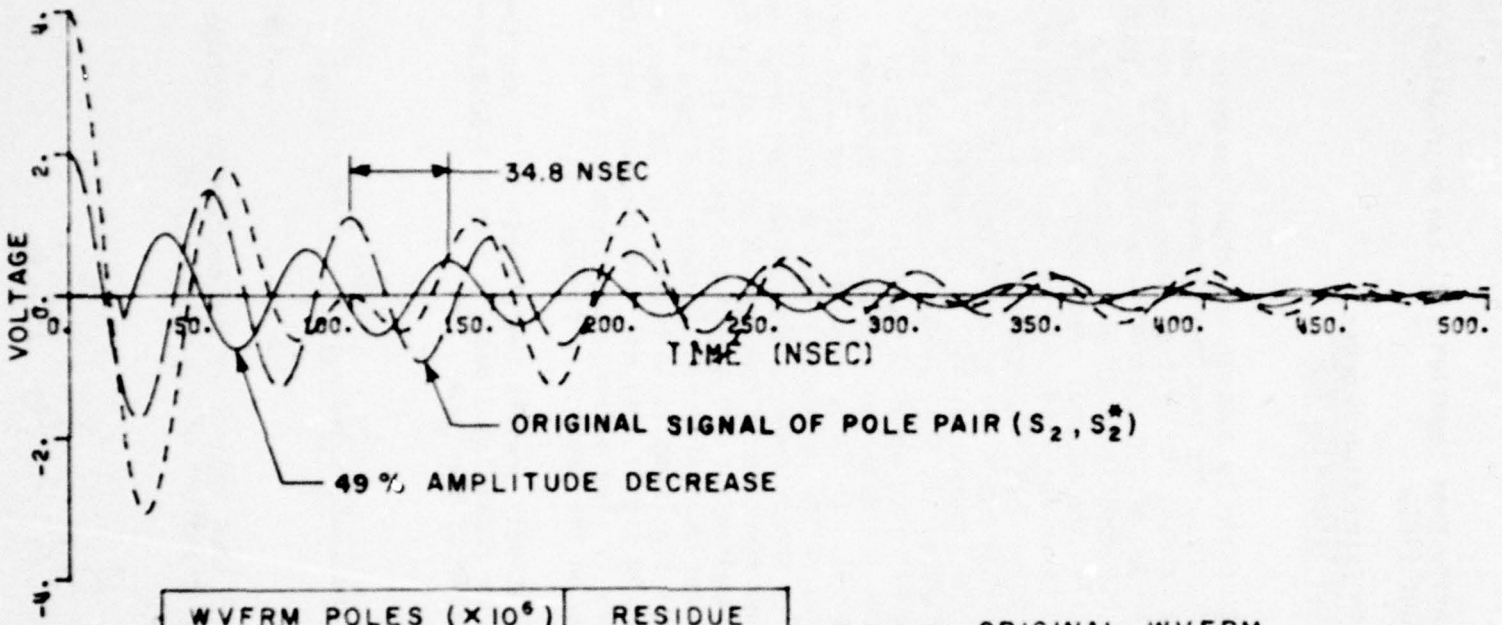

WVFRM POLES ($\times 10^6$)		RESIDUE	
σ_i	f_i	REAL	IMAG
-6.00	20.00	2.0	0.0
-6.00	15.00	2.0	0.0

---- ORIGINAL WVFRM

——— FILTERED WVFRM

EXTRACTION INTERVAL = $5\,T_B$

EXTRACTED POLES ($\times 10^6$): σ_i f_i

-6.0 15.0

Figure 7. Example on the amplitude and phase effects due to the pole extraction process.

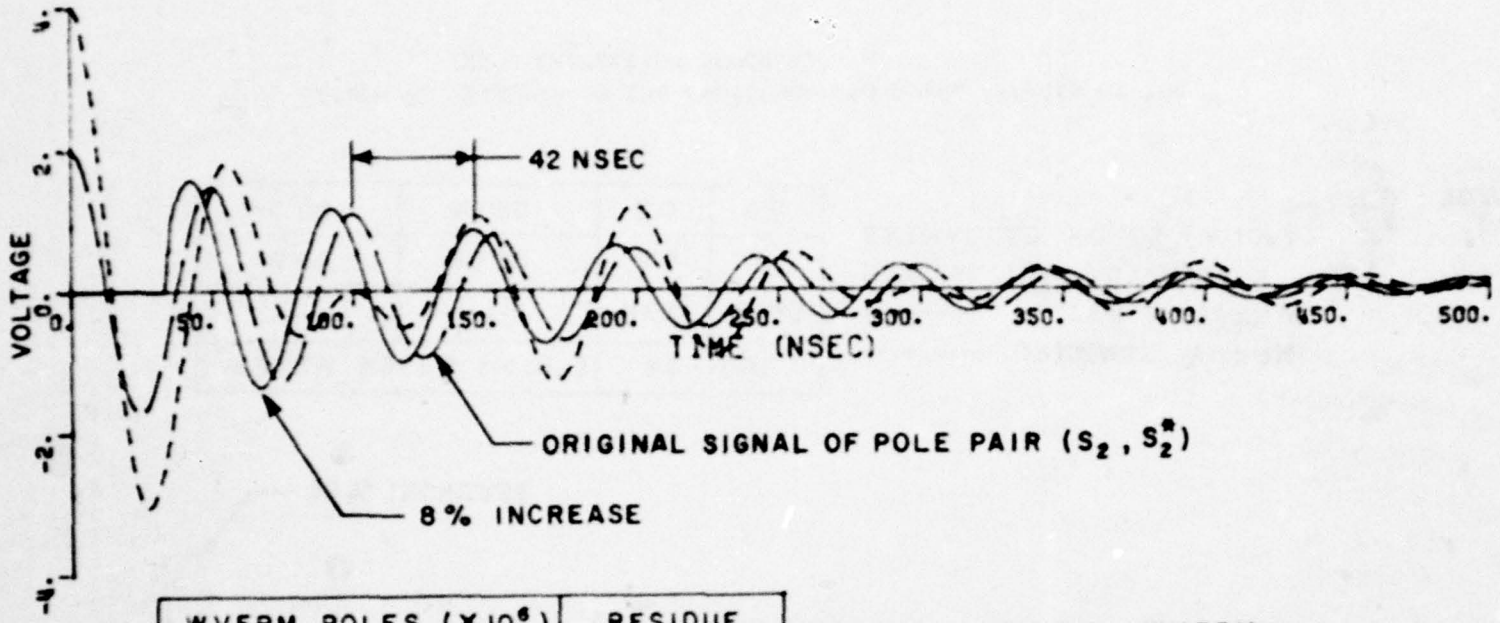

WVFRM POLES ($\times 10^6$)		RESIDUE	
σ_i	f_i	REAL	IMAG
-6.00	20.00	2.0	0.0
-6.00	15.00	2.0	0.0

---- ORIGINAL WVFRM
——— FILTERED WVFRM
EXTRACTION INTERVAL = $9T_s$
EXTRACTED POLES ($\times 10^6$): σ_i f_i
-6.0 15.0

Figure 8. Example on the amplitude and phase effects due to the pole extraction process.

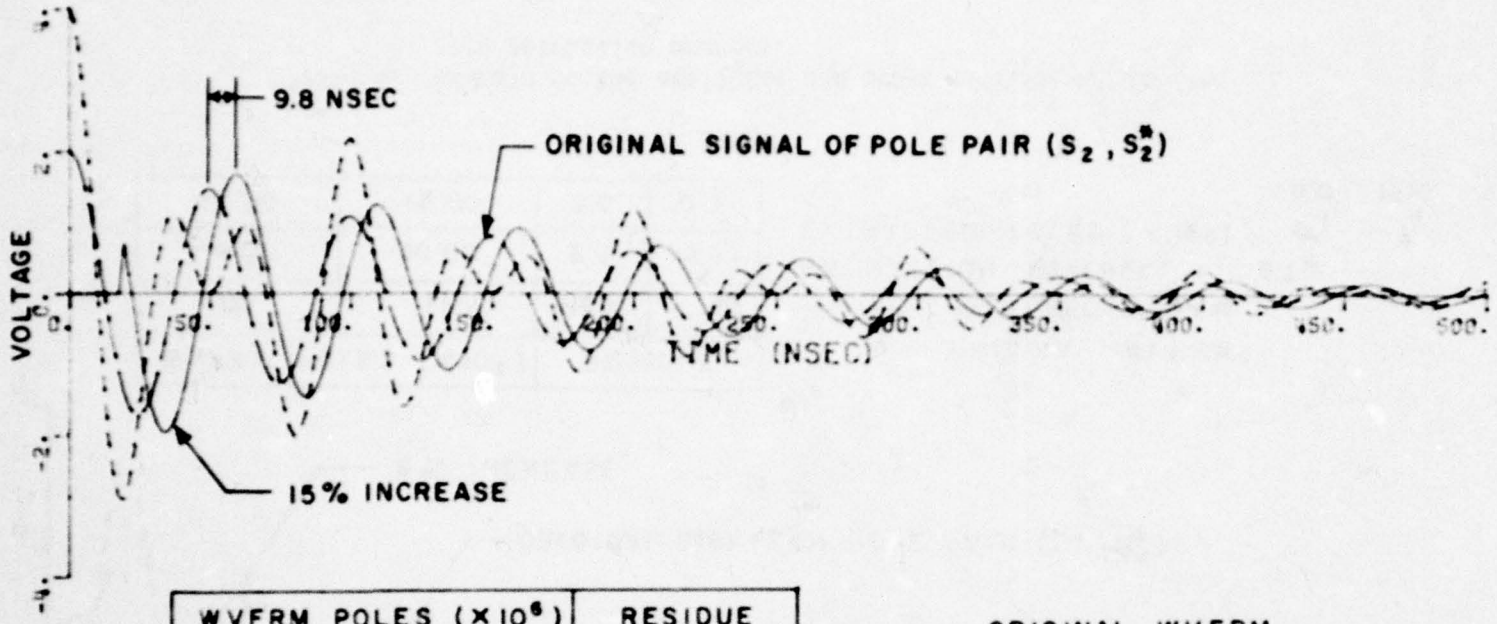

WVFRM POLES ($\times 10^6$)		RESIDUE	
σ_i	f_i	REAL	IMAG
-6.00	20.00	2.0	0.0
-6.00	30.00	2.0	0.0

---- ORIGINAL WVFRM
——— FILTERED WVFRM
EXTRACTION INTERVAL = $5T_B$
EXTRACTED POLES ($\times 10^6$): σ_i f_i
-6.0 30.0

Figure 9. Example on the amplitude and phase effects of the pole extraction process.

The extraction of pole pair (z_1, z_1^*) involves the multiplication of R(z) by Equation (10). Then, the transform of the filtered waveform is given by

$$R_p(z) = A_1(1-z^{-1}z_1^*) + A_1^*(1-z^{-1}z_1) +$$

$$\frac{A_2^*(1-2\mathrm{Re}(z_1)z^{-1}+|z_1|^2z^{-2})}{1-z^{-1}z_2^*} +$$

$$\frac{A_2(1-2\mathrm{Re}(z_1)z^{-1}+|z_1|^2z^{-2})}{1-z^{-1}z_2} \quad . \tag{21}$$

Expanding the last term of the above equation, we have

$$\frac{A_2(1-2\mathrm{Re}(z_1)z^{-1}+|z_1|^2z^{-2})}{1-z^{-1}z_2} =$$

$$\frac{A_2}{1-z^{-1}z_2} - 2\mathrm{Re}(z_1)\ \frac{z^{-1}}{1-z^{-1}z_2} + |z_1|^2\ \frac{z^2}{1-z^{-1}z_2} \tag{22}$$

Performing long divisions, we find that

$$\frac{z^{-1}}{1-z^{-1}z_2} = -\frac{z_2^*}{|z_2|^2} + \frac{z_2^*}{|z_2|^2(1-z^{-1}z_2)} \tag{23}$$

and

$$\frac{z^{-2}}{1-z^{-1}z_2} = -\frac{(z_2^*)^2}{|z_2|^4} - \frac{z_2^*}{|z_2|^2}\,z^{-1} + \frac{(z_2^*)^2}{|z_2|^4(1-z^{-1}z_2)} \tag{24}$$

The expansion of the third term of Equation (21) is similar to the above, if A_1, z_2 and z_2 are replaced by A_1, z_2 and z_2, respectively.

After substitution of the above expansions in Equation (21), we can express $R_p(z)$ as follows:

$$R_p(z) =$$

$$\left[2\mathrm{Re}(A_1)+2\mathrm{Re}(z_1)\left(\frac{A_2z_2^*+A_2z_2}{|z_2|^2}\right) - |z_1|^2\left(\frac{A_2(z_2^*)^2+A_2^*(z_2)^2}{|z_2|^4}\right)\right]$$

$$- z^{-1}\left[A_1z_1^* + A_1^*z_1 + \frac{|z_1|^2}{|z_2|^4}(A_2z_2^*+A_2^*z_2)\right]$$

$$+ \left[\frac{A_2}{1-z^{-1}z_2} + \frac{A_2^*}{1-z^{-1}z_2^*}\right]$$

$$+ \left[-2\mathrm{Re}(z_1)\frac{A_2z_2^*}{|z_2|^2} + |z_1|^2\frac{A_2(z_2^*)^2}{|z_2|^4}\right]\frac{1}{1-z^{-1}z_2}$$

$$+ \left[-2\mathrm{Re}(z_1)\frac{A_2^*z_2}{|z_2|^2} + |z_1|^2\frac{A_2^*(z_2)^2}{|z_2|^4}\right]\frac{1}{1-z^{-1}z_2^*} \quad . \qquad (25)$$

The first and second term of $R_p(z)$ in Equation (25) corresponds to impulses at $t=0$ and $t=T_e=N_eT_B$, respectively. As was indicated previously, these points cannot be calculated by Equation (12). Therefore, they will be discarded in the rest of our discussion. The third term corresponds to the original pole pair, (z_2,z_2^*). This is the desired result. The fourth and fifth terms are distortion terms and correspond to the variations on the magnitude and phase of the residue for the signal associated with the remaining pole pair. Therefore, $R_p(z)$ can effectively be written as the sum of the original signal with poles at (z_2,z_2^*) and the distortion terms. Note that these terms involve z_1 and z_2 which are functions of T_e.

In order to understand the effects of the distortion terms let us proceed by first inverting them into time domain. Thus,

Distortion Terms =

$$-2|A_2|\frac{\mathrm{Re}(z_1)}{|z_2|^2}e^{\sigma_2 T_e}e^{\sigma_2(nT_e+kT_B)}\left\{e^{j\left[\omega_2(nT_e+kT_B)+\alpha_2-\omega_2T_e\right]}\right.$$

$$\left.+\,e^{-j\left[\omega_2(nT_e+kT_B)+\alpha_2-\omega_2T_e\right]}\right\}$$

$$+|A_2|\frac{|z_1|^2}{|z_2|^4}e^{2\sigma_2 T_e}e^{\sigma_2(nT_e+kT_B)}\left\{e^{j\left[\omega_2(nT_e+kT_B)+\alpha_2-2\omega_2T_e\right]}\right.$$

$$\left.+\,e^{-j\left[\omega_2(nT_e+kT_B)+\alpha_2-2\omega_2T_e\right]}\right\};\ k=0,1,\ldots,N_e-1,\quad n=0,1,\ldots \quad (26)$$

or

Distortion Terms =

$$-4|A_2|e^{(\sigma_1-\sigma_2)T_e}\cos(\omega_1T_e)e^{\sigma_2(nT_e+kT_B)}\cos\left[\omega_2(nT_e+kT_B)+\alpha_2-\omega_2T_e\right]$$

$$+2|A_2|e^{2(\sigma_1-\sigma_2)T_e}e^{\sigma_2(nT_e+kT_B)}\cos\left[\omega_2(nT_e+kT_B)+\alpha_2-2\omega_2T_e\right];$$

$$k=0,1,\ldots,N_e-1$$
$$n=0,1,\ldots \quad . \quad (27)$$

For our waveforms, typical values of σ_1 and σ_2 are in order of -10^6 Nepers/sec, while those of T_e in 10^{-9} nsec. We can then use the approximation

$$e^{\sigma_1 T_e} \approx e^{\sigma_2 T_e} \approx 1. \quad (28)$$

According to this approximation, $r_p(t)$ (Equation (25)) can be expressed as follows:

$$r_p(nT_e+kT_B) = 2|A_2|e^{(\sigma_1-\sigma_2)T_e}\ e^{\sigma_2(nT_e+kT_B)}\cos\left[\omega_2(nT_e+kT_B)+\alpha_2\right]$$

$$-4|A_2|e^{(\sigma_1-\sigma_2)T_e}\ e^{\sigma_2(nT_e+kT_B)}\cos(\omega_1T_e)\cos\left[\omega_2(nT_e+kT_B)+\alpha_2-\omega_2T_e\right]$$

$$+2|A_2|e^{(\sigma_1-\sigma_2)T_e}\ e^{\sigma_2(nT_e+kT_B)}\cos\left[\omega_2(nT_e+kT_B)+\alpha_2-2\omega_2T_e\right]\ ;$$

$$k=0,1,\ldots,N_e-1$$
$$n=0,1,\ldots\quad .\qquad (29)$$

After further manipulation, by using some of the cosine identities, we arrive at the important result:

$$r_p(nT_e+kT_B)=4|A_2|e^{\sigma_2(nT_e+kT_B-T_e)}\cos\left[\omega_2(nT_e+kT_B)+\alpha_2-\omega_2T_e\right]\ x$$

$$e^{\sigma_1T_e}\left[\cos(\omega_2T_e)-\cos(\omega_1T_e)\right]\quad ;\quad k=0,1,\ldots,N_e-1$$
$$n=0,1,\ldots\quad .$$

(30)

We conclude that the signal associated with the remaining complex conjugate pole pair will be shifted in phase by

$$-\theta_s=\omega_2T_e=\omega_2N_eT_B=2\pi f_2N_eT_B(\text{rad}) \qquad (31)$$

or equivalently will be time increased by

$$t_s = \frac{\theta_s}{2\pi f_2} = N_eT_B = T_e\ . \qquad (32)$$

It will also be amplitude distorted by a factor

$$AF=2e^{\sigma_1T_e}\left[\cos(2\pi f_2N_eT_B)-\cos(2\pi f_1N_eT_B)\right]\ . \qquad (33)$$

We observe that the time shift does not depend on the interacting pole pairs. It is equal to the extraction interval. Conversely the amplitude factor does depend upon the frequencies of the pole pairs and also T_B. If it is negative, this is equivalent to an additional phase shift of $\theta_s=-\pi$ or a time increase of $t_s = \frac{1}{2f_2}$. When sampling at the Nyquist rate (Equation (13)) of f_2 then θ_s is multiples of π. The amplitude factor (Equation (33)) is plotted in Figure 10 as a function of f_2. It is interesting

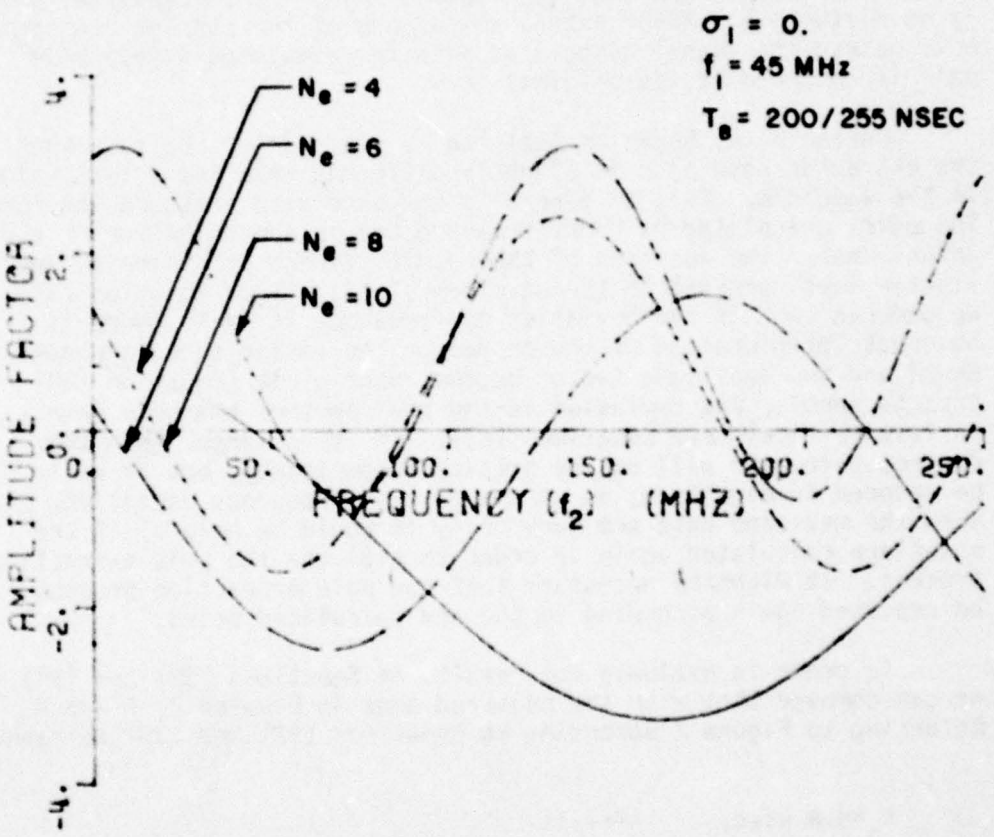

Figure 10. Amplitude response of the pole extraction process (Equation (33)) vs. frequency (f_2) of the remaining pole.

to note that the amplitude of the filtered waveform can increase fourfold when $\omega_2 N_e T_B = 2n\pi$ and $\omega_1 N_e T_B = (2n+1)\pi$, and conversely. But,

as seen in Figure 10, it can also vanish to zero when $\omega_2 N_e T_B = 2n\pi$ and $\omega_1 N_e T_B = 2k\pi$. Therefore, we must always select a sampling interval which does not bring us close to the zero crossings of the amplitude response. In addition, when N_e is small, then the two cosine terms approach 1. Thus, the amplitude factor tends to zero. This is the reason for performing the pole extraction process at a sampling interval close to the Nyquist interval of the extracted pole pair with the highest frequency [7].

It should be noted that Equation (30) is not valid when $z_1 = z_2$. For this case Equation (20) must be modified to treat double poles. It can be easily shown that when double poles are encountered, there is no distortion. After extraction of one of the complex conjugate pole pairs, the signal associated with the remaining single pole pair is returned in its original form.

Furthermore, Equation (33) can be studied for the case when the extracted pole pair is slightly different than its actual value in the waveform. This is generally the case with measured waveforms. The poles calculated by Prony's method are an approximation of the actual ones. The accuracy of the results depend on the noise and clutter level present in the waveform [7,18]. From Equation (33) we observe that if the deviation in frequency is small there is no great deterioration of the process. The cosine terms are almost equal and the amplitude factor becomes negligible (Equation (30) goes to zero). Any deviation in the real part of the pole pair is less critical (see Equation (28)). If it is large, then the desired pole pair will not be extracted completely, but it will be reduced in magnitude, as in the case of frequency deviation. When the measured data are very noisy it would be helpful if the poles are calculated again in order to evaluate the pole extraction process. It might be necessary that the pole extraction process be repeated again according to the new calculated poles.

In order to evaluate our results in Equations (32) and (33) we can compare them with the measured ones in Figures 7, 8 and 9. Referring to Figure 7 according to Equations (32) and (33) we have:

$t_s = 9.8$ nsec, AF=-.51

or

$t_s = 38.8$ nsec, AF=.51 .

Similarly, for Figures 8 and 9 we calculate;

$t_s = 42.6$ nsec, AF=.92

and

$$t_s = 9.8 \text{ nsec}, \qquad AF = 1.14,$$

respectively. As seen, Equations (32) and (33) perfectly predict the time shift and amplitude distortions.

E. Correction Process Involving Interaction of Two Complex Conjugate Pole Pairs

The amplitude and phase distortions on the signal associated with the remaining pole pair due to the pole extraction process is an undesirable effect. We want to obtain the remaining portion of the waveform in its original form. Otherwise, errors will occur in the tunnel identification process to follow. It will be seen in Chapters IV and V that if the resultant target response is not properly time placed, then errors will occur when determining the target's depth and position. Furthermore, amplitude distortions could obviously diminish the original tunnel response.

It is essential, then, to correct for the amplitude and phase distortions after the pole extraction process has been completed. This is easily accomplished, using Equation (30), as follows:

$$r_c(t) = r_p(t+t_s)/AF, \tag{34}$$

where $r_c(t)$ is the corrected waveform.

The correction process of Equation (34) was applied to the filtered waveforms in Figures 7, 8 and 9. The result (solid line) after correction is shown in Figures 11, 12 and 13, respectively. For comparison, the actual form of the signal associated with the original pole pair (s_2, s_2^*) is also plotted. As seen there is a perfect match of the corrected and original signal associated with pole pair (s_2, s_2^*).

The correction process will be incorporated in all subsequent pole extractions. When we refer to filtered waveforms it is assumed that correction has been already performed.

F. Correction Process Involving Multiple (Complex Conjugate) Pole Pairs

In the previous section we discussed the correction process (Equation (34)) when two pole pairs (complex conjugate) were involved. Obviously, measured waveforms will not necessarily consist of only two pole pairs. Two questions can then be raised: How is the re-

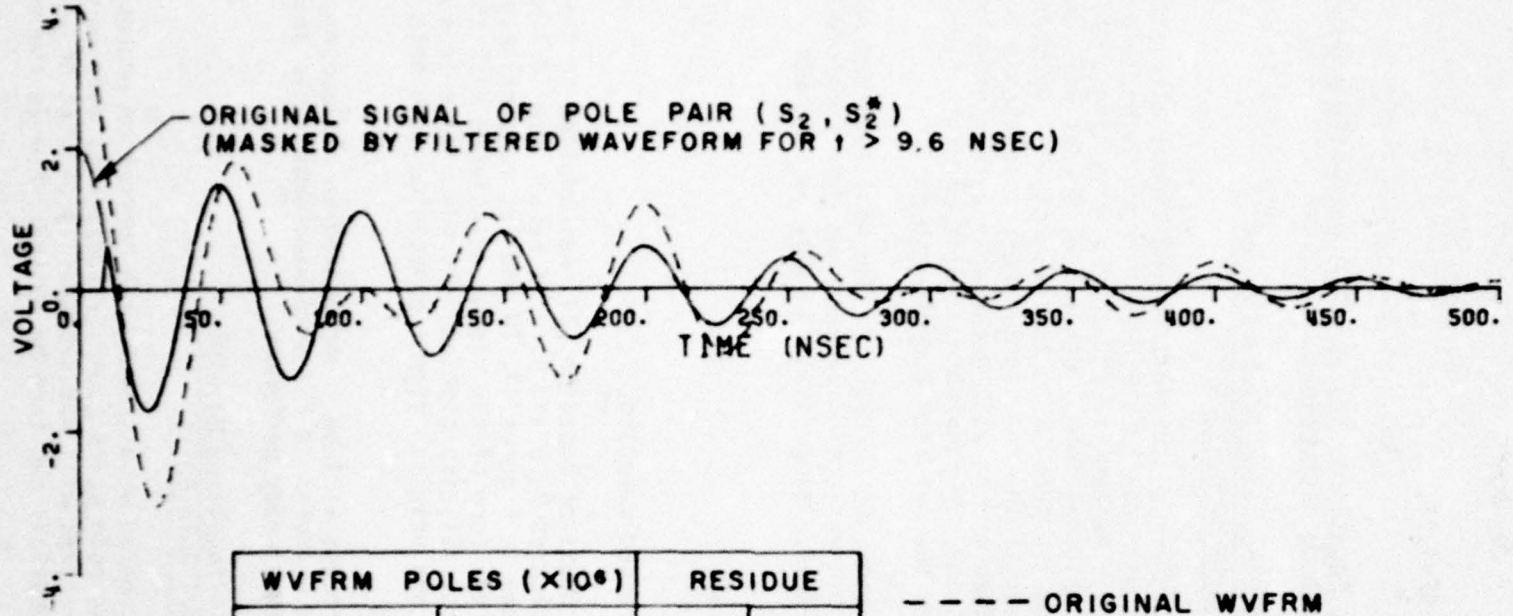

WVFRM POLES ($\times 10^6$)		RESIDUE	
σ_i	f_i	REAL	IMAG
−6.00	20.00	2.0	0.0
−6.00	15.00	2.0	0.0

– – – – ORIGINAL WVFRM

——— FILTERED (CORRECTED) WVFRM

EXTRACTION INTERVAL = $5T_B$

EXTRACTED POLES ($\times 10^6$): σ_i f_i

−6.0 15.0

Figure 11. Application of the correction process to the result of Figure 7.

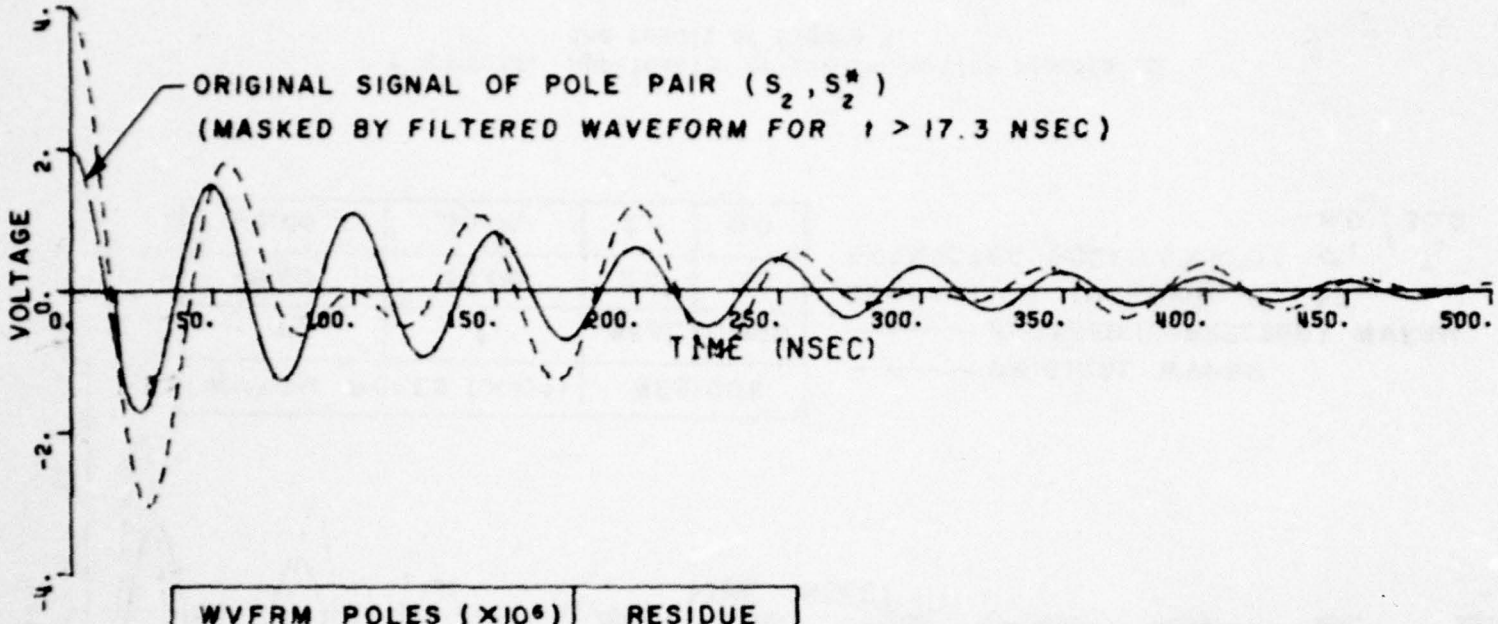

WVFRM POLES ($\times 10^6$)		RESIDUE	
σ_i	f_i	REAL	IMAG
-6.00	20.00	2.0	0.0
-6.00	15.00	2.0	0.0

- - - - ORIGINAL WVFRM

——— FILTERED (CORRECTED) WVFRM

EXTRACTION INTERVAL = $9\,T_0$

EXTRACTED POLES ($\times 10^6$): σ_i f_i

-6.0 15.0

Figure 12. Application of the correction process to the result of Figure 8.

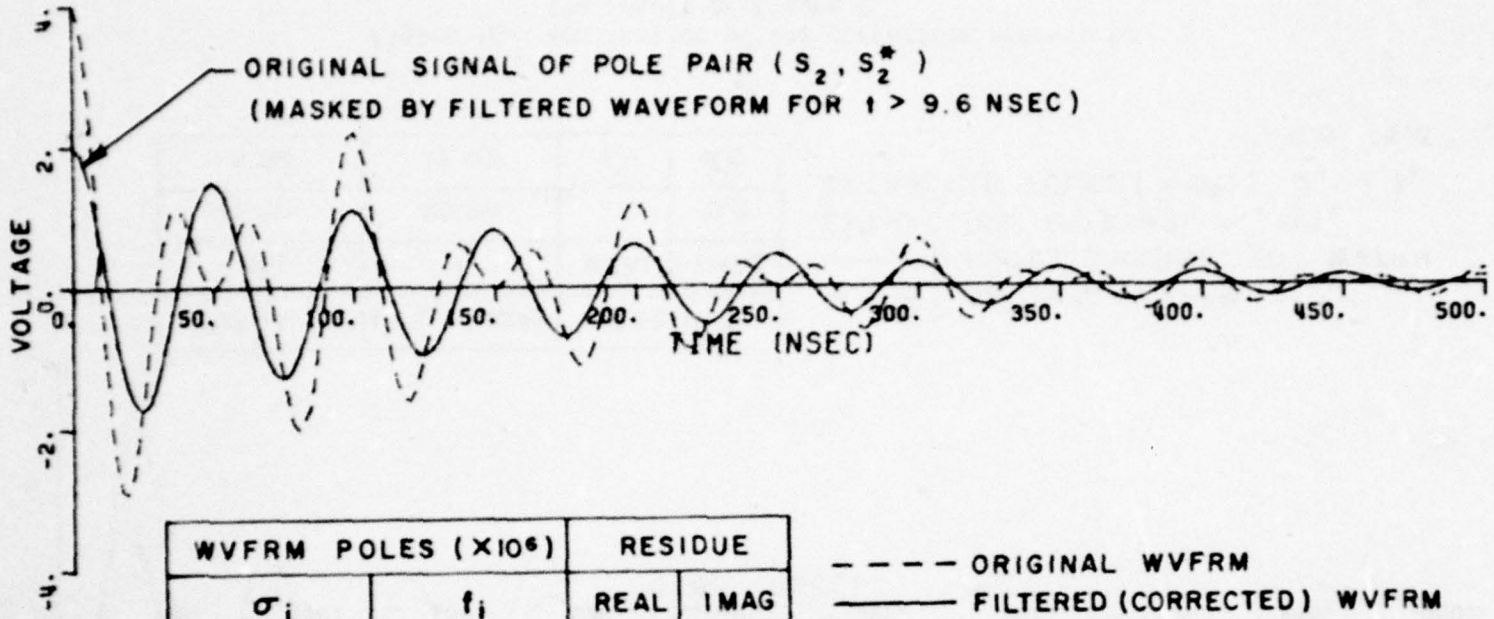

WVFRM POLES ($\times 10^6$)		RESIDUE	
σ_i	f_i	REAL	IMAG
-6.00	20.00	2.0	0.0
-6.00	30.00	2.0	0.0

- - - - ORIGINAL WVFRM

——— FILTERED (CORRECTED) WVFRM

EXTRACTION INTERVAL = $5T_B$

EXTRACTED POLES ($\times 10^6$): σ_i f_i

-6.0 30.0

Figure 13. Application of the correction process to the result of Figure 9.

maining waveform effected when two or more pole pairs are extracted concurrently, and, how do we account for the case of a remaining signal associated with more than one pole pair?

The first question is easily answered by observing that each extracted pole pair will affect the signal associated with each remaining pole independently according to Equations (32) and (33). Therefore, the correction process is performed by the application of Equation (34) for each of the extracted pole pairs on the remaining. This type of multiple correction is included in the pole extraction subroutine in Appendix C. An example of multiple pole pair extraction and correction is shown in Figure 14, corresponding to the uncorrected case of Figure 6. The original signal associated with the pole pair (s_2, s_2^*) is also plotted for comparison.

The second question can be difficult since the correction process requires the separation of the signal associated with the remaining waveform pole pairs. This case is not encountered in tunnel identification, since the tunnel can be characterized by a single pole pair. A method for performing such an operation is diagrammed in Figure 15. We have an original waveform consisting of pole pairs A, B, C and D. We wish to extract only A and B. Pole pairs C and D are to remain. The pole extraction process takes two directions in this case. In one direction the signal of pole pair C is isolated and corrected appropriately, and in the other the signal of pole pair D is treated likewise. The last step involves the addition of the corrected signals with pole pairs C and D. This approach is effective on a theoretical basis. The author has not exploited the method when dealing with measured waveforms.

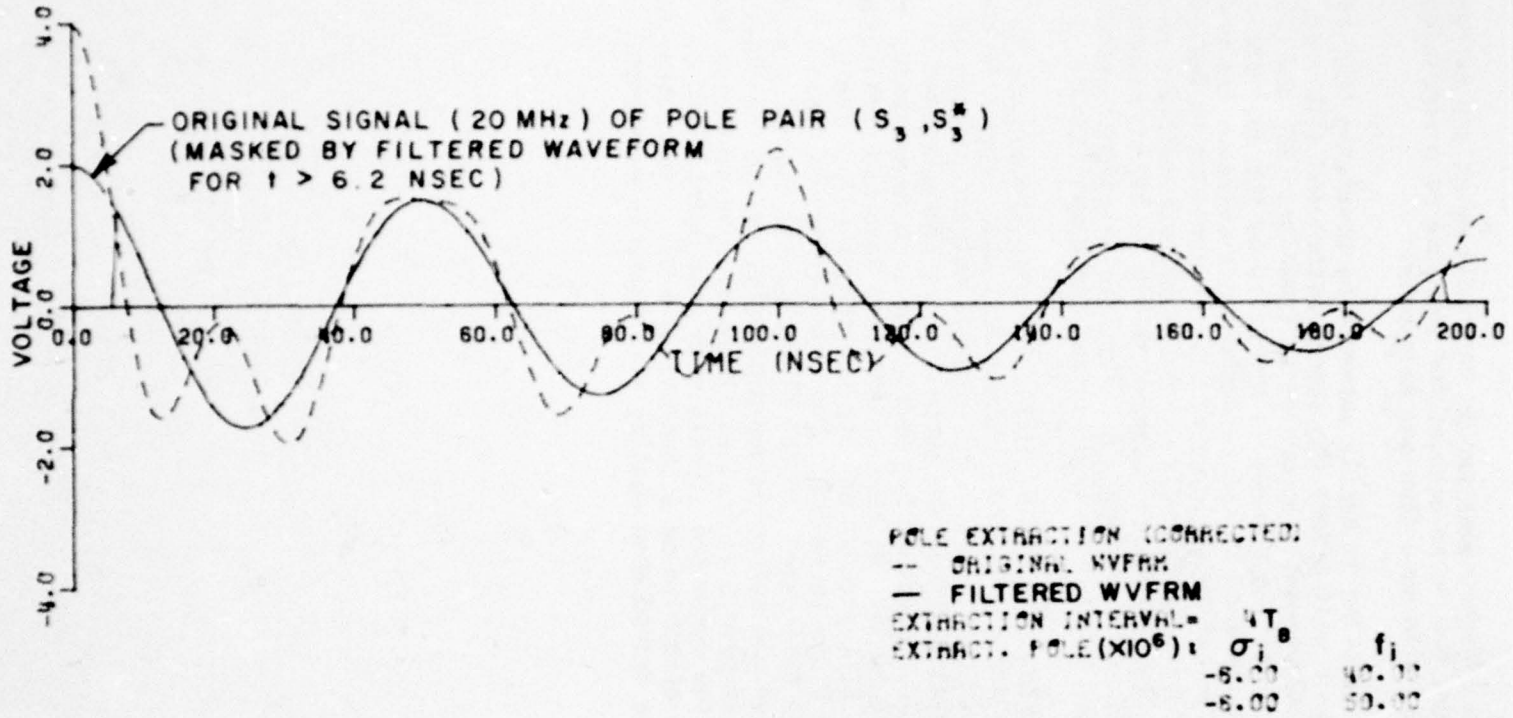

Figure 14. Pole extraction and correction involving multiple extracted pole pairs.

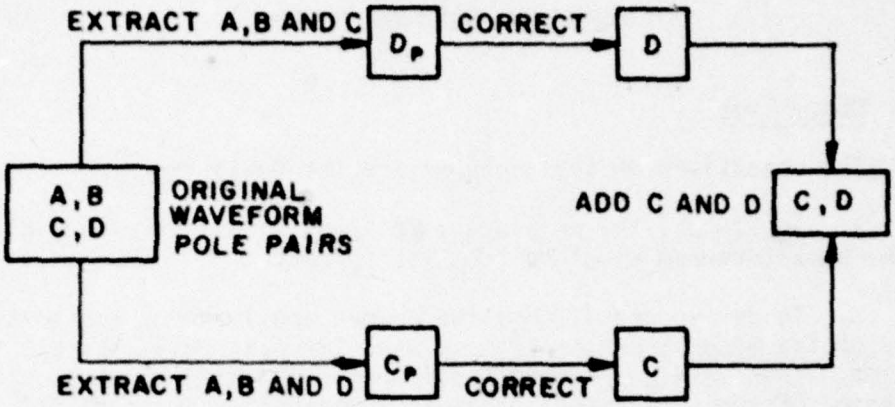

Figure 15. Pole extraction and correction with multiple extracted and remaining complex conjugate pole pairs.

CHAPTER III
THE RECONSTRUCTION PROCESS

A. Objectives

The objectives of this chapter are the following:

1. To discuss the problems associated with clutter and clipping in the backscattered waveform from the tunnel.

2. To derive and discuss the proper application, and advantages of the Reconstruction Process used for overcoming the clutter problem. This involves a simple difference equation which uses a portion of the late tunnel response to reconstruct its earlier time portion. A criterion for selecting this late portion of the tunnel response is also presented. For the sake of completeness the reconstruction process is generalized to reconstruct target responses characterized with more than one pole pair.

3. To apply the reconstruction process on measured tunnel responses. This is accomplished by first extracting the antenna pole pair and possibly other false target resonances. The character of the residual signal after the pole extraction process is classified and discussed for the correct and effective application of the reconstruction process (Figure 17). It will be indicated that the later time of the filtered waveform will contain the tunnel response exclusively, except for clutter and noise. Therefore, the portion of this, under a mean square error criterion, is chosen for reconstructing the tunnel response. Thus, we obtain a "clutter and noise free" tunnel response if we can indeed find such a window in the late tunnel response. The reconstructed tunnel response will be used later for estimating the tunnel depth.

B. The Clutter Problem

In the introduction it was noted that the early portion of the backscattered echoes were dominated by clutter. This is mainly due to ground reflections. Such clutter creates high voltage peaks which were clipped before processing by the recording oscilloscope. Typical tunnel backscattered echoes are shown in Figure 16. These were obtained from the tunnel site to be discussed in Chapter V. Their late time portion was found by Prony's method to contain two natural resonances or pole pairs (complex conjugate), one corresponding to the antenna and the other to the tunnel.

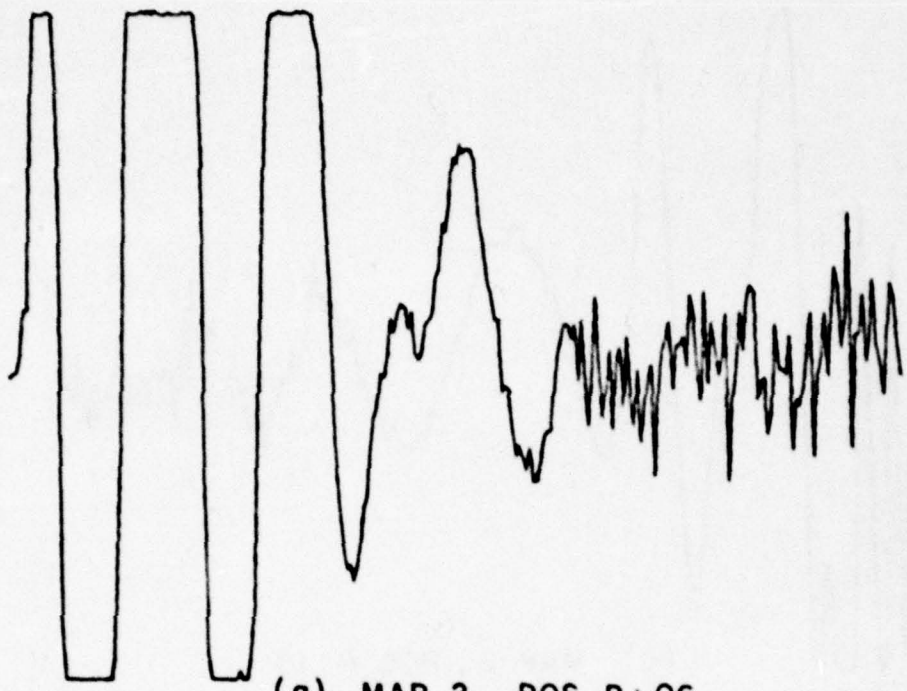

(a) MAP 2 , POS P : 06

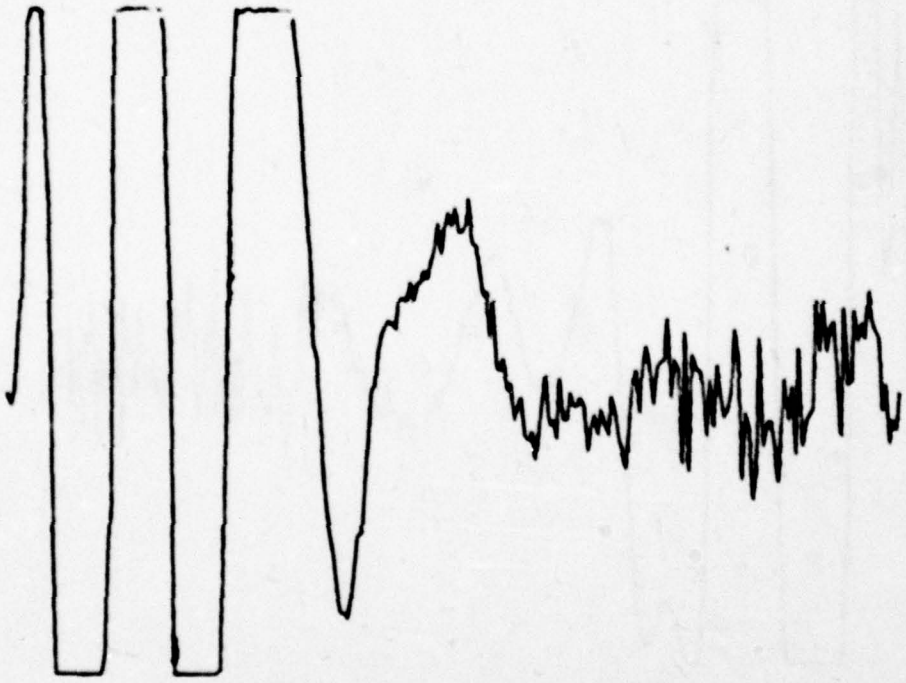

(b) MAP 2 , POS Q : 08

Figure 16. Examples of measured waveforms indicating clutter and clipping effects.

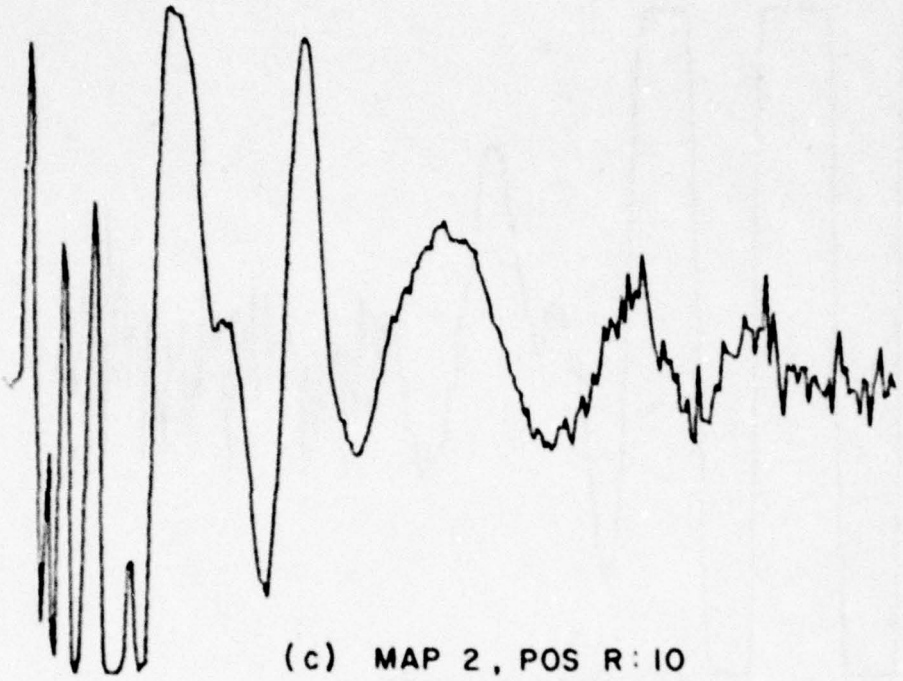

(c) MAP 2, POS R: 10

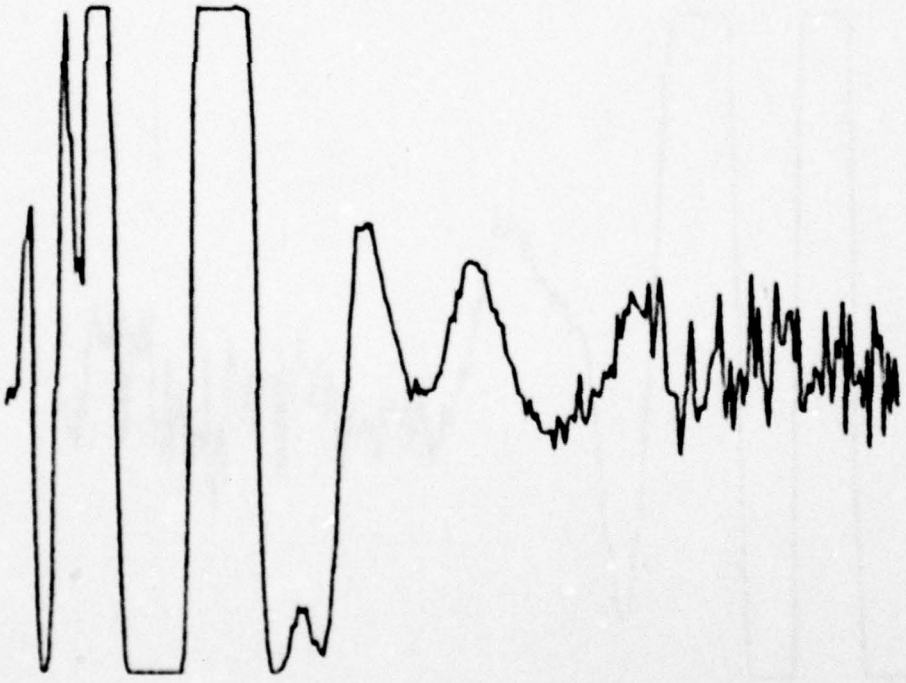

(d) MAP 2, POS S: 12

Figure 16. (Continued)

Appearance of clutter in the early portion of the recorded waveform disrupts useful information. The most important one is the arrival time of the tunnel response. Knowledge of this is essential since it will enable us to estimate the distance of the tunnel's top from the antenna. Furthermore, maps constructed from echoes of a set of measurements when the radar is placed above the tunnel become difficult to read and the region corresponding to the tunnel depth cannot be identified unless some previous knowledge about the depth is given. Basically, clutter is an undesired effect that contains no apparent useful data. In addition it disrupts the good data to follow.

Stapp [22] and a group at GEO-CENTERS, INC. attempted to construct maps without accounting for the clutter interference in the recorded waveforms. Their maps are confused and do not clearly contain the distinct tunnel behavior as a function of radar position when the radar data are used to develop a map. It is quite difficult to obtain precise information about the target using their maps.

C. Derivation of a Difference Equation for Reconstructing the Early Tunnel Response

A method is introduced here to overcome the clutter problem. It is used in conjunction with the pole extraction process and it will be referred to as Reconstruction Process. It is applied after ALL undesired poles (mainly the antenna pole pair) have been extracted from the original waveform. Thus, a "tunnel response alone" is obtained. The reconstruction process assumes that any information contained in the early portion of the recorded waveform cannot be extracted. Therefore, it is discarded. In consequence the late tunnel response is used to reconstruct its early response based on the knowledge of the tunnel pole pair as determined by Prony's method. This is accomplished by applying a difference equation to predict early points from later ones. The derivation of the difference equation used for reconstruction will now follow:

Let us assume an original echo consisting of m_o+2 complex poles. The two correspond to the tunnel pole pair and the other m_o are undesired. After their removal, the z-transform of the filtered waveform (it was noted at the end of the last chapter that all filtered waveforms are assumed to be corrected according to Equation (34). The reconstruction process has no usefulness unless the filtered waveform is corrected before reconstruction) can be expressed as

$$R_c(z) = \frac{a_0+a_1z^{-1}}{1-2\mathrm{Re}(z_1)z^{-1}+|z_1|^2z^{-2}} \qquad (35)$$

where (z_1, z_1^*) is the remaining tunnel pole pair. Multiplying both sides of Equation (35) by the denominator of the fraction on the right hand side gives

$$(1-2\mathrm{Re}(z_1)z^{-1}+|z_1|^2z^{-2})R_c(z) = a_0+a_1z^{-1} \quad . \tag{36}$$

The right hand side of Equation (36) is a first degree polynomial in z^{-1}. Thus it can be expressed as

$$(1-2\mathrm{Re}(z_1)z^{-1}+|z_1|^2z^{-2})R_c(z)=A(z) \quad . \tag{37}$$

Transforming Equation (37) to a discrete time function, we obtain

$$r_c(nT_r+kT_B) - 2\mathrm{Re}(z_1)r_c(nT_r+kT_B-T_r)+$$

$$|z_1|^2r_c(nT_r+kT_B-2T_r) = r_A(nT_r+kT_B) \quad ; \quad k=0,1,\ldots,N_r-1, \quad n=0,1,\ldots \tag{38}$$

where $r_A(nT_r) = \mathcal{Z}^{-1}[A(z)]$. Note that T_r again is not the basic sampling interval of the original waveform, T_B. It is a multiple of T_B, i.e.,

$$T_r = N_rT_B \quad . \tag{39}$$

The important observation to be made in Equation (38) is that:

$$r_A(nT_r)=0 \qquad \text{for } n \geq 2 \quad . \tag{40}$$

Therefore,

$$r_c(nT_r+kT_B)-2\mathrm{Re}(z_1)r_c(nT_r+kT_B-T_r)+|z_1|^2r_c(nT_r+kT_B-2T_r)=0;$$

$$n \geq 2, \quad k=0,1,\ldots,N_r-1 \quad . \tag{41}$$

Rearranging the above equation, gives

$$r_c(nT_r+kT_B-2T_r)= \frac{2Re(z_1)}{|z_1|^2}\, r_c(nT_r+kT_B-T_r)- \frac{1}{|z_1|^2}\, r_c(nT_r+kT_B);$$

$$n \geq 2, \quad k=0,1,\ldots,N_r-1. \qquad (42)$$

This equation can predict an early point based on the knowledge of two later points and the (tunnel) pole pair associated with the portion of the waveform to be reconstructed. The equation is only good when applied in the region where the tunnel pole pair is correctly described. Therefore, it is true for the region

$$nT_r \geq t_c+m_eN_eT_B+2T_r \qquad (43)$$

where t_c represents the starting time of the portion of the waveform associated with the desired target, i.e., the tunnel as shall be discussed later in detail. As before N_eT_B is the extraction interval used when extracting the m_e undesired complex poles. The term $m_eN_eT_B$ accounts for the error region due to clutter and clipping. These points are better illustrated in Figure 17. There, the antenna pole pair [-27. Meganepers/sec $\pm$ j2πx45.5 Megarad/sec] of the echo in Figure 16(b) is extracted. The respective regions are indicated on the graph. The late portion of the filtered waveform contains the scattered field from the target (tunnel) almost exclusively. There are, of course, other signals that could be present, caused by clutter and other scatterers if their resonances are within the radar bandwidth. In this case the poles of these scatterers (false targets) must be removed by the extraction process as was done with the antenna pole pair for obtaining the target response exclusively.

Note that in Equation (42) newly generated sample points can be used for reconstructing earlier ones. Therefore, only an initial "errorless" time window of length $2N_rT_B$ is needed for the reconstruction process to begin. In practice (see Figure 17) we actually never encounter an "errorless" time window. For this case we strive to choose the window that best describes the tunnel pole pair calculated by Prony's method. This is the subject of the next section. The implementation of Equation (42) is similar to that shown in Figure 3, except that reconstructed samples are used for the region out of the chosen initial time window.

Furthermore, it is essential to realize that Equation (42) does not assume the presence of any dc term in the filtered waveform. It is imperative then that any dc is removed before the process is applied.

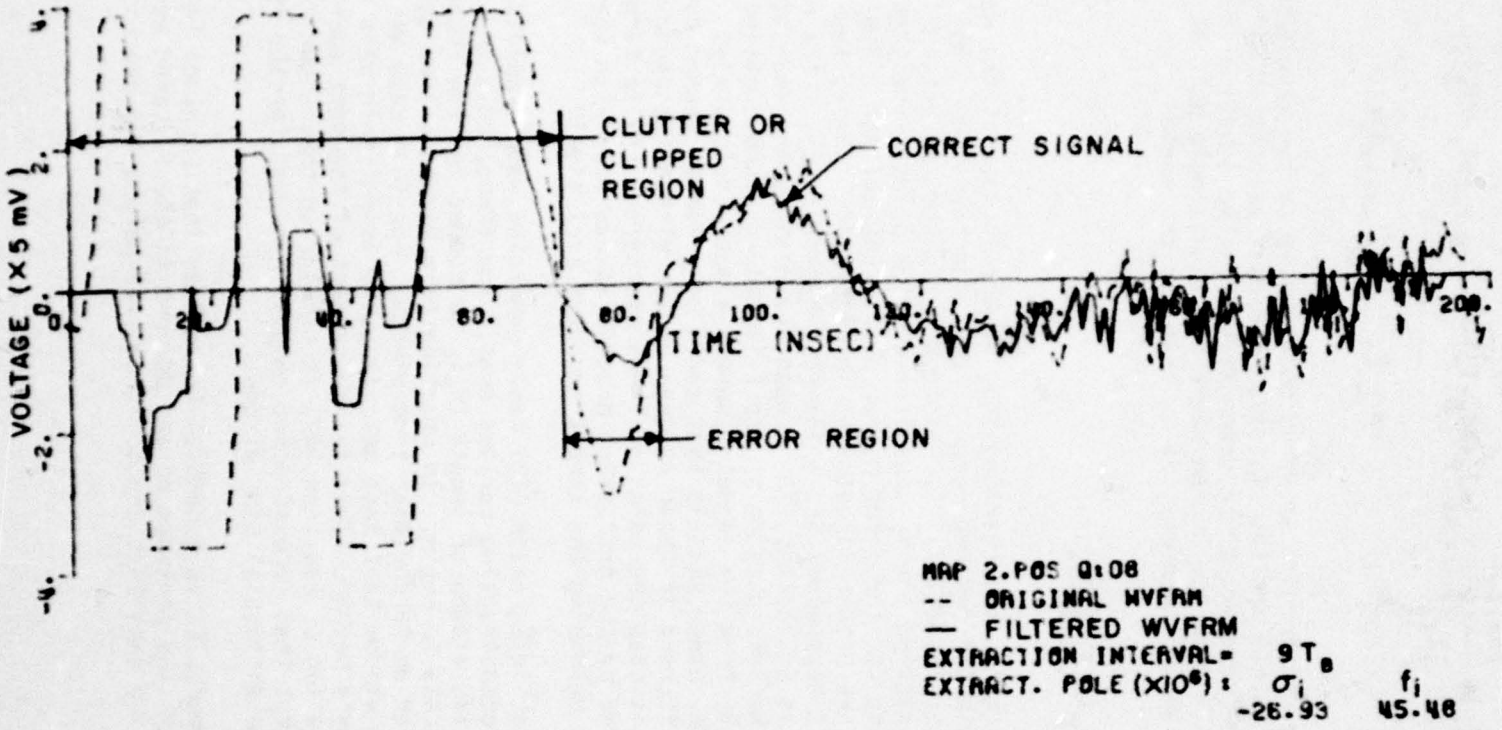

Figure 17. Pole extraction involving clutter and clipping in the early portion of the original waveform.

D. Error Criterion for Selecting the Base Time Window

The problem to be encountered now is the selection of the initial (base) time window to be used for reconstruction. The criterion for such a decision was chosen so that the first reconstructed points must best fit the filtered waveform. In this case the reconstruction process is applied by using different base windows. Actually, the portion of the filtered waveform beyond the clutter region is scanned by shifting the base window from right to left by T_B. For each base window used, an error, e_r, is calculated as

$$e_r = \frac{\sum_{i=257-N_s-k}^{256-N_s} \left[r_c(iT_B) - r_r(iT_B) \right]^2}{k} , \qquad (44)$$

where $r_c(iT_B)$ is the filtered waveform, $r_r(iT_B)$ is the reconstructed waveform, N_s is the reconstruction starting point, counted from the end of the waveform, and k is the number of first reconstructed points that e_r will be based upon. The waveforms are assumed to be 256 points long. As seen, e_r is an average square error between the filtered and reconstructed waveforms. When scanning is completed, the window with the smallest e_r is chosen as the base for reconstruction. Other error criteria are possible. This criterion will be used for selecting the proper or best base window to predict the early target response. Experience has proven it to be effective. It should be understood that the reconstructed tunnel response is only true up to the arrival time of the actual tunnel response. The reconstructed section previous to this time is just ficticious, but it will be found important for evaluating more precisely the distance to the target. A theoretical study in the next chapter demonstrates that the first zero crossing of the reconstructed waveform after its deviation from the filtered corresponds well to the target (tunnel) - antenna distance.

E. A Discussion on the Reconstruction Interval, T_r

Another important aspect to be examined is the reconstruction interval. It must always satisfy the Nyquist criterion for the tunnel pole pair to be reconstructed. It does not play as important a role as the pole extraction interval. T_r should never be too small, for example equal to T_B. Then, the process may fail. It will attempt to reconstruct noise since it is within its frequency band. An example is shown in Figure 18. Here the filtered waveform

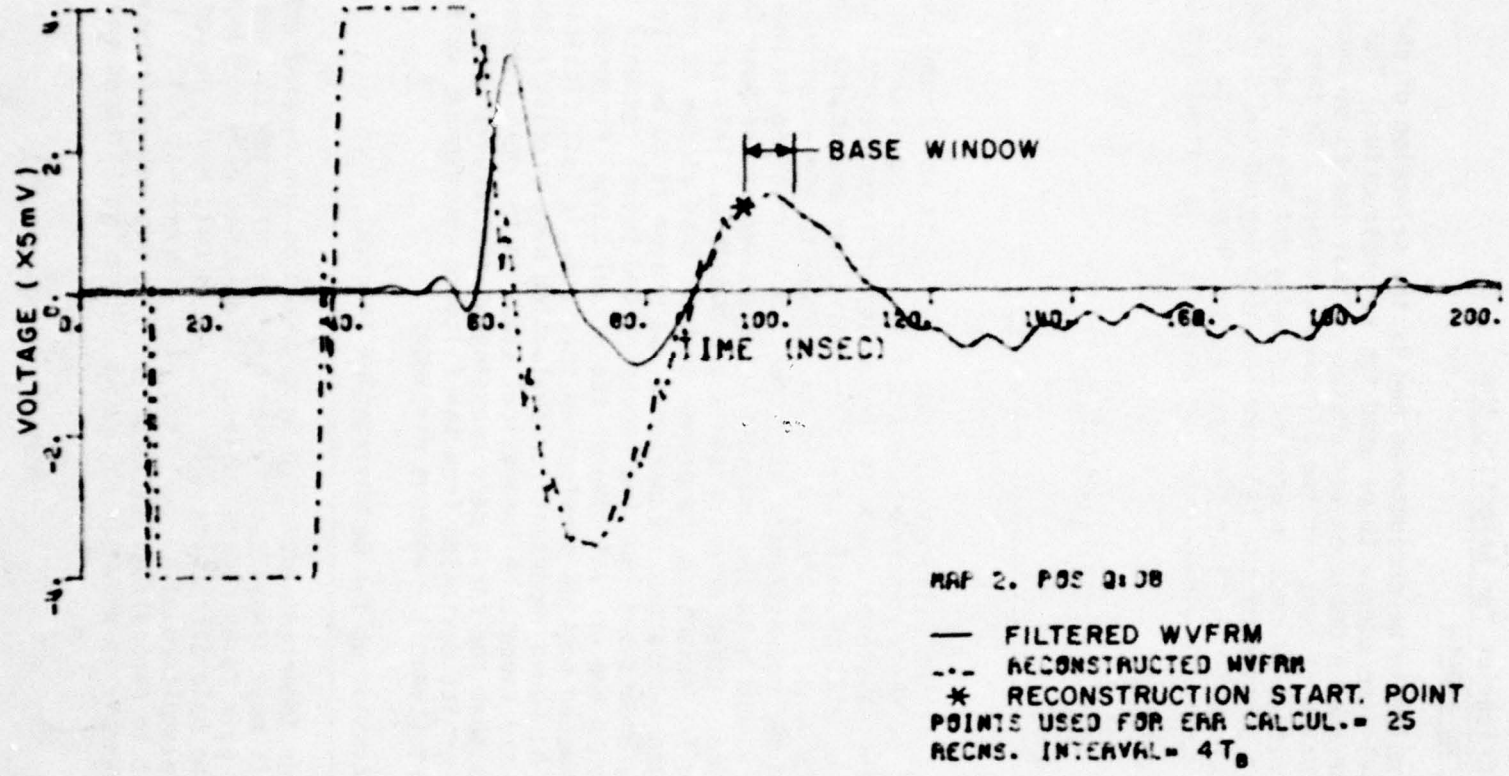

Figure 18. Example of the reconstruction process when using a small T_r.

in Figure 17 is reconstructed after bandpass filtering through a trapezoidal filter with corners at 5,100 and 175 MHz. This filtering removed any dc term and high frequency components. The chosen T_r was small ($4T_B$) as compared to the tunnel pole pair [-38. Meganepers/sec $\pm$ j2πx19.37 Megarad/sec] Nyquist interval. It is seen that some noise is carried along in the reconstructed section.

A reconstruction interval close to that required by the Nyquist criterion for the tunnel natural resonance is usually best. But this may require a long base window. Such a window, within which the tunnel pole pair is described correctly, is usually not available. For example, a pole pair at 20 MHz has a Nyquist interval of $25T_B$ (T_B=200/255 nsec). A base window of about $50T_B$ would then be needed. It was found, the interval used by Prony's method for calculating the natural resonances (poles) works well for the pole extraction and reconstruction processes. This interval was used for reconstructing the filtered waveform in Figure 17. The result is shown in Figure 19. Comparing Figures 18 and 19 we see that use of a larger reconstruction interval (N_r=9) reduces the reconstruction of noise. Therefore, T_r can be effectively used for filtering out undesired high frequency components.

The reconstructed waveforms are calculated by the computer subroutine given in Appendix D. Another example of the process is shown in Figure 20. The filtered waveform is the result after the extraction of the antenna pole pair [-43.6 Meganepers/sec $\pm$ j2πx69.0 Megarad/sec] of the echo in Figure 16(c). It was also filtered by the trapezoidal filter discussed previously. The reconstructed tunnel pole pair was located at [-42.6 Meganepers/sec $\pm$ j2πx21.9 Megarad/sec].

F. Generalization of the Reconstruction Process

The reconstruction process as given in Equation (42) can only reconstruct one pole pair. The antenna pole pair and all false target resonances must first be extracted before its application. Therefore, Equation (42) can only be used to reconstruct a target response consisting of only one natural resonance (tunnel). Most targets are characterized by more than one pole pair. For the sake of completeness we will just derive the difference equation used for reconstructing target responses containing more than one resonance.

Let us, for example assume a target response characterized by two pole pairs (complex conjugate). After the removal of the antenna pole pair and other false target resonances from its backscattered response then we wish to reconstruct the early target response for determining its depth. In this case Equation (42) must be modified to reconstruct two pole pairs, (z_1,z_1^*) and (z_2,z_2^*). This can be accomplished in a similar way to that used for deriving Equation (42).

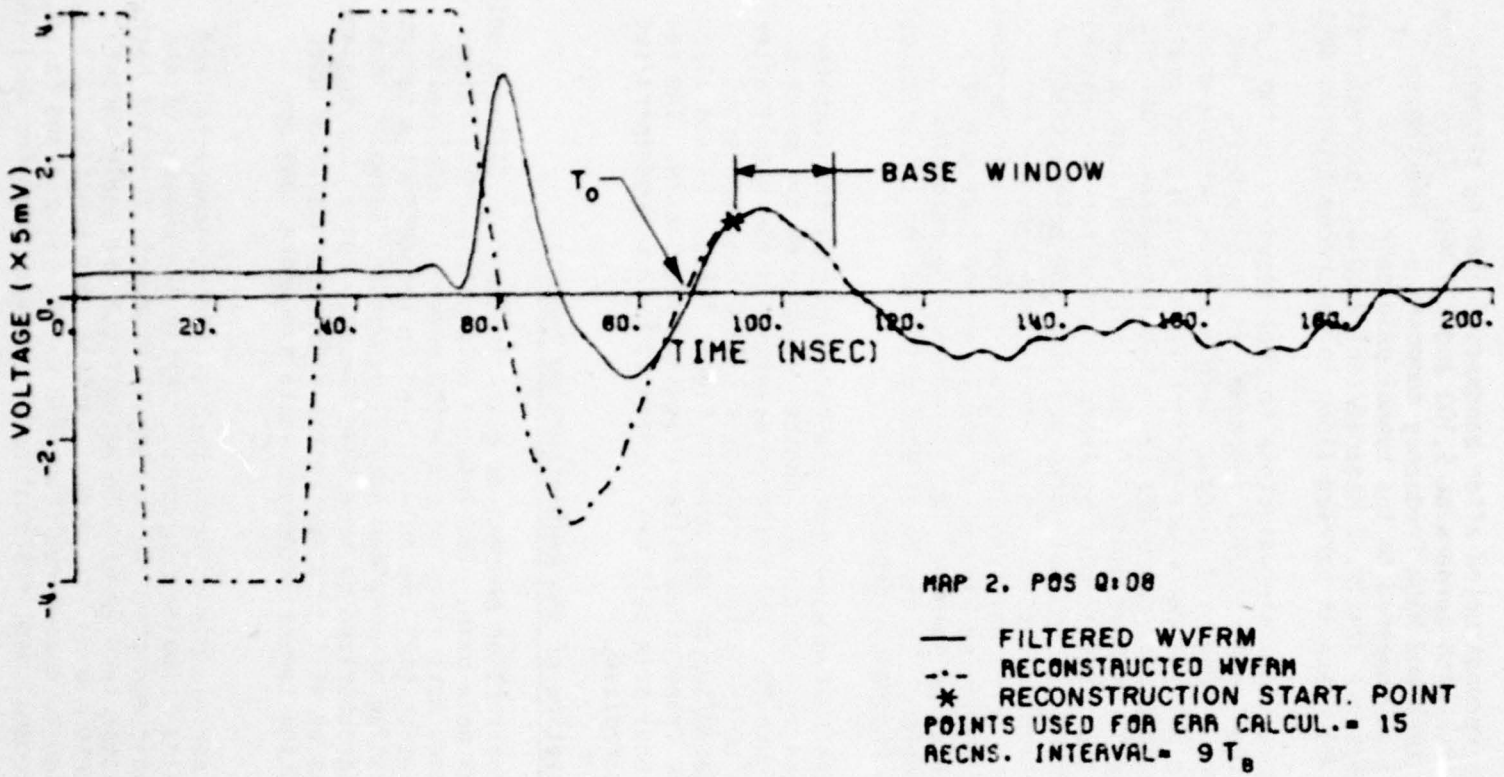

Figure 19. Example of the reconstruction process when using the same interval as was used to evaluate the natural resonance.

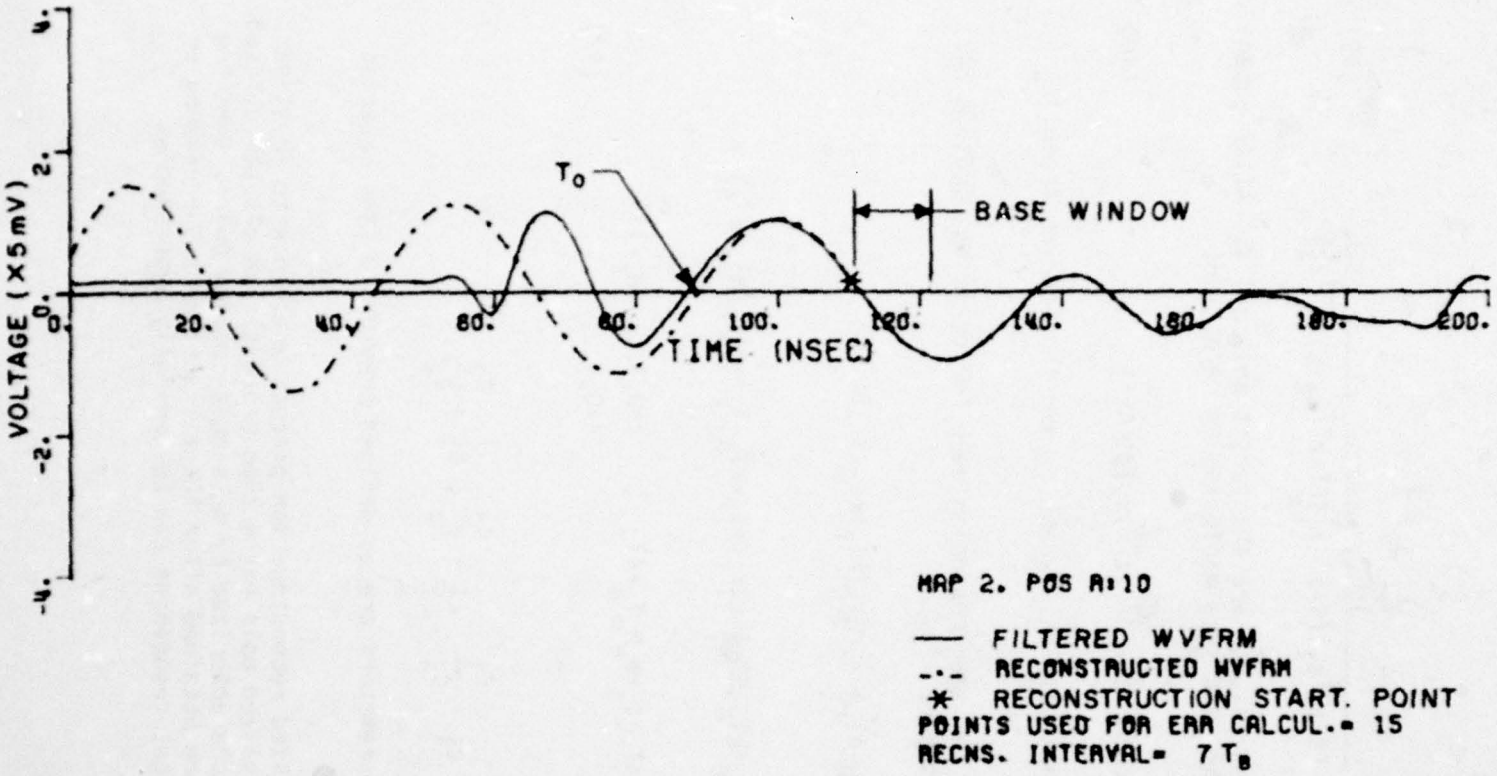

Figure 20. Another example of the reconstruction process.

The $\mathcal{Z}$-transform of the filtered waveform (in its late portion) can be given as

$$R_c(z) = \frac{\sum_{j=0}^{3} a_j z^{-j}}{(1-z^{-1}z_1)(1-z^{-1}z_1^*)(1-z^{-1}z_2)(1-z^{-1}z_2^*)} \qquad (45)$$

where (z_1, z_1^*) and (z_2, z_2^*) are the target pole pairs. After expansion of the denominator and some manipulation we obtain,

$$(1-c_1z^{-1}+c_2z^{-2}-c_3z^{-3}+c_4z^{-4})R_c(z)=A(z) \qquad (46)$$

where the constants c_1, c_2, c_3 and c_4 are the same as those in Equation (15).

Following the same reasoning used for deriving Equation (42) we can finally arrive at

$$r_c(nT_r+kT_B-4T_r) = c_3'r_c(nT_r+kT_B-3T_r)-$$

$$c_2'r_c(nT_r+kT_B-2T_r)+c_1'r_c(nT_r+kT_B-T_r)-c_0'r_c(nT_r+kT_B) \; ;$$

$$nT_r \geq t_c+m_eN_eT_B+4T_r \quad , \quad \begin{matrix} k=0,1,\ldots,N_r-1 \\ n=0,1,\ldots \end{matrix} \qquad (47)$$

where

$$c_0' = \frac{1}{c_4} \; , \; c_1' = \frac{c_1}{c_4} \; , \; c_2' = \frac{c_2}{c_4} \; , \; c_3' = \frac{c_3}{c_4}$$

and all other parameters are as defined previously (see Equation (43)).

A generalized reconstruction process analogous to Equation (18) (the generalized pole extraction process) can also be derived. If a target is characterized by m_e single complex poles, then the filtered waveform obtained after the extraction of the antenna or other false target resonances can be generally expressed as

$$R_c(z) = \frac{\sum_{j=0}^{m_r-1} a_j z^{-j}}{\prod_{i=1}^{m_r} (1-z_i z^{-1})} \qquad (48)$$

where z_i represents the target (single) complex poles.

According to the previously outlined procedure, after manipulating Equation (48) we can arrive at the following generalized reconstruction process:

$$-r_c(nT_r+kT_B-m_rT_r) = \frac{1}{c_{m_r}} r_c(nT_r+kT_B) + \frac{(-1)^1}{c_{m_r}} \sum_{\ell_1=1}^{m_r} z_{\ell_1} r(nT_e+kT_B-T_r)$$

$$+ \frac{(-1)^2}{c_{m_r}} \sum_{\ell_1=1}^{m_r} \sum_{\substack{\ell_2=1 \\ \ell_1\neq\ell_2}}^{m_r} z_{\ell_1} z_{\ell_2} r(nT_r+kT_B-2T_r)$$

$$\vdots$$

$$+ \frac{(-1)^i}{c_{m_r}} \sum_{\substack{\ell_1,\ell_2,\ldots\ell_i \\ \ell_1\neq\ell_2\neq\ldots\neq\ell_i}}^{m_r} z_{\ell_1} z_{\ell_2} \ldots z_{\ell_i} r(nT_r+kT_B-iT_r)$$

$$\vdots$$

$$+ \frac{(-1)^{m_r-1}}{c_{m_r}} \sum_{\substack{\ell_1,\ell_2,\ldots,\ell_{m_r-1} \\ \ell_1\neq\ell_2\neq\ldots\neq\ell_{m_r-1}}}^{m_r} z_{\ell_1} z_{\ell_2} \ldots z_{m_r-1} r(nT_r+kT_B-(m_r-1)T_r);$$

$$nT_r \geq t_c+m_eN_eT_B+m_rT_r \quad , \quad \begin{matrix} k=0,1,\ldots,N_r-1 \\ n=0,1,\ldots \end{matrix} \qquad (49)$$

where

$$c_{m_r} = \sum_{\substack{\ell_1,\ell_2,\ldots,\ell_{m_r} \\ \ell_1 \neq \ell_2 \neq \ldots \neq \ell_{m_r}}}^{m_r} z_{\ell_1} z_{\ell_2} z_{\ell_3} \ldots z_{\ell_{m_r}} \quad .$$

Also, note again that in the above equation m_r does not represent the target's complex conjugate pole pairs but just its single poles which are twice in number than the complex conjugate pole pairs.

As a check one can easily derive Equations (42) and (47) from the generalized Equation (49). It should be understood that concurrent reconstruction of a large number of poles is impractical since it requires a large base window for the process to begin. Also, note that any dc term must be removed before applying Equation (49).

G. Assets of the Reconstruction Process

The reconstruction process is an important part of the tunnel identification. It accomplishes three tasks:

1. The clutter problem is solved as long as it appears in the early portion of the echo (it usually is). Exact knowledge of the tunnel response is not needed. Only a small window with fair accuracy is required so the true tunnel response can be isolated. The reconstruction process will predict the rest of the waveform based on this window.

2. Most of the times the later portion of the received echo is not noise or clutter free. Based on the error criterion in Equation (44) the reconstruction process can detect the window which best describes the tunnel pole pair. Consequently, a more accurate early time response can be derived. Equation (44) is minimized when uniformity occurs in the base window. If noise or clutter is present in the base window under testing the predictability of the reconstruction process is disrupted. This causes an error increase. Note, also, that use of the error criterion satisfies Equation (43).

3. In the next chapter it will be demonstrated that the reconstructed waveform can play a very important role in the identification process. A comparison of the filtered and reconstructed waveforms can give us a very good estimate of the tunnel's response arrival time. Thus, its distance from the antenna can be estimated. In turn, mapping can present a complete picture of the tunnel's depth, structure and relative position.

In the next chapter a simple experimental model of the Radar-Tunnel Structure is examined. The study uses the pole extraction and reconstruction processes in order to extract information from the theoretical echoes and determine the limitations involved. In Chapter V the results of the model are used and a study on measured echoes is pursued.

CHAPTER IV
STUDY OF A SIMPLE TRANSMISSION LINE MODEL OF AN UNDERGROUND RADAR-TUNNEL STRUCTURE

A. Objectives

The goals of this chapter are the following:

1. To present a physical and mathematical study of a transmission line model which approximates the actual tunnel scattering behavior.

2. To relate the model to the actual radar-tunnel structure and derive methods to extract information from the theoretical echoes. These methods can then be used when dealing with measured echoes.

3. To demonstrate the role and significance of the pole extraction and reconstruction processes to be used in the identification process.

B. The Model

We are attempting to construct an experimental model of the Radar-Tunnel structure to study and extract information from the received backscattered echoes. This will help us to analyze the measured responses.

The input to the antenna must, of course, have a wide spectrum to ensure excitation of the tunnel's natural resonances. It is unfortunate though, that this is not easily achieved since the dipole antenna is in itself a resonant structure. If the input has a wide spectrum, say a gaussian pulse, the antenna will act as a filter. For excitation the tunnel's natural resonance must occur close to the antenna's resonance.

Since the target and the antenna are both resonant structures, they can be modeled as low-Q analog filters. Such can be a simple RLC circuit shown in Figure 21. The impedance, Z, of the network is given by

$$Z(s=j\omega) = \frac{s^2/C}{s^2+s/RC+1/LC} \quad . \tag{50}$$

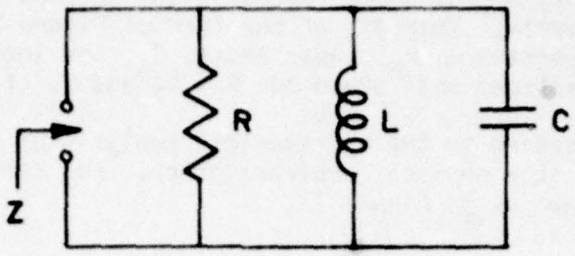

Figure 21. Simple RLC network.

The poles of Z are located at

$$s, s^* = -\frac{1}{2RC} \pm j\sqrt{\frac{1}{LC} - \left(\frac{1}{2RC}\right)^2} \quad \text{(rad)} \quad . \tag{51}$$

The theoretical model can then be constructed of two RLC networks separated by a lossy transmission line of characteristic impedance $Z_o(\omega)$. The transmission line is introduced to simulate ground medium to some degree.

The input to the system will be a gaussian pulse generator (wide spectrum) of internal resistance R_s as shown in Figure 22.

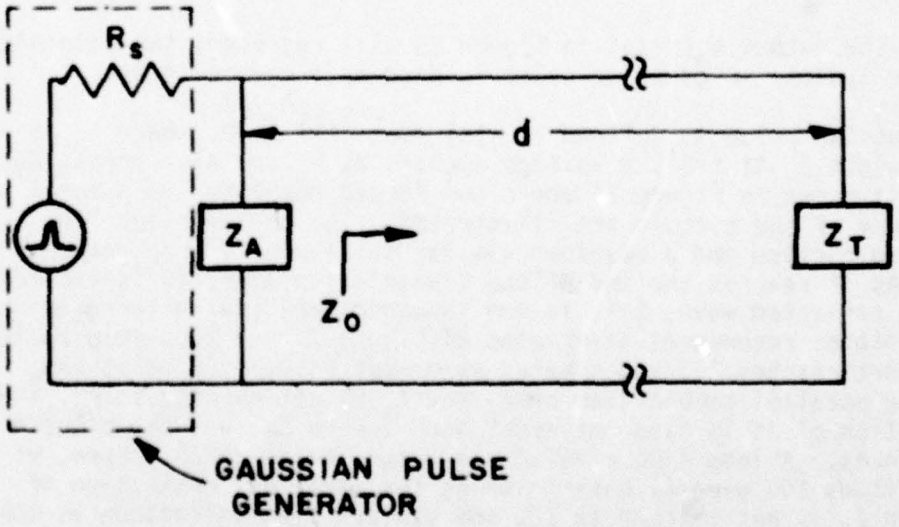

Figure 22. Transmission line model.

Impedances Z_A and Z_T of the model represent the antenna and target (tunnel), respectively. They are of the form of Figure 22. Z_A will consist of resistance, R_A, capacitance, C_A, and inductance, L_A. Similar definitions will stand for R_T, C_T and L_T of Z_T.

Before proceeding to the mathematical analysis of the model, let us first give it a physical interpretation. For convenience the model is redrawn as in Figure 23.

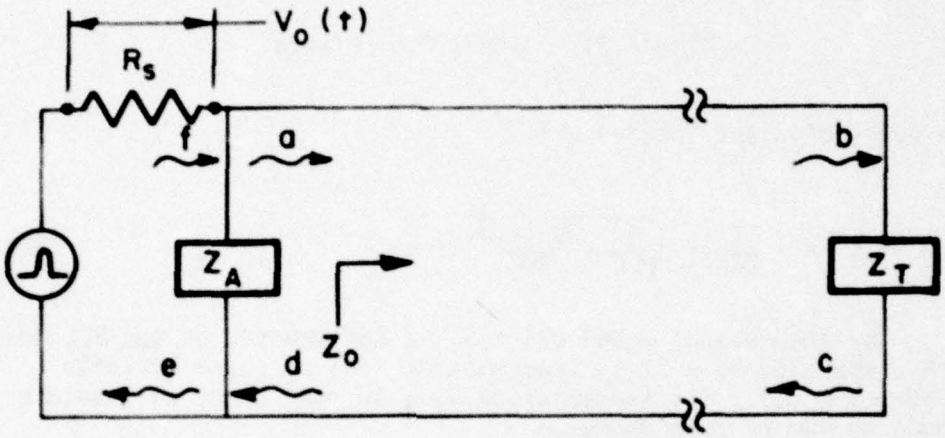

Figure 23. Transmission line model indicating wave propagation.

The output $V_0(s=j\omega)$ in Figure 23 will represent the response of the system. A gaussian pulse is used as a source at t=0. (A gaussian pulse is defined as $g(t) = e^{-(5.5t^2)/t_p^2}$, where t_p is its time width.) At $t=0^+$, a voltage appears at R_s and also across Z_A,(a). This is shown in Figure 24 where the forced response and natural response of the circuit are illustrated. The transmission line is also excited and a waveform similar to Figure 24 propagates toward Z_T. As it reaches the end of the transmission line, Z_T is excited and a reflected wave, (c), is now launched back toward the generator. It contains resonances associated with both Z_A and Z_T. This reflected waveform reaches Z_A, and creates an output voltage ($V_0(s)$), (e). If the parallel combination of R_s and Z_A is not matched to Z_0, then a portion of it is also reflected back toward Z_T, and the process continues. A long time waveform is shown in Figure 25. Here, we will study the general case in which the parallel combination of R_s and Z_A is not matched to Z_0, and discuss its limitations as the transmission line becomes short.

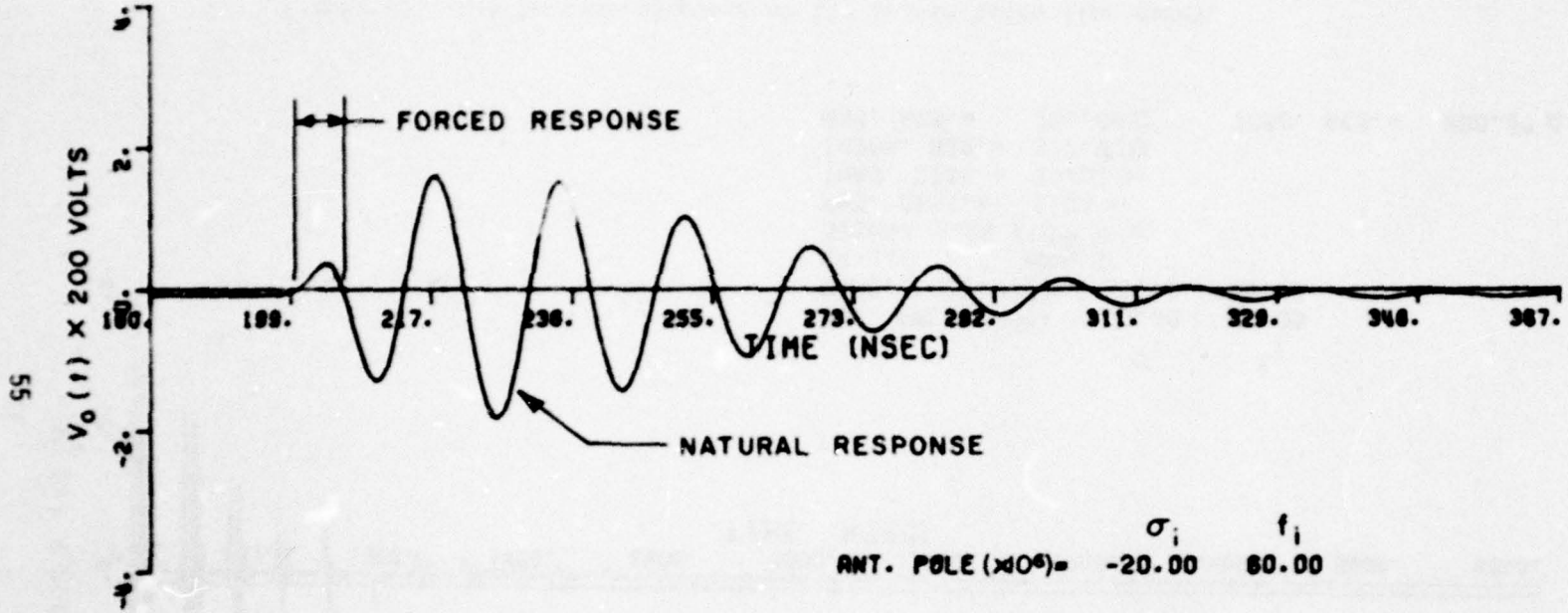

Figure 24. Response of an RLC resonant network to a Gaussian input pulse.

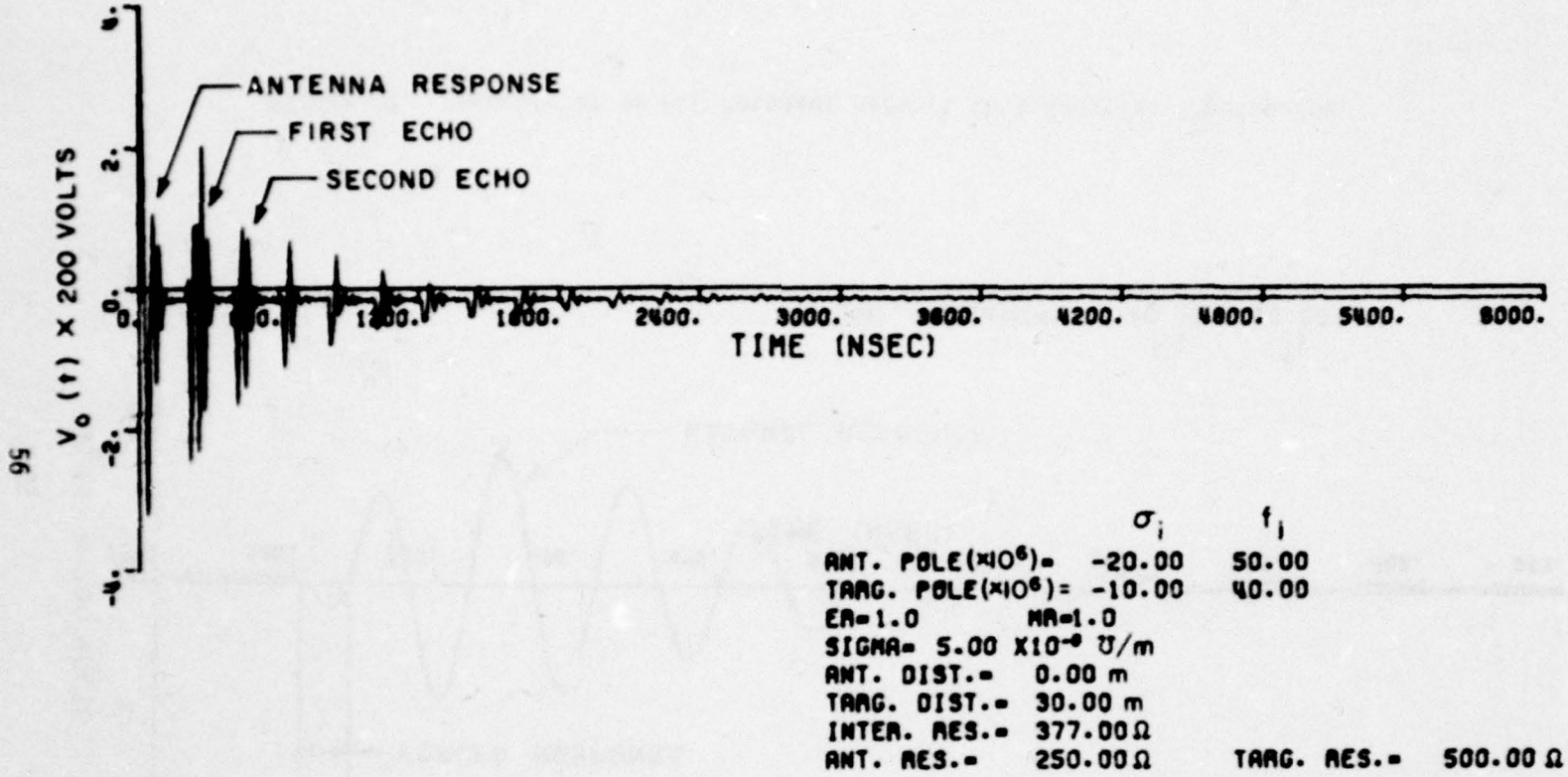

Figure 25. Finite time response of the transmission line model.

Our goal is to isolate the resonances associated with Z_T and to evaluate the length of the transmission line. The procedures introduced in the first three chapters are applied to isolate the desired parameters.

Since we already know them precisely, we can then better understand the limitation of our techniques when applied to unknown systems, such as a tunnel. Observe that the data will be corrupted by the presence of whatever parameters are used. One set of parameters is studied here in detail, but results for various other parameters are given in Appendix E.

C. Mathematical Analysis of the Model

A quantitative description of the transmission line model will now follow.

The method of analysis pursued in this study involves transforming the gaussian pulse (generator output) to the frequency domain, evaluating $V_o(j\omega)$ and then inverse transforming it to the time domain, $(v_o(t))$.

Two approaches will be used and compared for calculating the system's response of Figure 23. The first follows the actual physical multiple reflection process just described and transforms the desired voltage to time domain after each reflection. The second obtains the complete solution in the frequency domain and transforms the total voltage to time domain. The approaches are equivalent and both are used here to ensure that no computational errors are generated.

Defining the input as a gaussian pulse of spectrum $G(s=j\omega)$, the propagation constant as $\gamma=\alpha+j\beta$, and reflection and transmission coefficients as

$$\tau_v(s) = \frac{Z_{Ao}}{Z_{Ao}+R_s} \tag{52a}$$

$$\rho_A(s) = \frac{Z_{As}-Z_o}{Z_{As}-Z_o} \tag{52b}$$

$$\tau_A(s) = \frac{2\ Z_{As}}{Z_{As}+Z_o} \tag{52c}$$

$$\rho_T(s) = \frac{Z_T-Z_o}{Z_T+Z_o} \tag{52d}$$

where

$$Z_{Ao} = \frac{Z_A Z_o}{Z_A + Z_o}$$

and

$$Z_{As} = \frac{R_s Z_A}{R_s + Z_A} \quad ,$$

the voltage at the indicated points in Figure 23 can be expressed as follows:

$$V_a(s) = G(s)\ \tau_v(s) \tag{53a}$$

$$V_b(s) = G(s)\ \tau_v(s) \tag{53b}$$

$$V_c(s) = G(s)\ \tau_v(s)\ \rho_T(s)\ e^{-\gamma d} \tag{53c}$$

$$V_d(s) = G(s)\ \tau_v(s)\ \rho_T(s)\ e^{-2\gamma d} \tag{53d}$$

$$V_e(s) = G(s)\ \tau_v(s)\ \rho_T(s)\ \tau_A(s)\ e^{-2\gamma d} \tag{53e}$$

$V_e(s)$ is the first echo seen across Z_A. Consequently, the first echo across R_s can be expressed as

$$V_{1st}(s) = G(s) - V_e(s) \approx - V_e(s). \tag{54}$$

It appears after a time delay of

$$t = \frac{2d}{Im(\gamma)}$$

or

$$t = 2d\sqrt{\epsilon\mu} = 6.667\ d\sqrt{\epsilon_r \mu_r}\ \ (\text{nsec}) \tag{55}$$

for lossless media. d is in meters, and ϵ_r and μ_r are the relative permittivity and permeability of the medium, respectively.

The second echo across R_s will be delayed by 13.333 $d\sqrt{\epsilon_r \mu_r}$ nsec. According to the above analysis it is given by

$$V_{2nd}(s) = \left[1-\tau_v(s)\ \rho_T(s)\ \tau_A(s)\ e^{-4\gamma d}\right] G(j\omega) \quad . \tag{56}$$

The continuous time voltage seen across R_s is the sum of all the echoes, i.e.,

$$V_o(s) = V_{1st}(s) + V_{2nd}(s) + V_{3rd}(s) + \ldots \quad . \tag{57}$$

In obtaining the frequency response of $V_o(j\omega)$ we substitute for Z_A and Z_T in Equations (52). After some simple manipulation we have:

$$\tau_v(s) = \frac{s/C_A R_s}{s^2 + \frac{s}{C_A}\left(\frac{1}{R_A} + \frac{1}{R_s} + \frac{1}{Z_o}\right) + \frac{1}{L_A C_A}} \tag{58a}$$

$$\rho_A(s) = -\frac{s^2 + \frac{s}{C_A}\left(\frac{1}{R_s} + \frac{1}{R_A} - \frac{1}{Z_o}\right) + \frac{1}{L_A C_A}}{s^2 + \frac{s}{C_A}\left(\frac{1}{R_s} + \frac{1}{R_A} + \frac{1}{Z_o}\right) + \frac{1}{L_A C_A}} \tag{58b}$$

$$\tau_A(s) = \frac{s^2 + \frac{s}{C_A}\left(\frac{1}{R_s} + \frac{1}{R_A}\right) + \frac{1}{L_A C_A}}{s^2 + \frac{s}{C_A}\left(\frac{1}{R_s} + \frac{1}{Z_o} + \frac{1}{R_A}\right) + \frac{1}{L_A C_A}} \tag{58c}$$

$$\rho_T(s) = -\frac{s^2 + \frac{s}{C_T}\left(\frac{1}{R_T} - \frac{1}{Z_o}\right) + \frac{1}{L_T C_T}}{s^2 + \frac{s}{C_T}\left(\frac{1}{R_T} + \frac{1}{Z_o}\right) + \frac{1}{L_T C_T}} \tag{58d}$$

The poles of $\tau_v(s)$, $\rho_A(s)$ and $\tau_A(s)$ are located at

$$s_{A'}, s_{A'}^* = -\frac{1}{2R_A' C_A} \pm j\sqrt{\frac{1}{L_A C_A} - \left(\frac{1}{2R_A' C_A}\right)^2} \tag{59}$$

where

$$\frac{1}{R'_A} = \frac{1}{Z_o} + \frac{1}{R_A} + \frac{1}{R_s}$$

and the poles of $\rho_T(s)$ at

$$s_{T_1}, s^*_{T_1} = -\frac{1}{2R'_T C_T} \pm j\sqrt{\frac{1}{L_T C_T} - \left(\frac{1}{2R'_T C_T}\right)^2} \qquad (60)$$

where

$$\frac{1}{R'_T} = \frac{1}{Z_o} + \frac{1}{R_T} \quad .$$

The imaginary parts of Equations (59) and (60) correspond to the complex resonances of the coefficients of Equations (52).

Furthermore, if

$$\frac{1}{L_A C_A} >> \left(\frac{1}{2R'_A C_A}\right)^2 \text{ and } \frac{1}{L_T C_T} >> \left(\frac{1}{2R'_T C_T}\right)^2 \qquad (61)$$

then the complex resonances of the coefficients will be approximately equal to the natural resonances of Z_A and Z_T, as defined in Equation (51). If Equation (61) is not satisfied then the resonances of the coefficients will deviate from the actual ones of the target or the antenna, and the target structure can not be determined correctly according to the relationships given later. In all our studies we will always attempt to satisfy Equation (61).

According to the above discussion the first echo, $V_{1st}(s)$, has double pole pair at $(s_{A_1}, s^*_{A_1})$ and single pole pair at (s_{T_1}, s^*_T) Consequently, $V_{2nd}(s)$ is characterized with triple pole pair at $(s_{A_1}, s^*_{A_1})$ and double at $(s_{T_1}, s^*_{T_1})$. The poles of the subsequent echoes can be determined in a similar way.

The above analysis of the transmission line model can serve the purpose of a good understanding of the response, but it becomes difficult to implement for a computer analysis.

A more concise method of looking at the transmission line is to represent an equivalent impedance of Z_T at the input terminals of the line. According to the wave equations governing the transmission line, the equivalent impedance of Z_T (Figure 22) at the input terminals is given [27] by

$$Z_{Teq} = Z_o \frac{Z_o + Z_T \tanh(\gamma d)}{Z_T + Z_o \tanh(\gamma d)} \quad . \tag{62}$$

Representing the parallel combination of Z_{Teq} and Z_A as

$$Z_{in} = \frac{Z_{Teq} Z_A}{Z_A + Z_{Teq}} \quad , \tag{63}$$

then $V_o(s)$ can be expressed as

$$V_o(s) = \frac{R_s}{Z_{in} + R_s} = - \frac{Z_{in}}{R_s + Z_{in}} \quad . \tag{64}$$

The above expression is equivalent to that given in Equation (57).

D. Testing of the Model

Equation (64) was used for implementation of a computer model for the transmission line, given in Appendix E. The characteristic impedance of the line in the computer model was defined as

$$Z_o = \sqrt{\frac{r + j\omega\mu_r\mu_o}{\sigma + j\omega\epsilon_r\epsilon_o}} \tag{65}$$

and the propagation constant as

$$\gamma = \frac{r + j\omega\mu_r\mu_o}{Z_o} \quad . \tag{66}$$

The parameters r and σ represent the series and shunt losses per unit length of the line, while $\mu_r\mu_o$ and $\epsilon_r\epsilon_o$ correspond to the inductance and capacitance, repsectively, per unit length of the line.

It was necessary to introduce some loss in the line (complex γ) in order for $v_o(t)$ (the inverse Fourier transform of $V_o(j\omega)$) to be completely diminished within the chosen time window, T_w. A finite time window is a limitation of the Fast Fourier Transform used for time inversion of the 8192-point, complex, discrete array, $V_o(j\omega)$. This array was produced by an incremental frequency interval equal to

$$\Delta\omega = \frac{2\pi}{T_w} \quad \text{(rad)}. \tag{67}$$

The above matters should be carefully arranged for the successfulness of the computer model.

Furthermore, for simplicity, Z_o was kept real by defining r as

$$r = \sigma \frac{\mu_o \mu_r}{\epsilon_o \epsilon_r} \quad . \tag{68}$$

The output voltage shown in Figure 25 was calculated by the computer model in Appendix E. The input was a 6 nsec gaussian pulse. The pole pair of Z_A was placed at

$$s_A, s_A^* = -20\times10^6 \text{ nepers/sec} \pm j2\pi\times50\times10^6 \text{ rad/sec}$$

and that of Z_T at

$$s_T, s_T^* = -10\times10^6 \text{ nepers/sec} \pm j2\pi\times40\times10^6 \text{ rad/sec} \quad .$$

Other parameters as indicated in Figure 25 are

$R_A = 250\Omega$ $\qquad$ $\epsilon_o = 8.8456\times10^{-12}$ Farads/meter

$R_T = 500\Omega$ $\qquad$ $\mu_o = 1.256\times10^{-6}$ Henrys/meter

$Z_o = 377\Omega$ $\qquad$ $\sigma = 5\times10^{-6}$ ℧/meter

$R_s = 377\Omega$ $\qquad$ $\epsilon_r = 1.$

$d = 30$ meters $\qquad$ $\mu_r = 1.$

Note that d was chosen long enough so that there would be no overlap of the echoes. The pole pair of Z_T was selected with respect to that of Z_A so that the maximum response of Z_T alone in the frequency domain would occur at the frequency where the response from Z_A (alone) would decay to its half power value.

As mentioned in Chapter I, we are interested in determining the structure of the tunnel (target) by examining the received voltage. The natural resonance of the tunnel (imaginary of s_T) will determine its structure. The peak response from the tunnel occurs when the reflection from the front and back interfaces are in phase. To a first order approximation, neglecting caustics, this occurs for

$$2\beta H = \pi \quad , \tag{69a}$$

where H is the tunnel height. Assuming the velocity of the wave in the tunnel to be that of free space, Equation (69a) gives

$$H = \frac{C}{4f_H} \tag{69b}$$

where f_H is a comparable first order resonance corresponding to the height of the tunnel,

$$f_H = \frac{C}{4H} \quad . \tag{69c}$$

Its depth, d, can be determined by the arrival time, T_a, of the first echo as follows:

$$d = \frac{T_a(\text{nsec})}{6.667\sqrt{\epsilon_r \mu_r}} \quad (\text{meters}). \tag{70}$$

From the above discussion it is instructive to use the first echo for analysis, since this is the simplest response containing information about Z_T. The time expanded first echo of Figure 25 is shown in Figure 26(a). For comparison, the first echo as calculated by Equation (54) is also shown in Figure 26(b). Note that it is identical to that in Figure 26(a). The poles of this echo were found by Prony's method to be located at

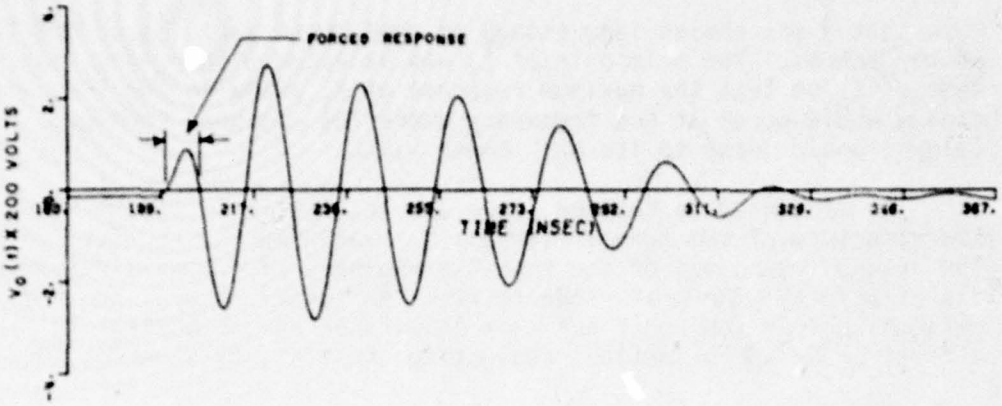

(a) Calculated from Equation (64)

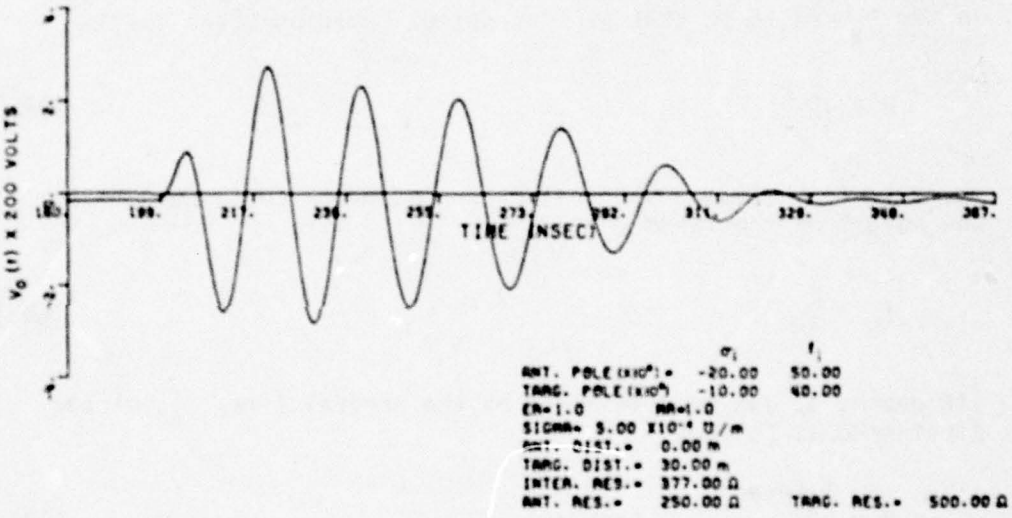

(b) Calculated from Equation (54)

Figure 26. First Echo of Figure 25 (d=30m.).

$$p_1, p_1^* = -48.5205 \text{ Meganepers/sec} \pm j2\pi x47.9588 \text{ Megarad/sec}$$

$$p_2, p_2 = -42.09545 \text{ Meganepers/sec} \pm j2\pi x50.62961 \text{ Megarad/sec}$$

$$p_3, p_3^* = -23.23658 \text{ Meganepers/sec} \pm j2\pi x39.83028 \text{ Megarad/sec}$$

with respective residues of

$$R_{p_1}, R_{p_1}^* = (2.866151 \pm j2.846461)x10^{-2}$$

$$R_{p_2}, R_{p_2}^* = (-2.354673 \pm j3.490129)x10^{-2}$$

$$R_{p_3}, R_{p_3}^* = (-.4535518 \pm j.07051006)x10^{-2} .$$

(The residues when calculated by Prony's method, do not have any absolute, but only relative meaning, since they depend on the starting point of the window used by Prony's method for finding the poles.) If Equations (52) are used for calculating the poles of $V_{1st}(s)$, we obtain

$$p_1', p_1'^* = -46.525 \text{ Meganepers/sec} \pm j2\pi x49.551 \text{ Megarad/sec}$$

$$p_2', p_2'^* = -46.525 \text{ Meganepers/sec} \pm j2\pi x49.551 \text{ Megarad/sec}$$

$$p_3', p_3'^* = -23.263 \text{ Meganepers/sec} \pm j2\pi x39.861 \text{ Megarad/sec}$$

These results agree very well with the ones generated by Prony's method. Note that the tunnel height corresponding to a 39.83 MHz resonance is found to be

$$H = \frac{c}{4x39.83x10^6} = 1.883 \text{ m.}$$

The arrival time in this case is easily detected to be

$$T_a = 6.667(30) = 200 \text{ nsec}$$

since the output data were produced from a theoretical model.

E. Use of the Reconstruction Process to Estimate the Arrival Time of the Target Response

It was noted previously that in general when actual echoes are encountered the early portion of the echo is dominated by clutter. Thus, we will attempt to describe a more clutter immune method for calculating the arrival time of the target response.

Employing the pole extraction process, the antenna double pole was extracted from the response of Figure 26. The result is shown in Figure 27. Note the peaking at the beginning of the resultant waveform. This is because the forced response cannot be characterized with a set of poles. The rest of the filtered waveform contains only the pole pair of Z_T (corrected), (p_3, p_3).

After removing the dc component of the target response (Figure 27), we can then reconstruct its early portion based on its late response, as shown in Figure 28. Concentrating in the interval of 19-37 nsec we observe that in this time span the reconstructed waveform deviates drastically from the course of the filtered waveform. The first zero crossing of the reconstructed portion after its deviation from the filtered waveform corresponds to the tail end of the forced response (see Figure 26). This phenomenon was tested for many such responses in order to examine its validity (see Appendix E). It was found to be the same in every case that was studied. From Figure 28 the target's depth can be calculated as

$$d = \frac{T_o - t_p}{6.667\sqrt{\epsilon_r \mu_r}} = \frac{200}{6.667} = 30 \text{ meters}, \qquad (71)$$

where t_p is the gaussian pulse width in nsec and T_o is the time in nsec corresponding to the first zero crossing of the reconstructed waveform after its deviation. (Note that the origin of Figure 28 corresponds to 180 nsec, see Figure 26.)

The previously studied response was obtained with a long transmission line (30m). The echoes then did not overlap. We can now shorten the line in order to determine if it is still possible to detect the target. By shortening the line, there will be overlap of the echoes and probably the antenna response, $V_a(s)$ (Equation (53a)). We will neglect the antenna response since for the parameters

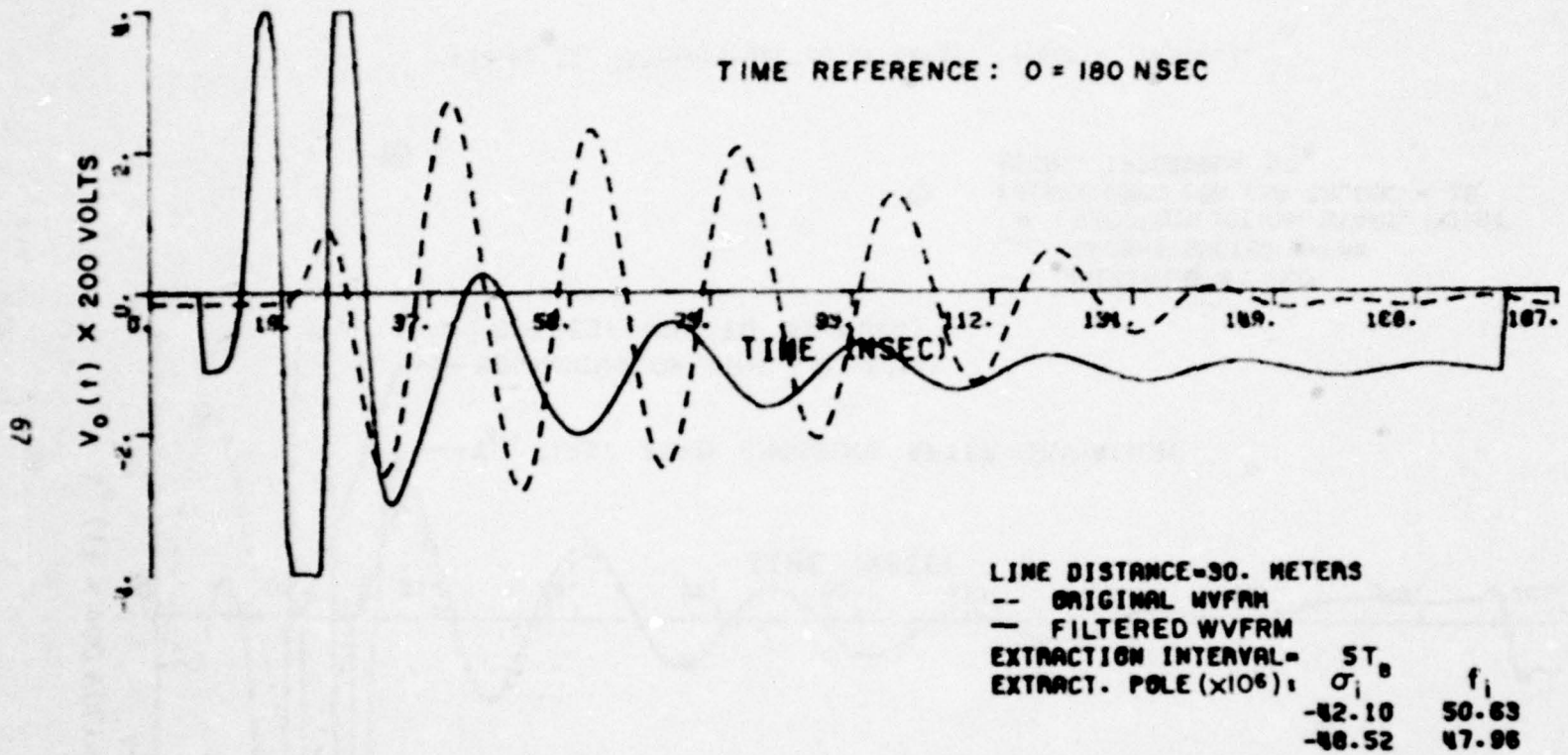

Figure 27. Extraction of antenna double pole pair from first echo.

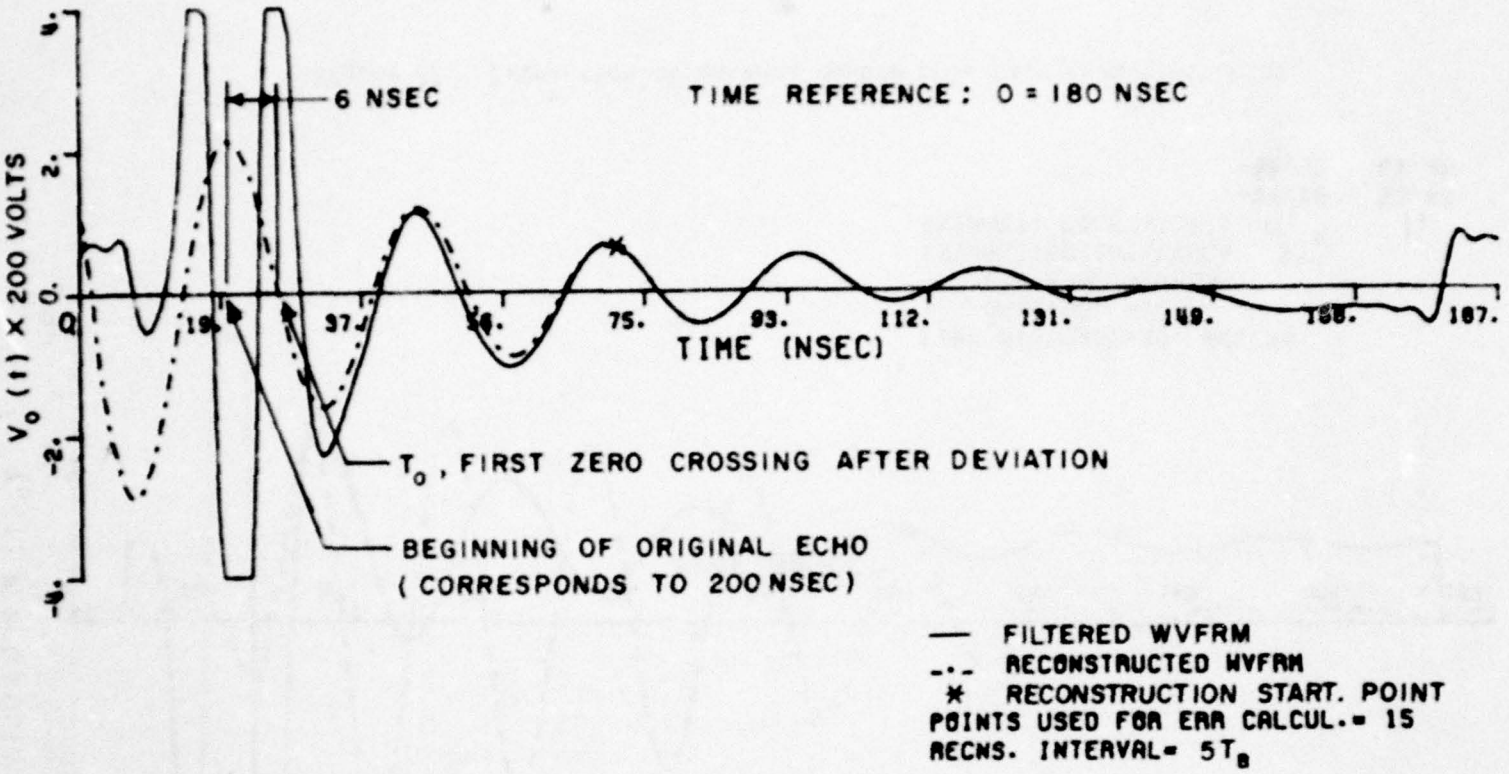

Figure 28. Reconstruction of target response (d=30m.).

chosen it would be negligible by the arrival of the first echo. If it did not, then an increased residue of the antenna pole pair would have to be encountered in the first echo.

Using the same parameters as those for d=30m. on page 65, the first echo response for depths 20, 18, 15 and 10 meters are shown in Figures 29, 30, 31 and 32 (dotted lines), respectively. Note the window in each waveform containing the first echo only. This window was used by Prony's method for calculating the poles of the first echo (sampling interval is T_R=6000/8191 nsec). We could not use the total window shown in the figures since Prony's method assumes that the response associated with all the poles in the region being sampled has been introduced pior to the original sample.

For example, let us randomly select a time window out of the total span of the waveform and use Prony's method to find its poles. In this time window there could be a superposition of two or more echoes. It was found that Prony's method will probably find all of the complex resonances of the poles but the calculated real parts will be far off from the ones existing in the waveform if a resonance is initiated within this time window. In fact Prony's method requires that no forced response be present in the data if the real parts of the poles are to be calculated accurately.

The poles obtained by Prony's method for the echoes in Figures 29, 30 and 31 are shown in Table 1. These are much the same with those obtained for d=30m., as expected. In order to determine the depth of the target we first extract the antenna double pole pair. The result is the solid line on the same figures (Figures 29, 30, and 31). After centering, the reconstructed early portion of the target response is shown in Figures 33, 34 and 35 for depths at 20, 18 and 15 meters, respectively. Detecting the first zero crossing of the reconstructed target responses after their deviation from the filtered waveform (solid line) we obtain the following results:

T_o = 120 + 20.12 = 140.2 nsec ; d=20m.

T_o = 108 + 17.8 = 125.8 nsec ; d=18m.

T_o = 90 + 16.5 = 106.5 nsec ; d=15m.

Using the above results in Equation (71) the depths are calculated to be 20.13, 17.97, 15.07 meters as compared to the actual depths of 20, 18 and 15 meters, respectively.

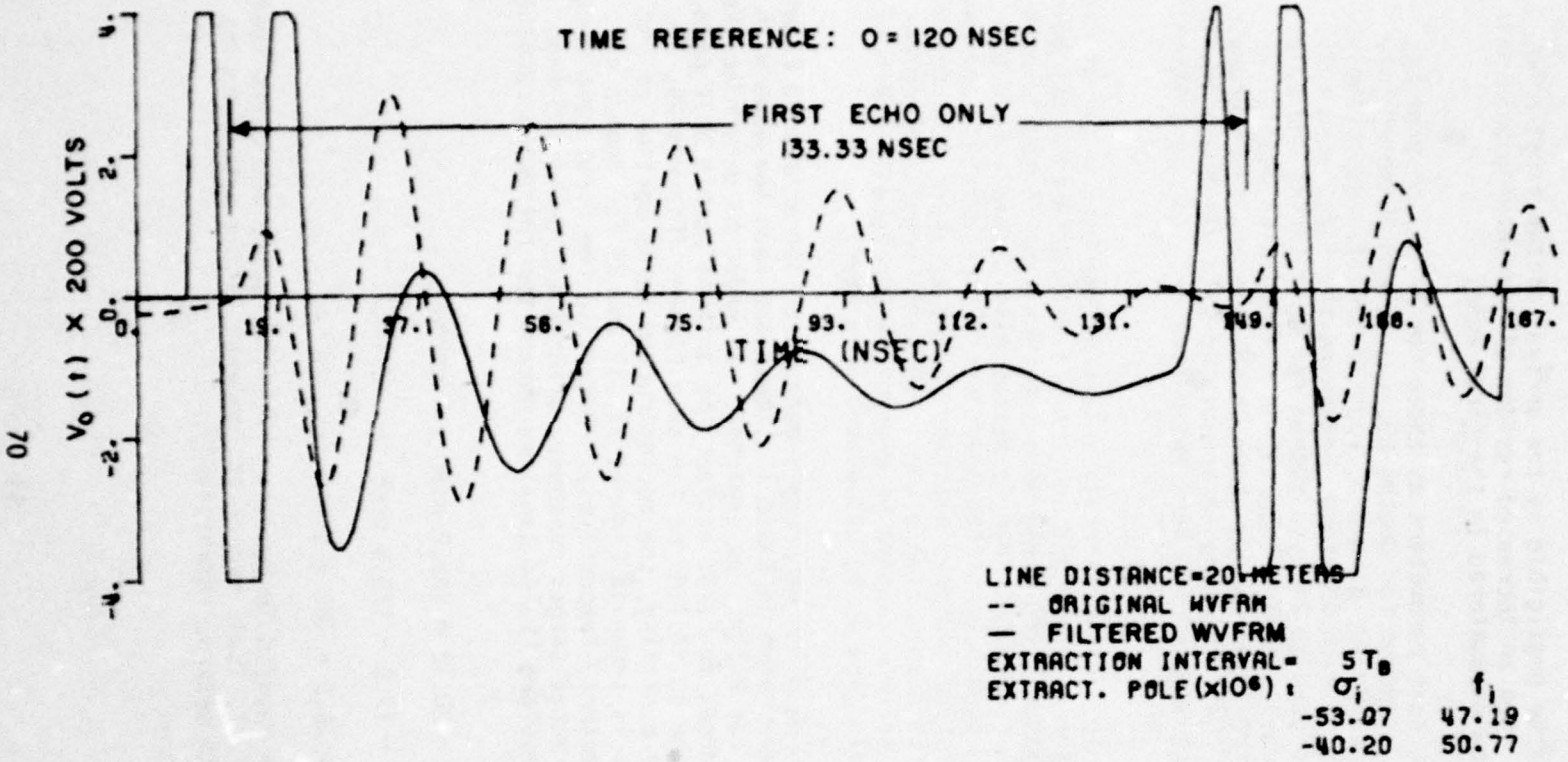

Figure 29. Extraction of antenna double pole pair from first echo (d=20m.).

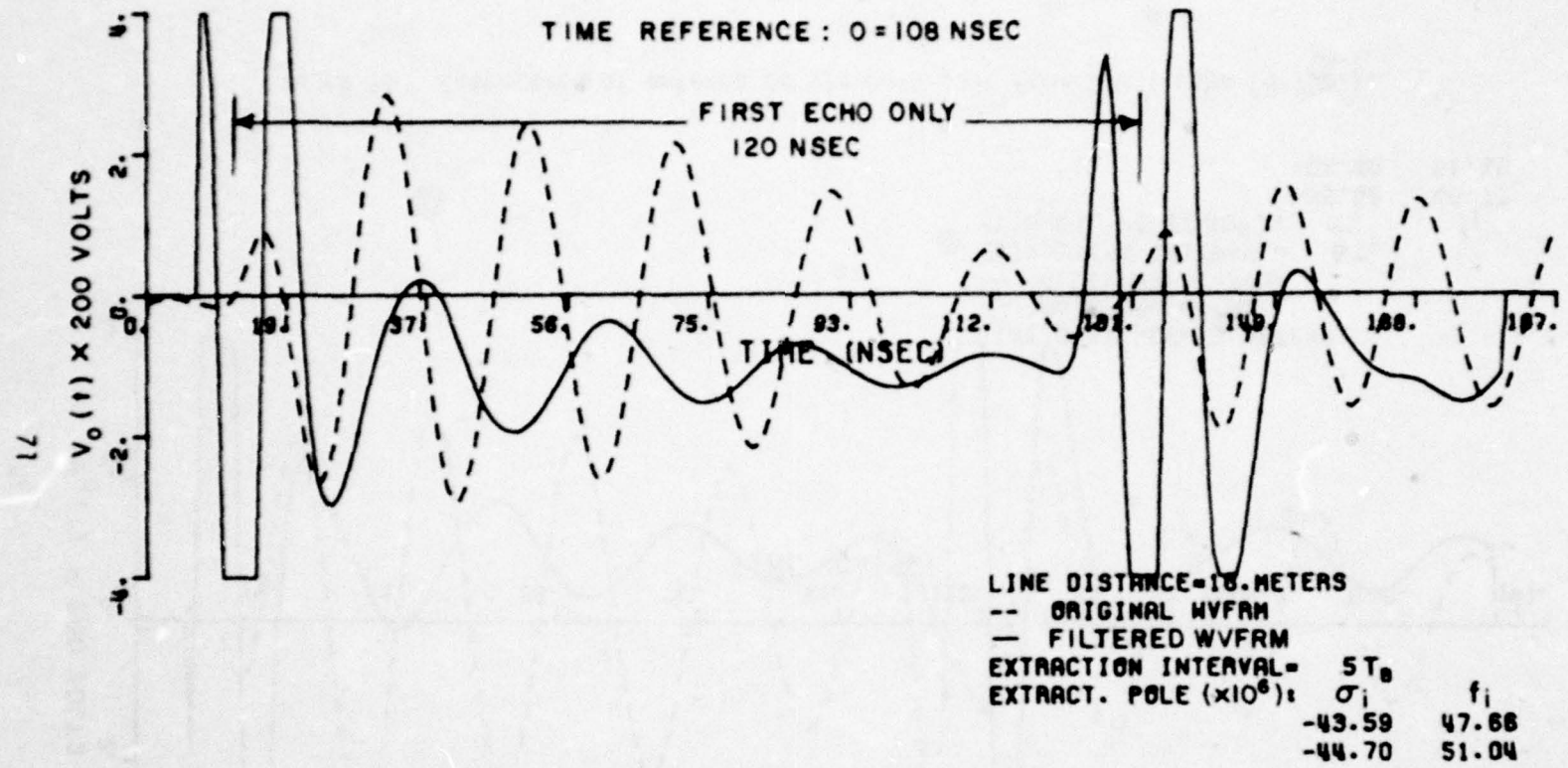

Figure 30. Extraction of antenna double pole pair from first echo.

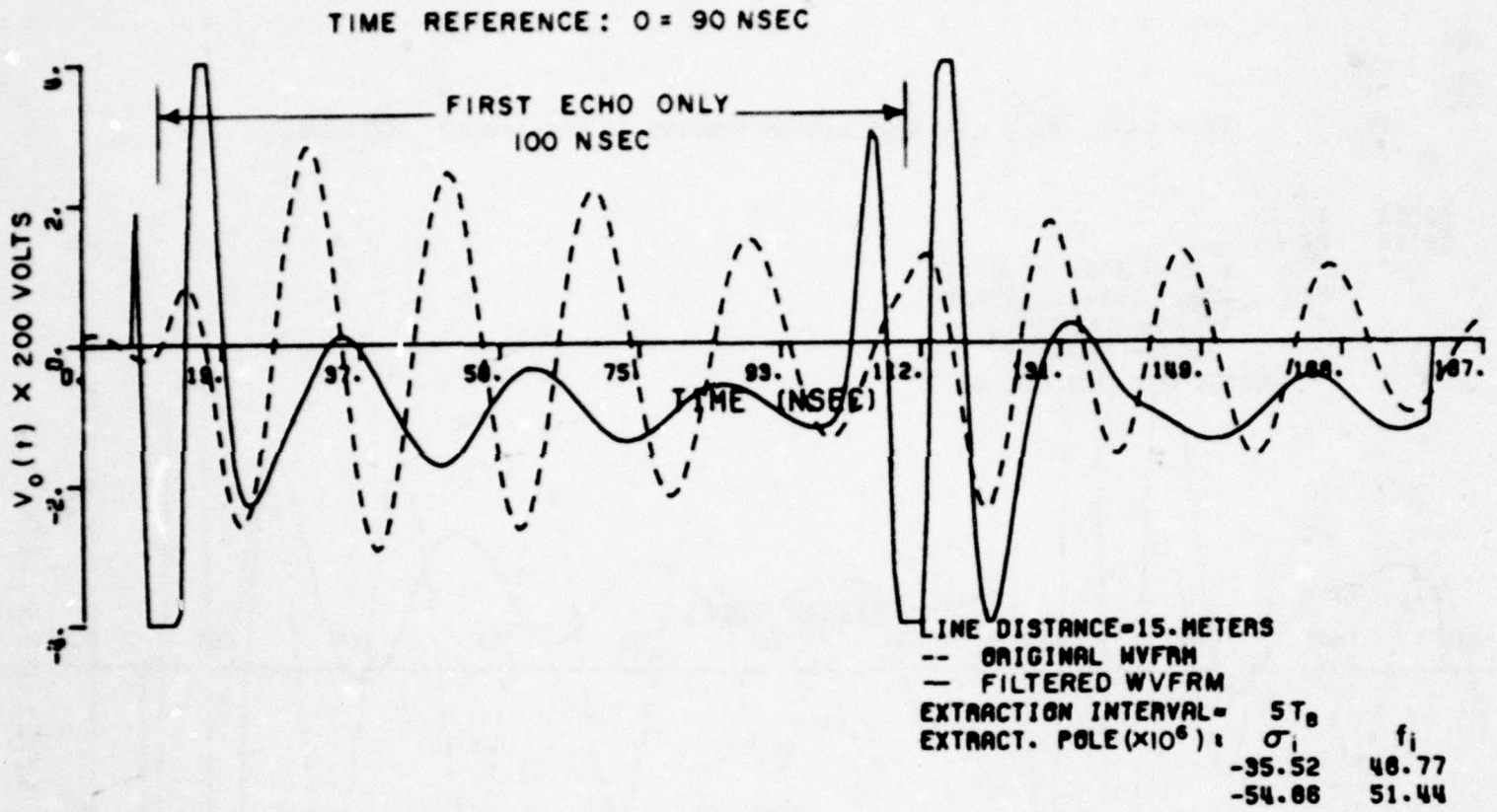

Figure 31. Extraction of antenna double pole pair from first echo (d=15m.).

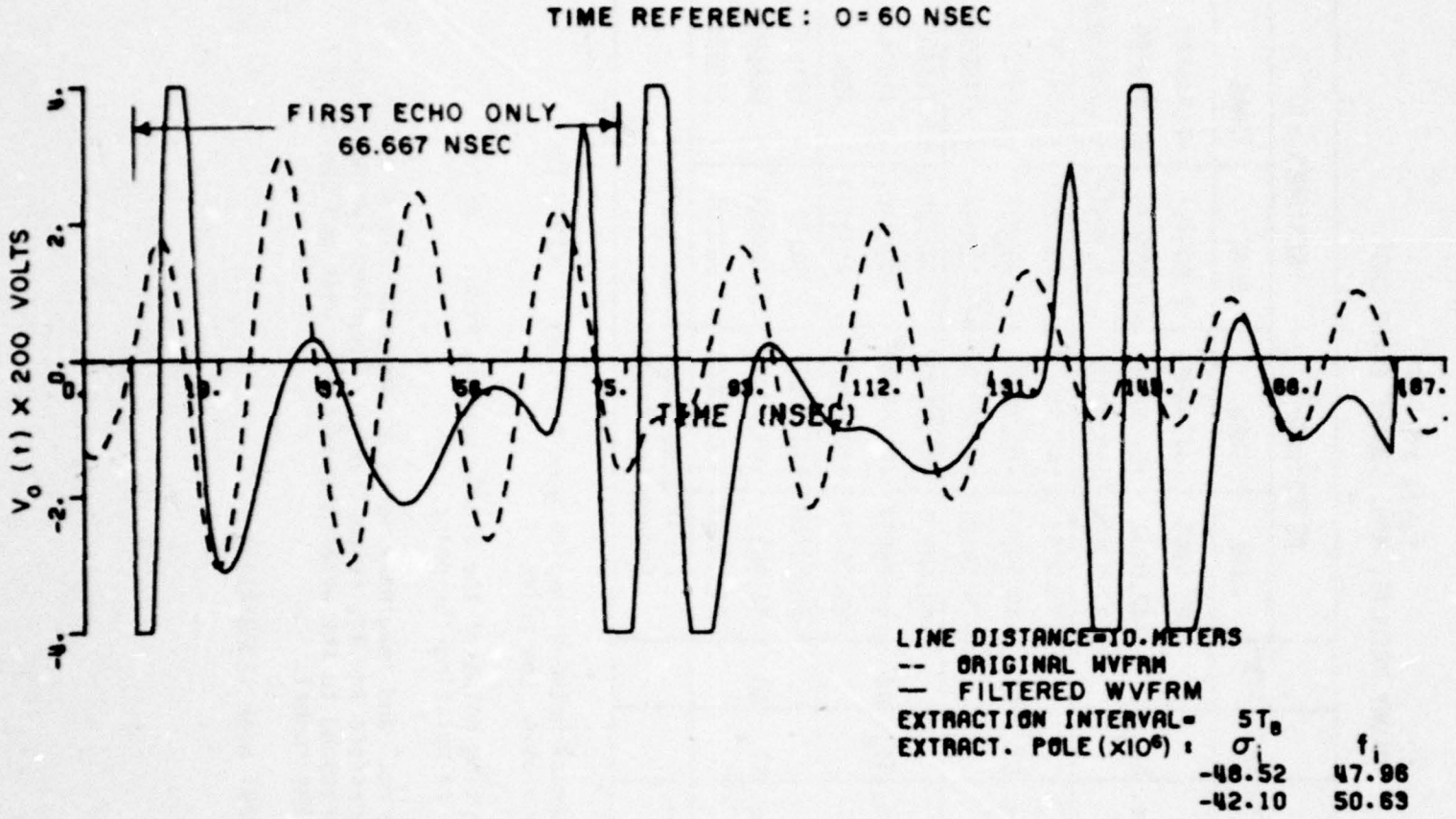

Figure 32. Extraction of antenna double pole pair from first echo (d=10m.).

Table 1
PRONY RESULTS; MIN. SQUARE ERROR CASE

[2]WVFRM	DEPTH	IBS[1]	ITS[2]	POLES[3](x10^6)		RESIDUES(x10^{-2})	
				REAL	IMAG	REAL	IMAG
Fig. 26	30 m.	$6T_B$[4]	51	-48.5205	±47.95888	2.866151	±2.846461
				-42.0954	±50.62961	-2.354673	±3.490129
				-23.23658	±39.83028	- .4535518	± .07051006
Fig. 29	20 m.	$5T_B$	45	-53.0749	±47.19403	.1067881	±2.831341
				-40.19853	±50.76860	.8886122	±2.994219
				-25.16282	±40.15106	- .4398645	± .3466342
Fig. 30	19 m.	$5T_B$	44	-43.58974	±47.65909	.842728	±3.228905
				-44.69857	±51.03842	.0540642	±3.139947
				-25.06127	±39.62526	- .2190129	± .408473
Fig. 31	15 m.	$4T_V$	40	-35.51768	±48.77227	2.961494	± .2245375
				-54.8633	±51.44039	-2.166434	± .5655805
				-21.13081	±39.51648	- .301001	± .212935
Fig. 32	10 m.			First Echo Time Window not Wide Enough for Processing			

[1]IBS = Interval between samples used by Prony's method for calculating the poles.

[2]ITS = Starting point of the window used by Prony's method for calculating the poles.

[3] The real and imaginary parts of the poles are given in Nepers/sec and Hz, respectively. The first two pole pairs correspond to the antenna double pole pair and the third to the tunnel.

[4]T_B = .73251 nsec (6000/8191)

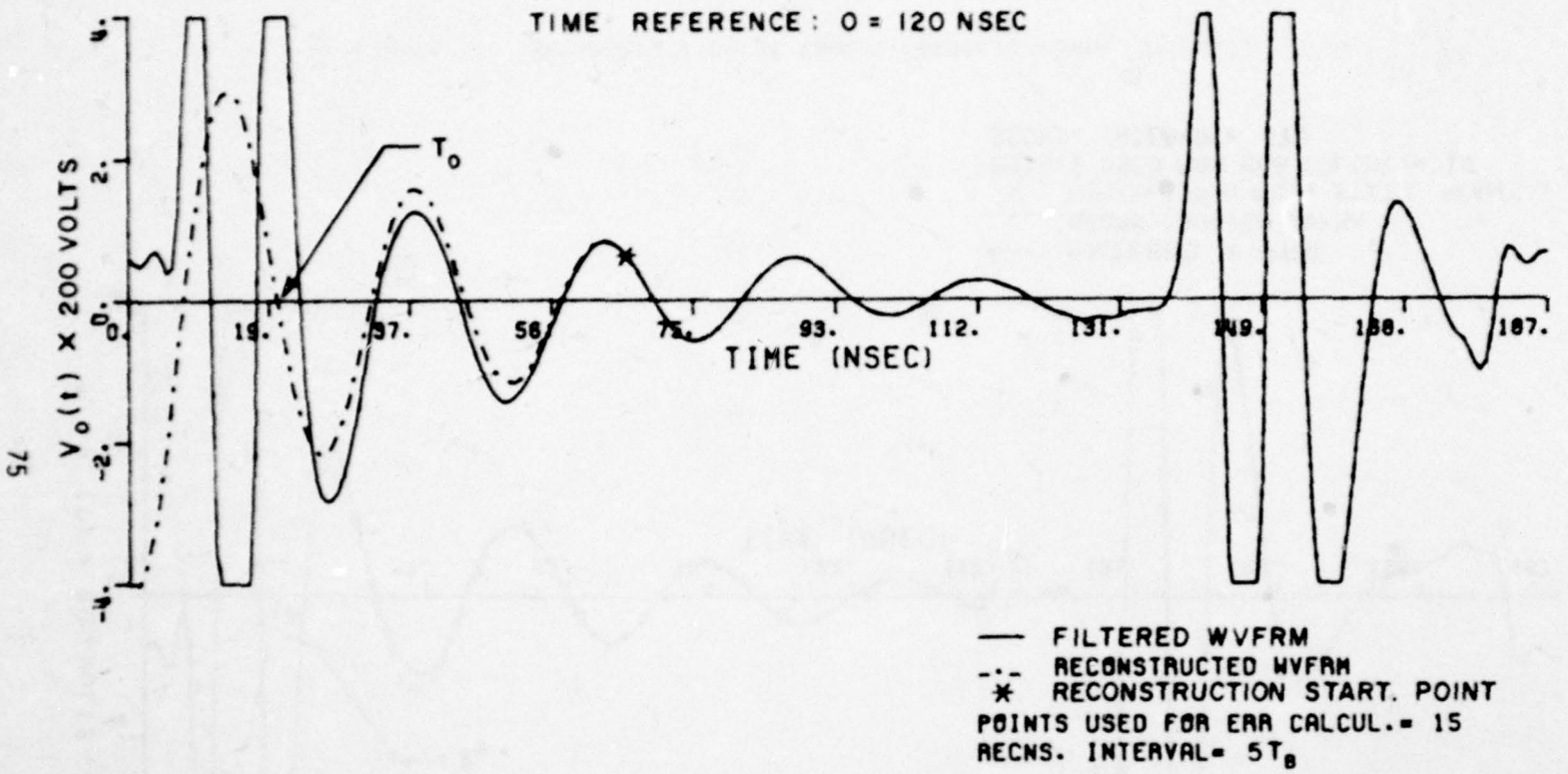

Figure 33. Reconstruction of target response alone (d=20m.).

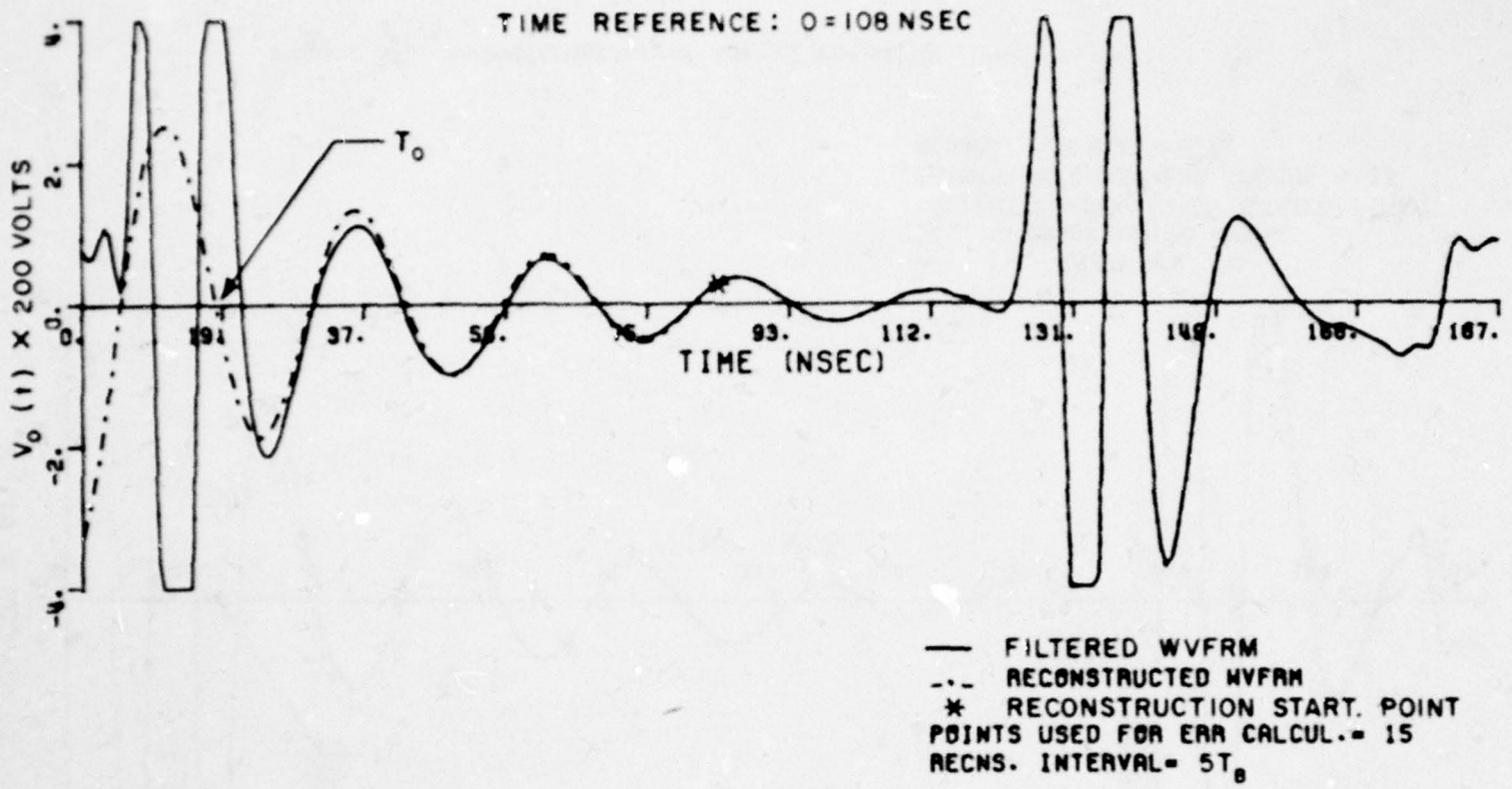

Figure 34. Reconstruction of target response alone (d=18m.).

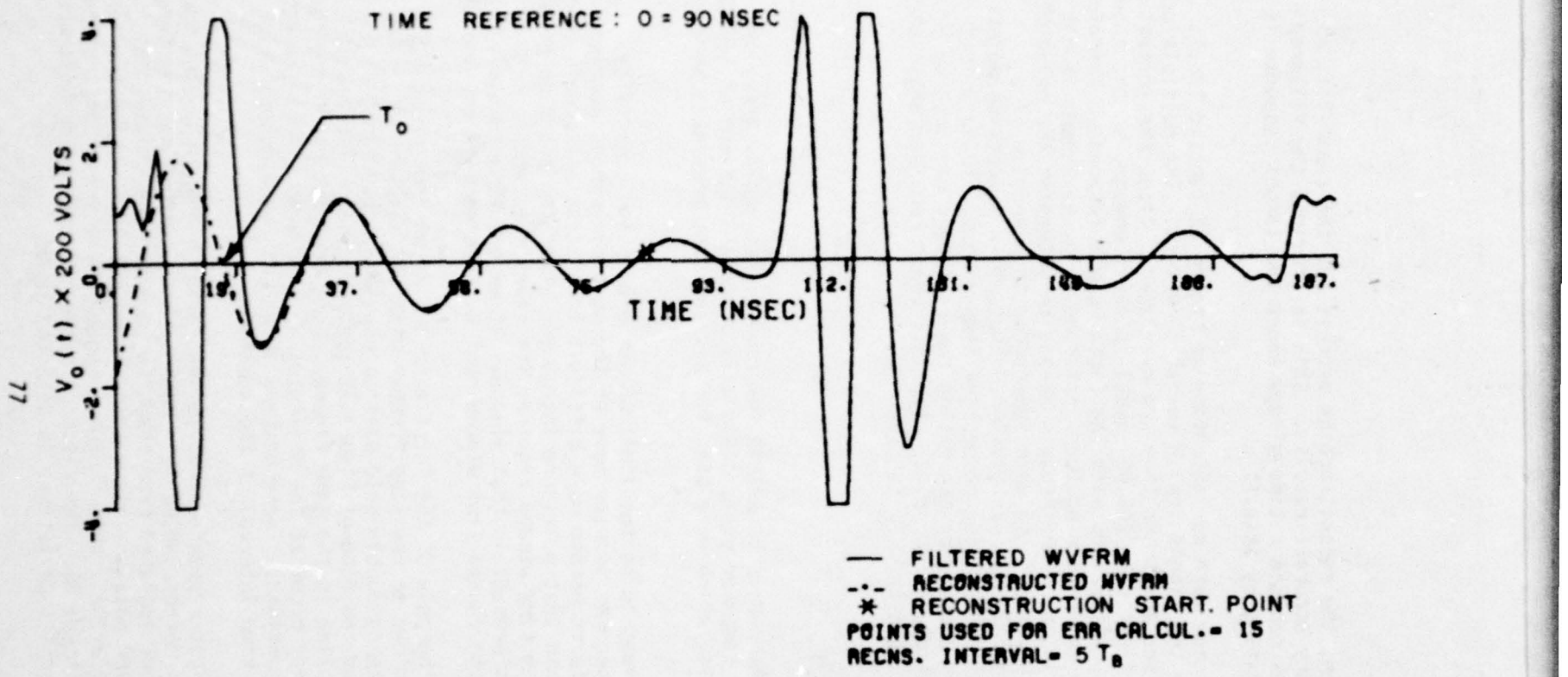

Figure 35. Reconstruction of target response alone (d=15m.).

As seen, the reconstruction process has the capability of producing very accurate results. This is provided the filtered waveform does contain a time window where the target response is actually existing by itself.

Let us now turn our attention to Figure 32 (dotted line). In this case the line's length was at 10 meters. The multiple echoes are 66.667 nsec apart and they are overlaped. Also, the arrival time of the first echo (66.667 nsec) is short enough, so the antenna (Z_A) response interferes with the first echo's response. Therefore, the time window containing the first echo only, as shown, is not wide enough in order for Prony's method to determine the poles of the first echo. We could have superseded this problem if our sampling interval, T_B, was smaller. Thus, more processing points would be available in the respective time window. These points could then be enough for generating the equations required by Prony's method to calculate the poles. But this would require larger array for $V_o(j\omega)$. Note that T_B is given by

$$T_B = \frac{T_W}{K-1}$$

where K is the number of points describing the complex array of $V_o(j\omega)$. The computer used, could only process a maximum of K=8192 complex points, which were used for all the data presented here and in Appendix E.

This seems to be the limit of our processing capability. As the line becomes shorter more of the multiple echoes overlap and the waveforms become more difficult to process. Its main complication is again that poles are introduced after the starting point of the minimum time window required for Prony's method to calculate all the poles present in that window. If we are to accurately process a response, the chosen time window must be coherent and continuous.

Since the pole of the first echo are known from previous processing we can go one step further with the response at d=10m. Using the antenna double pole pair as obtained for d=30m., it is extracted from the echo of Figure 32 (dotted line). The result is the solid line in the same figure. Note the peaking of the forced response. They occur at the beginning of each echo, where the forced response is confined. These peaking show that three echoes exist in the total time interval of the waveform.

The target response alone is indicated in the first echo for a time length corresponding to a cycle. Note, also, that the target response is not isolated from the other echoes, yet, since they consist of more poles. This was developed earlier. Using the target pole pair for d=30m., this target response alone was reconstructed as shown in Figure 36. The first zero crossing of the reconstructed waveform after its deviation, is detected to be

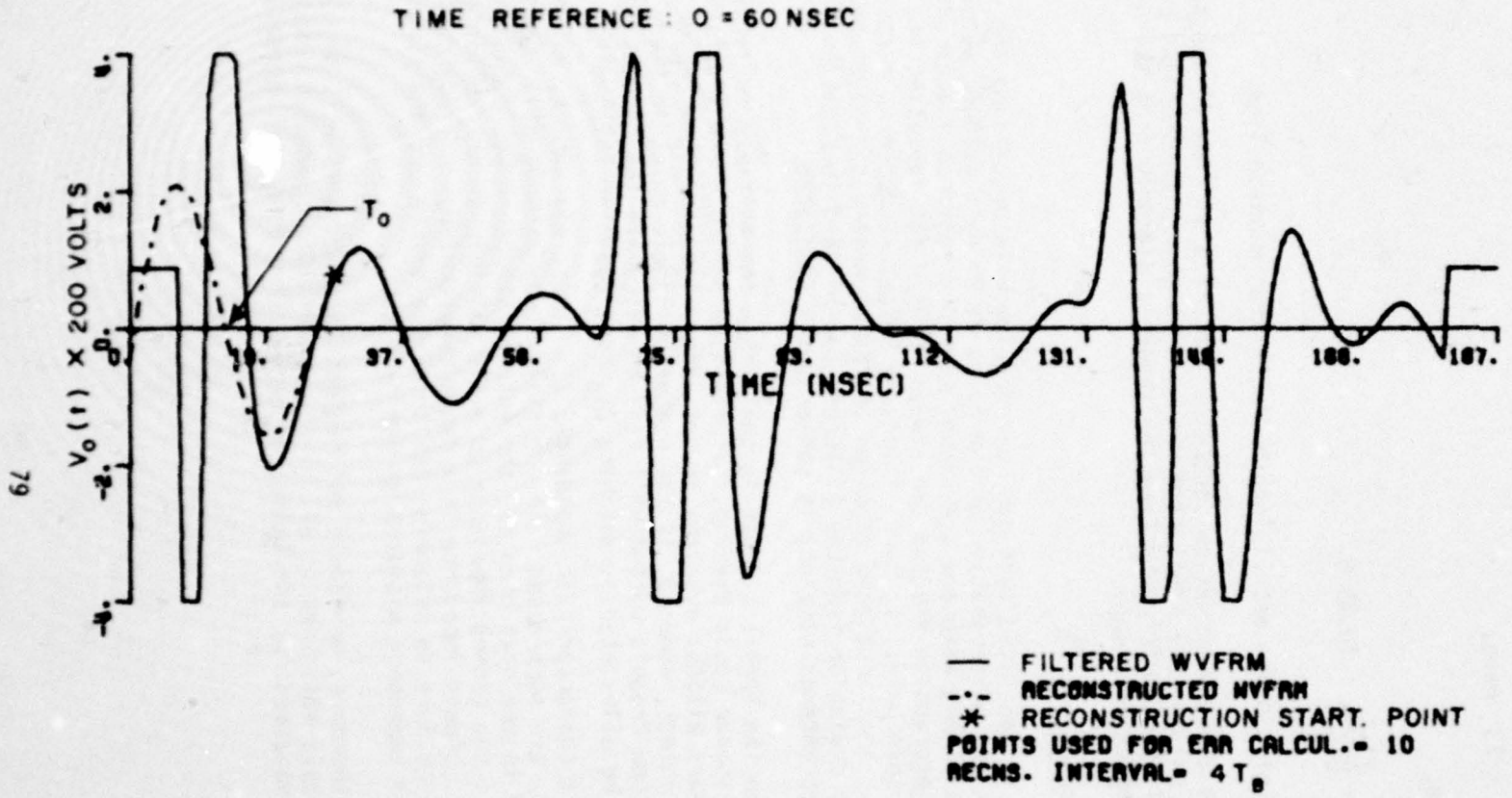

Figure 36. Reconstruction of target response alone (d=30m.).

T_o = 73 nsec.

Therefore,

$$d = \frac{73-6}{6.667} = 10.05 \text{ m.}$$

Indeed, this is the actual length of the transmission line.

The above observation indicates that if a portion of the target response exists in a small time window then the reconstruction process can still be used for detecting the target's distance from the antenna (or constructing a map).

F. Conclusions

It is concluded that our main problem with processing the echoes is the determination of the poles by Prony's method. Once the poles of the waveform are known, within a reasonable accuracy, the pole extraction process can always be used for isolating the target's pole pair. In turn, the early target response is reconstructed. The first zero crossing of the reconstructed waveform after its deviation from the filtered, can be used in Equation (71). The target-antenna distance is subsequently estimated.

When the target's depth is small then the multiple reflections of its response could overlap. If the time window where the first echo appears without overlaps is not large, (greater than $2N_p$ or $3N_p$ time points, where N_p is the number of single poles in the window) then Prony's method will fail to calculate the correct poles. This can be alleviated by matching Z_{As} (see Equation (52)) with the line's characteristic impedance, Z_o. Thus, all echoes, except the first, are suppressed. In our field study at Gold Hill, Colorado, discussed in the next chapter, the antenna structure was closely matched to the ground impedance to avoid multiple tunnel reflections. Of course, ground impedance is a dynamic parameter. A study could be attempted here to determine the tolerance of the antenna structure and ground impedance mismatch on our results.

Furthermore, we should not neglect that Equation (61) should be reasonably satisfied at all times. Otherwise, erroneous results could be obtained for the tunnel or target structure (see Appendix E).

CHAPTER V
APPLICATION OF THE POLE EXTRACTION AND RECONSTRUCTION PROCESSES ON MEASURED TUNNEL ECHOES

A. Objectives

The objectives of this chapter are the following:

1. To apply the pole extraction and reconstruction processes on measured tunnel echoes for detection and identification.

2. To evaluate our results and compare them with results from other processing attempts.

B. Echo Recording and Processing

During the summer of 1978 a group from the ElectroScience Laboratory recorded a set of echoes on a tunnel site at Gold Hill, Colorado. The position of the recorded waveforms with respect to the tunnel is indicated in Figure 37. As shown, two traverses were made over the rectangular tunnel [22]. At position R10 the tunnel was about 20 ft. (6.1 m.) deep, and of size 4'x9'. These data would correspond to a tunnel response arrival time of about 100 nsec (the ground relative permittivity was accurately measured to be $\varepsilon_r=6$) and a resonance at about 25 MHz.

A 6 nsec gaussian pulse was used for excitation with an 8-foot crossed dipole antenna, referred to as LBANT (Long Box Antenna) [14]. Some of the recorded echoes are shown in Figure 16. The later portion of all the waveforms was used by Prony's method for calculating their poles. Results are given in Tables 2 and 3. Two complex conjugate pole pairs are indicated. The one at 40-50 MHz corresponds to the antenna pole pair, and the other at 20-30 MHz to the tunnel pole pair. The real part of the calculated poles varied over a wide range. This is due to the nonuniformity of the ground, and also to the sensitivity of the real part in the calculations performed by Prony's method.

The antenna pole pair given in the tables was extracted from each particular echo by employing Equation (16) and was subsequently corrected for distortions according to Equation (34). The early portion of the tunnel response for each waveform was then reconstructed according to Equation (42), with the tunnel pole pair as given in

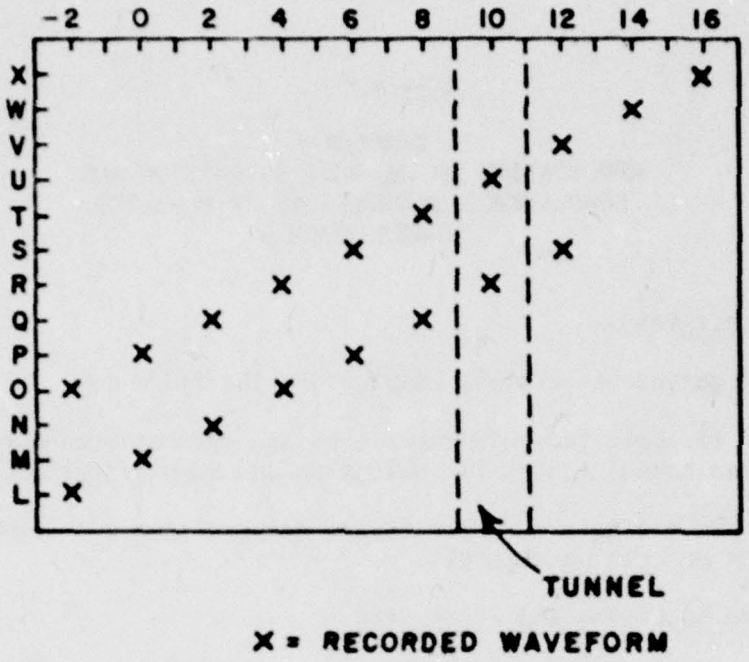

Figure 37. Measurement coordinates of Gold Hill Map 2.

the tables. The reconstructed waveforms at positions Q08 and R10 are shown in Figure 19 and 20, respectively. It should be mentioned that the intervals used during the pole extraction and reconstruction processes were the same as those used by Prony's method for calculating the waveform poles. These intervals are given in Tables 2 and 3 under the column of IBS (Interval Between Samples).

Table 2
PRONY RESULTS; MIN. SQUARE ERROR CASE

WVFRM POS.	IBS[1]	ITS[2]	POLES (Nepers$\times 10^6$/sec, MH_z)[3]		RESIDUES ($\times 5\times 10^{-3}$V)	
			REAL	IMAG	REAL	IMAG
M00	$9T_B$	107	-52.57866	$\pm$67.33230	.4162106	$\pm$ .4041063
			-24.88652	$\pm$25.85206	.1878496	$\pm$ .3247834
N02	$9T_B$	102	-10.79741	$\pm$51.30669	- .2334531	$\pm$ .1110562
			-32.04296	$\pm$24.91175	.0342021	$\pm$ .2627557
O02	$9T_B$	105	-17.33083	$\pm$47.07857	.3978992	$\pm$ .7173292
			-24.33710	$\pm$20.47811	- .702791	$\pm$ .3943723
P06	$8T_B$	112	-32.70187	$\pm$41.94802	- .1942287	$\pm$1.310707
			-30.30265	$\pm$18.21603	.6458865	$\pm$ .08358783
Q08	$9T_B$	101	-26.92599	$\pm$45.48387	.04361706	$\pm$ .5112753
			-38.10888	$\pm$19.36852	-1.484128	$\pm$ .7730645
R10	$7T_B$	96	-43.59402	$\pm$69.02293	- .000748475	$\pm$ .178899
			- 4.259986	$\pm$21.8921	- .5154413	$\pm$ .3856364
S12	$8T_B$	98	-57.71117	$\pm$46.79932	- .7286549	$\pm$ .6220561
			-18.19595	$\pm$25.17972	.06751176	$\pm$ .09678334

[1] IBS = Interval between samples used by Prony's method for calculating the poles (T_B=200/255 nsec).

[2] ITS = Starting point of the window used by Prony's method for calculating the poles.

[3] The first pole pair corresponds to the antenna and the second to the tunnel.

Table 3
PRONY RESULTS; MIN. SQUARE ERROR CASE

WVFRM POS.	IBS[1]	ITS[2]	POLES (Nepers x 10^6/sec, MHz)[3]		RESIDUES (x5x10^{-3}V)	
			REAL	IMAG	REAL	IMAG
S06	$8T_B$	95	-60.4619	±42.94669	.19806356	±1.508699
			-12.42679	±29.99758	- .424870	± .200000
T08	$9T_B$	107	-22.01400	±45.22787	.2006144	± .4037744
			-17.24408	±20.34345	.6929016	± .6932108
U10	$6T_B$	115	-77.43989	±49.73739	.9140537	± .5295426
			-20.49544	±29.20841	- .6743707	± .4071000
V12	$8T_B$	101	- 6.23398	±38.51152	.2606750	± .3271609
			-115.4021	±29.45295	- .294674	±2.649029
W14	$4T_B$	110	-24.31728	±56.38387	.06778622	± .2581218
			- 6.543068	±29.34473	.4046351	± .05179789
X16	$7T_B$	112	-58.65565	±67.08458	.3214495	± .2581229
			-44.09909	±37.64018	- .6434123	± .4217677

[1] IBS = Interval between samples used by Prony's method for calculating the poles (T_B=200/255 nsec).

[2] ITS = Starting point of the window used by Prony's method for calculating the poles.

[3] The first pole pair corresponds to the antenna and the second to the tunnel.

C. Results

The tunnel resonance as given by Prony's method (20-30 MHz) corresponds very much to the calculated one of 25 MHz. The deviation of the measured resonance at different recording positions is due to the changing height of the tunnel along its path.

Looking at Figures 19 and 20 we observe that the first zero crossing of the reconstructed tunnel response after its deviation from the filtered waveform occurs at about 90 nsec. This corresponds to the arrival time of the tunnel response and compares satisfactorily to the calculated one of 100 nsec.

In order to determine the relative position of the tunnel, grey-level mapping (see Reference [22]) of the reconstructed waveforms for each traverse could be performed. This mapping technique places the waveforms of the traverse in a two dimensional coordinate system of depth (time) versus waveform recording position. Each coordinate point corresponds to a waveform voltage. Voltages between successive positions are interpolated by using Lagrange polynomial approximations [22]. Thus, a continuous two dimentional array of voltages is obtained. A computer routine written by Stapp translates the array voltages into characters of quantized darkness levels. The highest voltage corresponds to the darkest character (black), and the lowest to white. These characters could then be plotted on a line printer to obtain a grey-level map of depth versus waveform recording position.

The grey-level map indicates the arrival time of the tunnel response at each echo recording position. As we approach the tunnel, the arrival time of its response becomes shorter. Such behavior creates a hyperbola on the map with its peak corresponding to the position with the shortest distance from the tunnel (for a leveled surface this position is right over the tunnel).

Figures 38-40 show generated maps for the lower traverse of the plan view given in Figure 37. As seen, multiple hyperbolas are created. But, these are ficticious due to the reconstruction process. The hyperbola corresponding to the tunnel is the one beginning at about 90 nsec (in the middle of the map). This is determined from the first zero crossing of the reconstructed waveform after its deviation from the filtered. Figure 38 indicates the map with interpolation in the position axis performed after rectification (Fold First). This rectification process was found necessary in Reference [22] to clearly depict the tunnels in the grey-level mapping. It is not needed after using the processing techniques outlined here. The black level was set at 3.5x5mV. Other descriptive material on these figures, not needed in the present discussion, is retained for the deeply interested reader and follows the definitions given in [22]. In Figures 39 and 40 interpolation was

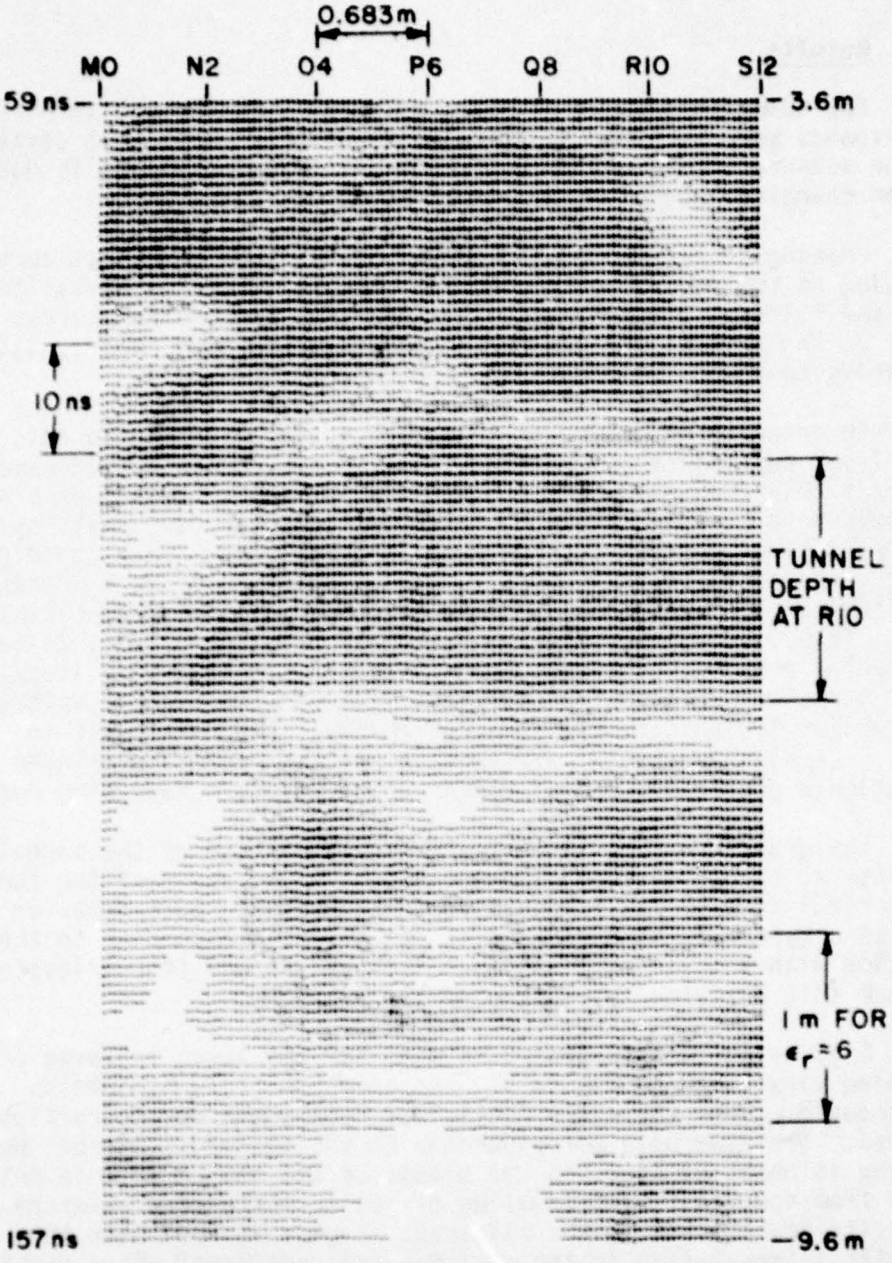

Long Box Antenna
NXDIV=19 NYDIV=0
LIX=3 LIY=1

Clipped at 3.5
Fold First

GOLD HILL MAP 2

Figure 38. Mapping of the lower traverse over the tunnel.

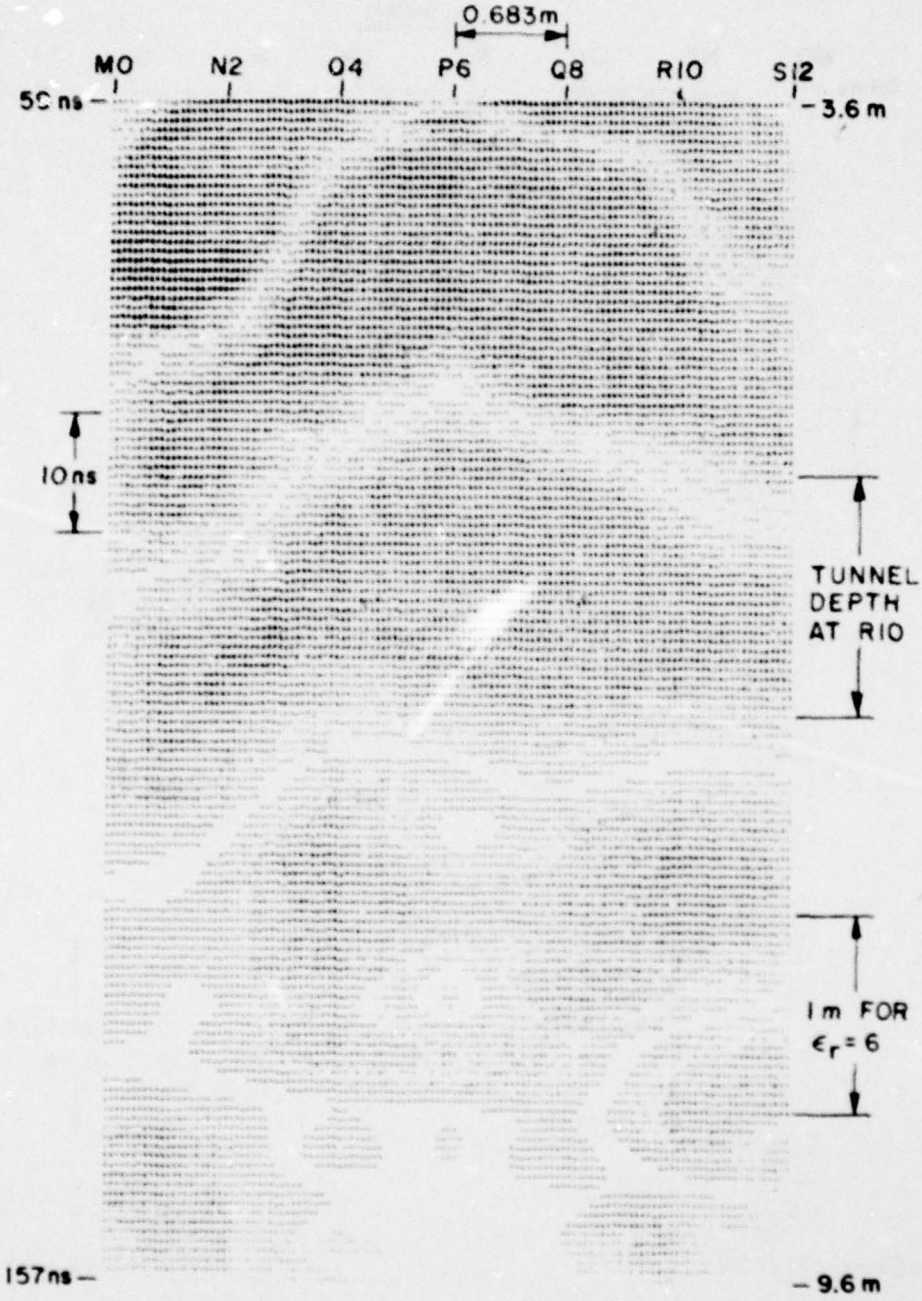

Long Box Antenna
NXDIV=19 NYDIV=0
LIX=3 LIY=1

Clipped at 3.5
Fold Last

GOLD HILL MAP 2

Figure 39. Mapping of the lower traverse over the tunnel.

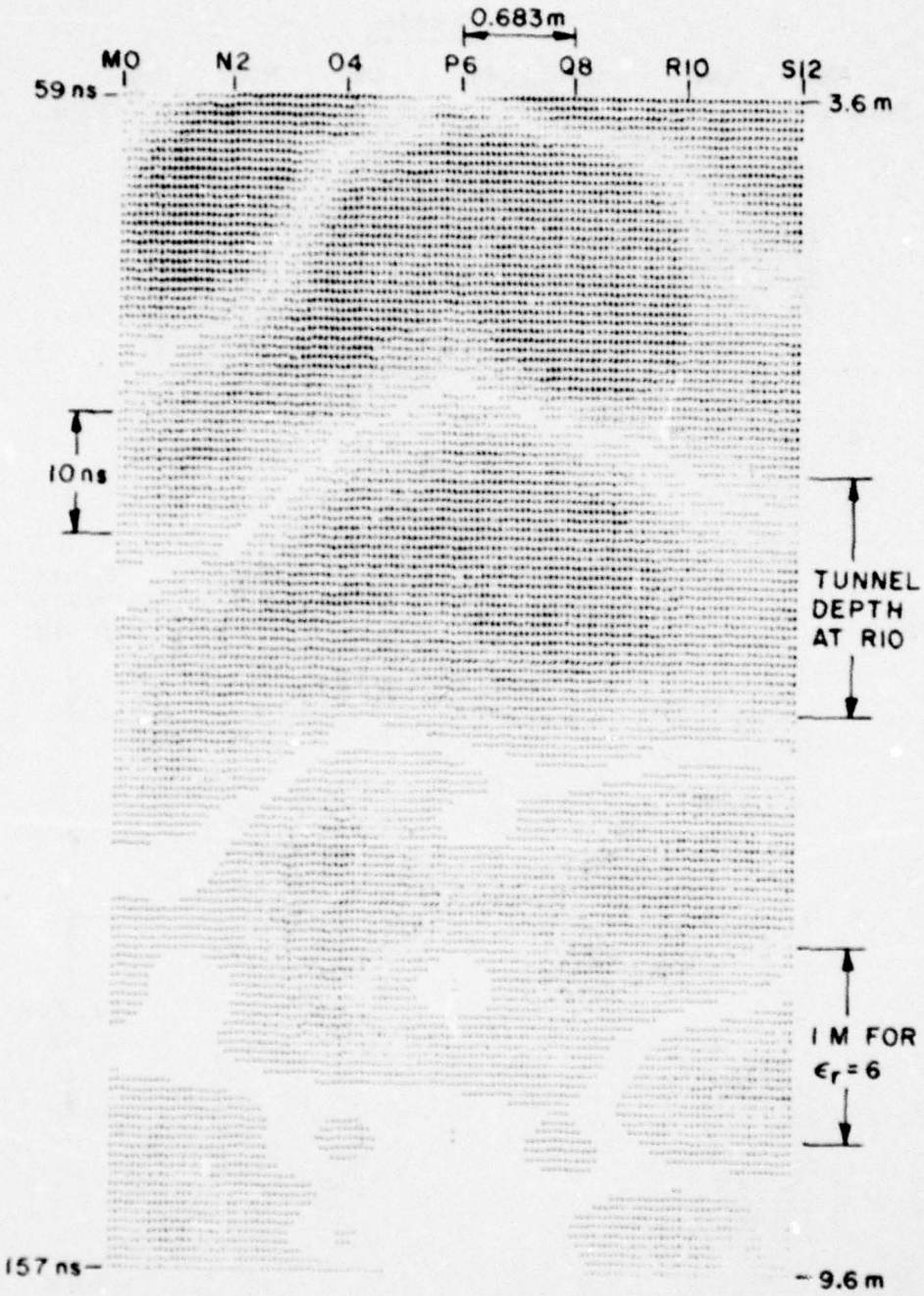

Long Box Antenna
NXDIV=19 NYDIV=0
LIX=3 LIY=1

Clipped at 5.0
Fold Last

GOLD HILL MAP 2

Figure 40. Mapping of the lower traverse over the tunnel.

performed before rectification (Fold Last) and with the black level set at 3.5x5 and 5x5mV, respectively. The actual tunnel position at recording coordinate R10 (position over the tunnel) is shown in all maps for comparison. This is exactly the position shown by the maps at this coordinate. But, the hyperbola does not peak at R10 as it would be expected. It peaks at P6-Q8, although, it does not differ much from position R10. This distortion can be well attributed to a 10^{0} ground slope not accounted for in the maps, which could have made the shortest distance from the tunnel to be at position P6.

In Figure 41 a grey-level map for the top traverse is shown. The actual tunnel position at coordinate U10 is the same as the one given by the map. Again, as discussed previously the hyperbola peaks at positions S6-T8.

It should be noted that in all maps the height of the tunnel at each recording position corresponds to the width of the hyperbola.

Our results as compared to measured ones are very good. In some instances measured and calculated results have a perfect correspondence, while in others, they are very close. The important point to be understood here is that our process is indeed capable of identifying the tunnel. A comparison of our maps with those generated by Stapp enhances the successfulness of the process. Figures 42 and 43 present an example of the maps given by Stapp for the top and lower traverse in Figure 37, respectively. They were produced by direct grey-level mapping of the echoes. As seen, the expected hyperbola which identifies the tunnel is not clearly indicated. More likely, the maps give a confused picture of the tunnel and limited conclusions can be made.

Stapp was forced to use various data processing techniques such as taking the absolute value, average nearest neighbor waveforms and adjusting the level at which the waveforms were clipped etc. Even then the results while acceptable left much room for improvement. However, by including the physical mechanisms, i.e. natural resonances, in the process, these rather arbitrary steps were not necessary and vastly improved maps were obtained.

AD-A078 328 OHIO STATE UNIV COLUMBUS ELECTROSCIENCE LAB F/G 17/9
IMPROVED IDENTIFICATION OF UNDERGROUND TARGETS USING VIDEO-PULS--ETC(U)
OCT 79 I L VOLAKIS N00014-78-C-0049
UNCLASSIFIED ESL-710816-4 NL

2 OF 2
AD-
A078328

END
DATE
FILMED
1-80
DDC

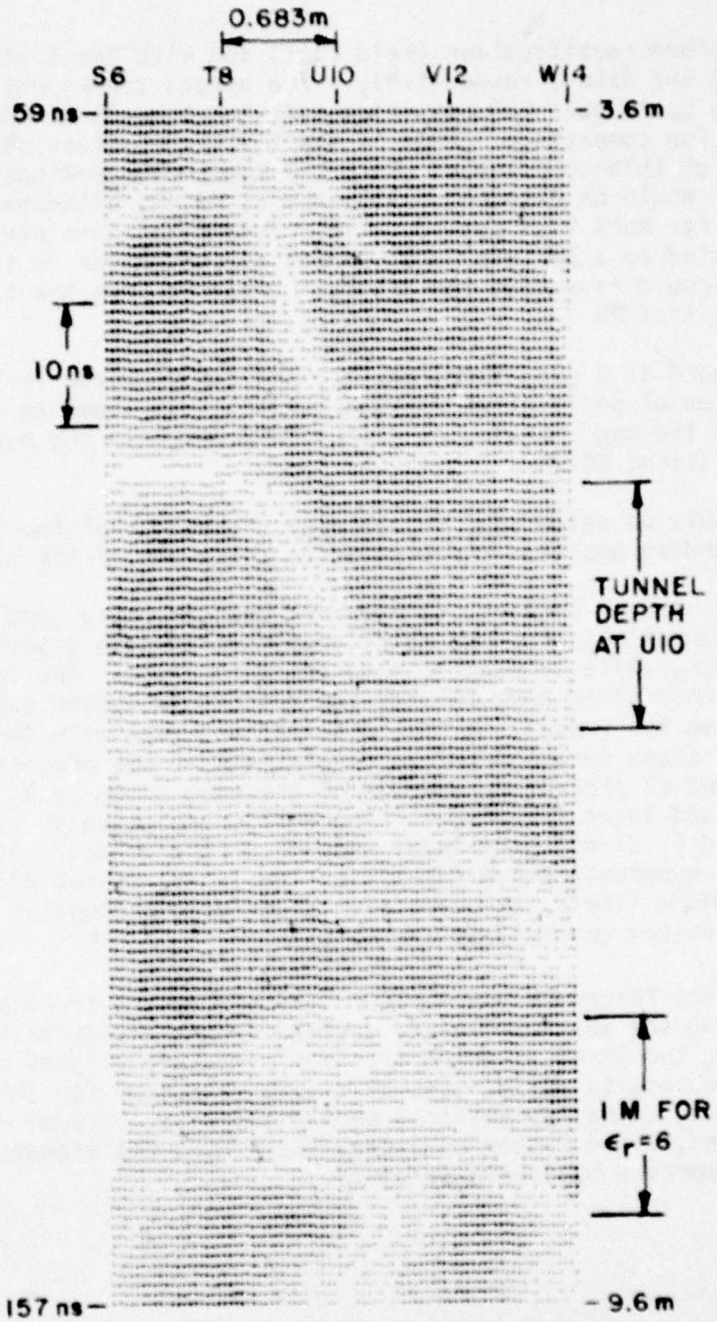

Long Box Antenna
NXDIV=19 NYDIV=0
LIX=3 LIY=1

Clipped at 3.5
Fold Last

GOLD HILL MAP 2

Figure 41. Mapping of the top traverse over the tunnel.

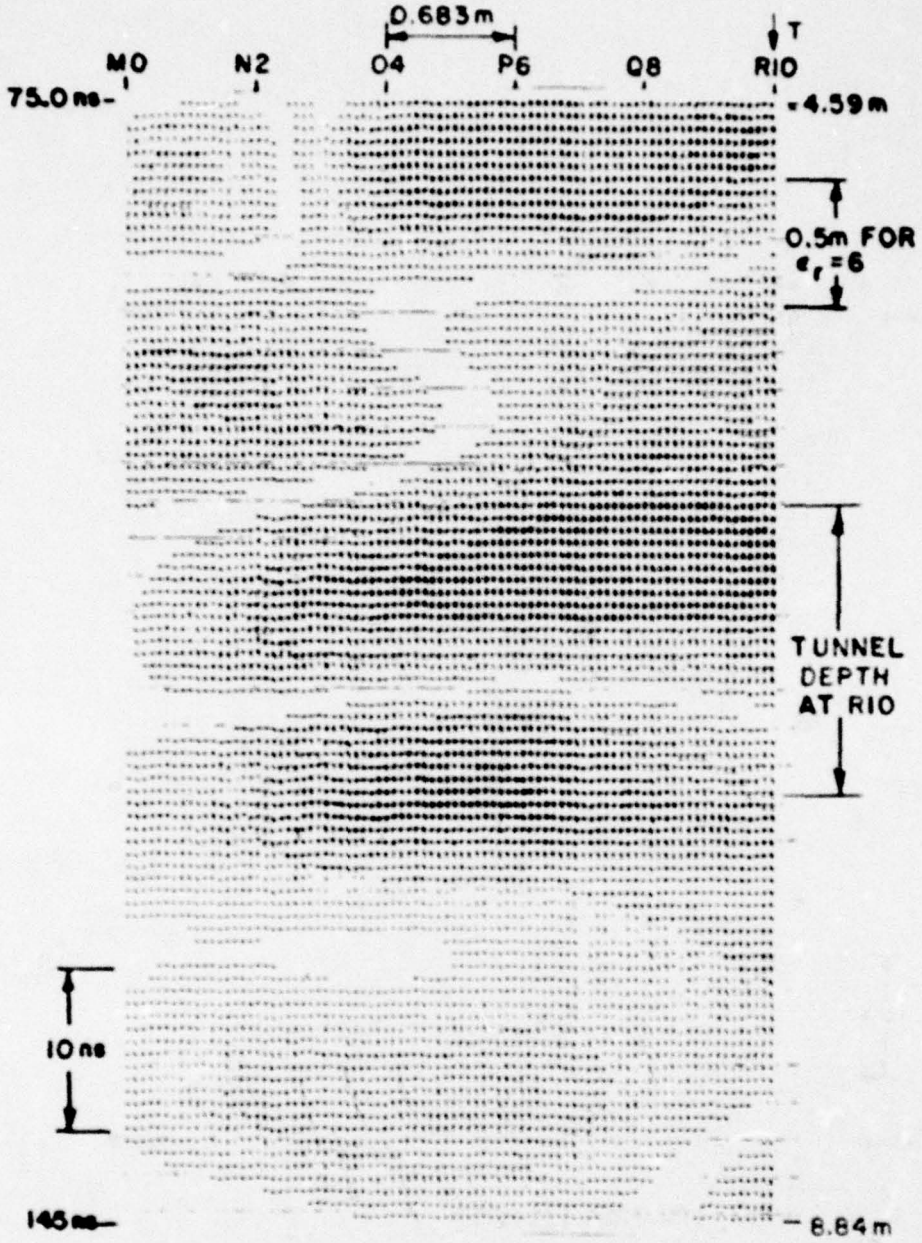

LOW-PASS FILTERED AND AVERAGED IN GROUPS OF 3

Long Box Antenna
NXDIV=16 NYDIV=0
LIX=3 LIY=1

Clipped at 1.61
Fold Last

GOLD HILL MAP 2

Figure 42. Mapping of the lower traverse over the tunnel as given by Stapp [22].

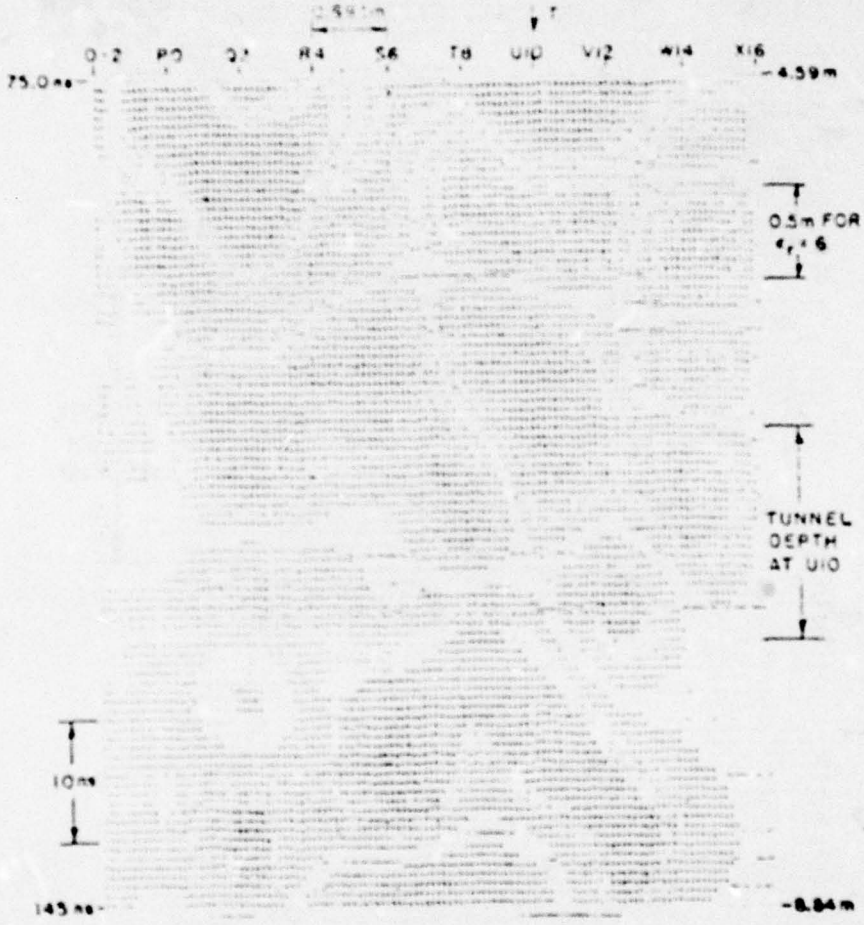

LOW-PASS FILTERED

Long Box Antenna
NXDIV=12 NYDIV=0
LIX=3 LIY=1

Clipped at 1.91
Fold Last

GOLD HILL MAP 2

Figure 43. Mapping of the top traverse over the tunnel as given by Stapp [22].

CHAPTER VI
SUMMARY AND CONCLUSIONS

The tunnel identification process consisted of three main tasks:

1. Recording of the echoes and calculation of their poles by Prony's method.

2. Processing of the echoes:

   a) Removal of the antenna pole pair and other undesired resonances (Chapter II).

   b) Reconstruction of the tunnel response (Chapter III).

3. Determination of tunnel's structure, depth, and relative position (mapping).

We concentrated on the processing of the echoes. The processing procedure was thoroughly analyzed and tested on theoretical (Chapter IV) and measured (Chapter V) tunnel echoes. Methods for identifying and determining the tunnel's structure and depth were outlined. The reconstruction process was used for combating the clutter problem. The relative tunnel position could be obtained by employing the grey-level mapping technique.

Our results from the measured echoes were very good. The tunnel position, depth and height were clearly indicated in the constructed maps, and they did correspond to the actual ones.

Thus, it was demonstrated that our processing can indeed identify and provide us with concise information about an underground tunnel from its backscattered responses.

The processing capability was very accurate as long as the calculated waveform poles by Prony's method are within reasonable accuracy (especially the imaginary part). The inaccuracy of Prony's method when dealing with data dominated by clutter and noise limits our processing capability. Once the proper waveform poles are known, the identification process can be performed within a great accuracy.

An important part of the processing, which can be performed in real time, is that the structure and depth of the tunnel can be determined before mapping. Mapping can give us a better overview of the relative tunnel position. But, it requires extensive computer time and storage, which is undesired. Furthermore, the construction of maps needs many recorded waveforms. This can be a problem since the ground surface may not be smooth enough for the antenna to be properly positioned in many spots.

It should be noted that our processing of the echoes, although it was used for identifying tunnels, is very general. It can be applied to any target backscattered waveform for isolating the target response and combating clutter and noise.

REFERENCES

1. E. M. Kennaugh and D. L. Moffatt, "Transient and Impulse Response Approximations," Proc. of IEEE, Vol. 53, August 1965, pp. 893-901.

2. D. L. Moffatt and R. K. Mains, "Detection and Discrimination of Radar Target," IEEE Trans. on Antennas and Propagation, Vol. AP-23, No. 3, May 1975.

3. J. D. Young and Ross Caldecott, "Underground Pipe Detector," United States Patent No. 3967282 and 4062010.

4. Arthur Eberle and J. D. Young, "The Development and Field Testing of a New Locator for Buried Plastic and Metallic Utility Lines," Transportation Research Board Fifty-Sixth Annual Meeting, Washington, D.C., January 1977, Also published in Transportation Research Record 631 published by Transportation Research Board, Commission on Sociotechnical Systems, National Research Council, National Academy of Sciences, Washington, D.C., pp. 47-52, Library of Congress, JE7,H5, No. 631 (TE175) 380.5' 085 625.7 .

5. L. C. Chan, D. L. Moffatt and L. Peters, Jr., "A Characterization of Subsurface Radar Targets," Proc. of the IEEE, Vol. 67, No. 7, July 1979, pp. 991-1000.

6. L. C. Chan and L. Peters, Jr., "Electromagnetic Mine Detection and Identification," Report 4722-1, December 1978, The Ohio State University ElectroScience Laboratory, Department of Electrical Engineering; prepared under Contract DAAK70-77-C-0114 for U. S. Army Mobility Equipment Research and Development Command, Fort Belvoir, Virginia.

7. L. C. Chan, "Subsurface Electromagnetic Target Characterization and Identification," Ph.D. Dissertation, The Ohio State University ElectroScience Laboratory, Department of Electrical Engineering.

8. L. C. Chan, "A Digital Processor for Transient Subsurface Radar Target Identification," Report 479X-3, December 1975, The Ohio State University ElectroScience Laboratory, Department of Electrical Engineering; prepared for Columbia Gas System Service Corporation, Columbus, Ohio.

9. C. W. Davis, III and L. Peters, Jr., "Summary of Studies on Tunnel Detection Radar System," Report 784460-11, January 1979, The Ohio State University ElectroScience Laboratory, Department of Electrical Engineering; prepared under Contract DAAG-53-76-C-0179 for the U. S. Army Mobility Equipment Research and Development Command, Ft. Belvoir, Virginia.

10. Y. T. Lin, "Classification of Objects With Complex Geometric Shapes by Means of Low Frequency Electromagnetic Responses," Report 3815-1, August 1974, The Ohio State University ElectroScience Laboratory, Department of Electrical Engineering; prepared under Grant AFOSR-74-2611 for Air Force Office of Scientific Research.

11. L. C. Chan and D. L. Moffatt, "Characterization of Subsurface Electromagnetic Soundings," Report 4490-2, December 1978, The Ohio State University ElectroScience Laboratory, Department of Electrical Engineering; prepared under Grant No. ENG76-04344 for National Science Foundation.

12. C. W. Davis, III and R. D. Gaglianello, "A Video Pulse Radar System for Tunnel Detection," Report 784460-9, January 1979, The Ohio State University ElectroScience Laboratory, Department of Electrical Engineering; prepared under Contract DAAG-53-76-C-0179 for the U. S. Army Mobility Equipment Research and Development Command, Ft. Belvoir, Virginia.

13. C. A. Tribuzi, "An Antenna for Use in the Underground (HFW) Radar System," Report 4460-4, The Ohio State University ElectroScience Laboratory, Department of Electrical Engineering; prepared under Contract DAAG53-76-C-1079 for U. S. Army Mobility Equipment Research and Development Command, November 1977.

14. L. W. Wald, "Modification of the HFW Underground Antenna Based on Experimental Studies," M.Sc. Thesis, The Ohio State University ElectroScience Laboratory, Department of Electrical Engineering, December 1978.

15. R. Prony, "Essou experimental et a nalytigus sur le lois de la dilatibilite de fluides elastiques et sur celles del la force expansive de la vapeur de l'alkool, a differentes temperatues," J. l'Ecole Polytech, (Paris), Vol. 1, No. 2, 1795, pp. 24-76.

16. C. W. Chuang and D. L. Moffatt, "Natural Resonances of Radar Targets Via Pronys Method and Target Discrimination," IEEE Trans. on Aerospace and Electronic Systems, Vol. AES-12, No. 5, September 1976, pp. 583-589.

17. M. L. Van Blaricum and R. Mittra, "A Technique for Extracting the Poles and Residues of a System Directly from Its Transient Response," IEEE Trans. on Antennas and Propagation, Vol. AP-23 No. 6, November 1975, pp. 777-781.

18. M. L. Van Blaricum, "Techniques for Extracting the Complex Resonances of a System Directly from Its Transient Response," Ph.D. Dissertation, 1976, University of Illinois at Urbana-Champaign, Department of Electrical Engineering.

19. M. L. Van Blaricum, "An Analysis of Existing Prony's Method Techniques," Mini-Symposium of Modal Analysis of Experimental Data, Albuquerque, New Mexico, March 1977.

20. M. L. Van Blaricum and R. Mittra, "Problems and Solutions Associated with Prony's Method for Processing Transient Data," IEEE Trans. on Antennas and Propagation. Vol. AP-26, No. 4, January 1978, pp. 174-182.

21. Carl E. Baum, "On the Use of Contour Integration for Finding Poles, Zeros, Saddles, and Other Function Values in the Singularity Expansion Method," Mathematics Notes, Note 35, 18 February 1974.

22. D. O. Stapp, "Method for Grey Scale Mapping of Underground Obstacles Using Video Pulse Radar Returns," M.Sc. Thesis, The Ohio State University ElectroScience Laboratory, Department of Electrical Engineering, December 1978.

23. "Tunnel Location Using Subsurface Radar Profiling and Computer Recognition," Final Technical Report GC-C-78-1015, December 1978; GEO-CENTERS, INC; prepared under Purchase Order Number 334182 for The Ohio State University Research Foundation.

24. M. S. Corrington, "Simplified Calculation of Transient Response," Proc. of IEEE, Vol. 53, No. 3, March 1965, pp. 287-292.

25. James A. Cadzow, Discrete Time Systems, Prentice-Hall, 1973.

26. William D. Stanley, Digital Signal Processing, Prentice-Hall, 1975.

27. J. D. Kraus and Keith R. Carver, Electromagnetics, 2nd Ed., McGraw-Hill, Inc., 1973.

APPENDIX A
DERIVATION OF A DIFFERENTIAL EQUATION FOR EXTRACTING ONE COMPLEX CONJUGATE POLE PAIR

Let us assume an original waveform, r(t), with a Laplace representation of

$$R(s) = \mathcal{L}\left[r(t)\right] \quad .$$

In general we can express R(s) as follows:

$$R(s) = \frac{N(s)}{(s-s_1)(s-s_1^*)D(s)} \tag{A1}$$

where (s_1, s_1^*) is the pole pair to be removed.

Multiplying both sides of Equation (A1) by the representation of the pole pair (s_1, s_1^*), we have

$$R_p(s) = (s^2 - 2s\mathrm{Re}(s_1) + |s_1|^2)R(s) = \frac{N(s)}{D(s)} \quad . \tag{A2}$$

$R_p(s)$ is the Laplace representation of the filtered waveform. Its poles are described by D(s).

Transforming $R_p(s)$ to time domain we obtain

$$r_p(t) = \left(\frac{d^2}{dt} - 2\mathrm{Re}(s_1)\,\frac{d}{dt} + |s_1|^2\right)r(t) \tag{A3}$$

where $r_p(t) = \mathcal{L}^{-1}\left[R_p(s)\right]$.

Equation (A3) indicates the analog implementation required for extracting the complex conjugate pole pair (s_1, s_1^*). It is equivalent to the digital one given in Equation (14) (see Chapter II).

In a similar manner we can derive differential equations equivalent to the difference equations given in Chapter II and III.

APPENDIX B
MAIN FORTRAN PROGRAM FOR CALLING THE POLE EXTRACTION AND RECONSTRUCTION ROUTINES, MANIPULATING DATA AND PLOTTING

```
C     * * * * * * * * * * * * * * * * * * * * * * *
C     THIS PROGRAM CALLS THE POLE EXTRACTION AND RECONSTRUCTION
C     PROCESSES
C     * * * * * * * * * * * * * * * * * * * * * * *
C     * * * * TASKS PERFORMED :
C     * 1. FILTERS THE INPUTED WAVEFORM (IFILT=1 OR 0
C          FOR NO FILTERING)
C     * 2. EXTRACTS UP TO 3 CONJUGATE POLE PAIRS (6 POLES).NP
C          (IDECF=1 OR 0 FOR NO POLE EXTRACTION)
C     * 3. THE "FILTERED" WAVEFORM IS CORRECTED IN PHASE
C          AND AMPLITUDE AFTER POLE EXTRACTION(IF SM2=0 NO
C          CORRECTION WILL BE PERFORMED)
C     * 4. FILTERS THE "FILTERED" WAVEFORM FOR RECONSTRUCTION
C          PURPOSES: NOTE THAT BEFORE RECONSTRUCTION OF THE EARLY
C          PORTION, THE WAVEFORM MUST BE CENTERED. (IFILT=1 OR 0 FOR
C          FOR NO FILTERING)
C     * 5. RECONSTRUCTS EARLY PORTION OF A WAVEFORM CHARACTERIZED
C          BY A COMPLEX CONJUGATE POLE PAIR FROM A BASE
C          WINDOW IN ITS LATE PORTION : THE PREDICTOR IS
C          CHOSEN BASED ON THE CRITERION THAT THE NEXT M-REF
C          POINTS MATCH BEST THE ORIGINAL WAVEFORM. (IDECR=1 OR
C          0 FOR NO RECONSTRUCTION)
C     * 6. THE FINAL "FILTERED" WAVEFORM IS STORED
C     * 7. ORIGINAL,POLE EXTRACTED AND RECONSTRUCTED WAVEFORMS
C          ARE PLOTTED OUT.
C     * * * * * * * * * * * * * * * * * * * * * * * * * * *
C     * * * * SELECTION OF OPTIONS :
C     * IDECF=1: POLE EXTRACTION IS PERFORMED                *
C              =0: POLE EXTRACTION ROUTINE IS SKIPPED          *
C     * IDECR=1: RECONSTRUCTION PROCESS IS PERFORMED          *
C              =0: RECONSTRUCTION PROCESS IS SKIPPED           *
C     * IFILT=1: RIDERAND FILTERING CAN BE PERFORMED
C                 BEFORE ANY PROCESSING                       *
C              =0: NO FILTERING IS PERFORMED                  *
C     * IFILT=1:CENTERING OF THE WAVEFORM CAN BE
C                 PERFORMED BEFORE RECONSTRUCTION             *
C              =0 NO FILTERING BEFORE RECONSTRUCTION          *
C     * * NOTE * * IT IS IMPORTANT THAT THE WAVEFORM IS *
C                 CENTERED BEFORE RECONSTRUCTION              *
C     * * * * * * * * * * * * * * * * * * * * * * * * * * *
C     * * * DESCRIPTION OF PARAMETERS:
C     * ND=ARRAY DIMENSION
C     * TB=BASIC SAMPLING INTERVAL OF WAVEFORM IN USEC
C     * TDE=INPUT WAVEFORM
C     * FTWF=FOURIER TRANSFORM OF THE WAVEFORM IN MANIPULATION
C     * TDDEC= "FILTERED" WAVEFORM(POLE EXTRACTED)
C     * TDREC=RECONSTRUCTED WAVEFORM
C     * TDDIFF=DIFFERENCE OF "FILTERED"(TDDEC) &RECONSTRUCTED
C              (TDDEC) WAVEFORMS
C     * TIME=X-AXIS ARRAY FOR PLOTS
C     * SR(I)=REAL PART OF ITH POLE PAIR TO BE EXTRACTED IN MEGAREPS(XE9
      6)
C     * SM(I)=IMAG. PART OF ITH POLE PAIR TO BE EXTRACTED IN MHZ
C     * SM2= IMAG. OF TUNNEL POLE PAIR IN MHZ (USED FOR CORRECTION)
C     * NP=NUMBER OF CONJUGATE POLE PAIRS TO BE EXTRACTED
C     * N=POLE EXTRACTION INTERVAL
C     * NS=WAVEFORM STARTING POINT FOR PROCESSING (ALL PREVIOUS
```

```
C          POINTS TO 'HS' ARE SET TO ZERO
C     * NH1,NH2,NH3=CORNER POINTS OF TYP HALF-TRAPEZOID PASSBAND
C     * ND4=DIMENSION OF ARRAY 'SS'
C     * * * * * * * * * * * * * * * * * * * * * * * * * * * *
      OPTIONS 32K
      OPTIONS DP
      INCLUDE FORTB,LIB2
      INCLUDE MESSE,SYSV
      INCLUDE FLSBS,A04C
      COMPLEX FTWF(256)
C     * * DIMENTION OF ARRAYS:FTWF,TWF,TIME,TWDEC,TWDECB AND
C     * * TWDIFF MUST BE 'ND'
      DIMENSION IDES(14),ISET(14),ICODE(4),IDOR(10),IDEC(10)
      DIMENSION IFILER(2),IUSERR(2),IBLNK(2),TWF(256),SS(64)
     &,TIME(256),TWDEC(256),ILB(6),IST(256),IFILES(2),IUSERS(2)
      DIMENSION TWDECB(256),IDBK(10),IDOC(11),IDIF(10),TWDIFF(256),
     &ISTR(15),NERR(15),IST(2),NBR(2),IFLAG(3),SR(3),SM(3),ZRL(3),
     &ZMAG(3),COEF(6),IDCNV(15),INTR(8),IREC(8),IFELT(11)
      DATA IA,IB/1HA,1HB/
      DATA IDOR/19H--  ORIGINAL WVFRM/
      DATA IDER/23H_.-  RECONSTRUCTED WVFRM/
      DATA IDOC/18H    FILTERED WVFRM/
      DATA IDIF/19HDIFFERENCE WAVEFORM/
      DATA ISTR/22HRECONST. START. POINT=/
      DATA NERR/28HPOINTS USED FOR ERR CALC'TL.=/
      DATA IDCNV/33HEXTRACT. POLE(MHZ) : REAL    IMAG/
      DATA INTR/20HEXTRACTION INTERVAL=/
      DATA IREC/16HRECNS. INTERVAL=/
      DATA IFELT/26HSOLID LINE: FILTERED WVFRM/
      PI=3.141592
      CALL SUPERR(1)
      CALL SUPERR(2)
      CALL SUPERR(3)
      CALL SUPERR(4)
      CALL SUPERR(5)
      CALL SUPERR(6)
      CALL SUPERR(7)
      CALL SUPERR(12)
      CALL SUPERR(13)
      CALL SUPERR(14)
      CALL ASSIGN(6HOUTPT,1,0,0,2)
C     * * * * *
C     * * INPUT DATA
CCC
      NP=0
      ND=256
      ND4=256/4
      TB=200./255
      TWF=TB*25.5
      WRITE(8,5)
5     FORMAT(/1X,'WAVEFORM INPUT')
9000  CALL RDFLNM(IFILER,IUSERR)
      WRITE(8,9001)
9001  FORMAT(1X,'A OR B: ')
      CALL RTEXTS(I,1)
      I=(I.SHIFT.1).SHIFT.-1
      IAOR=I
      IAB=0
      IF(I.SHIFT.-1.EQ.IA.SHIFT.-16)GO TO 9004
      IAB=1
      IF(I.SHIFT.-1.EQ.IB.SHIFT.-16)GO TO 9004
      WRITE(8,9002)
9002  FORMAT(1X,'?')
      GO TO 9000
```

```
      RRRR=1.
      WRITE(8,405)
405   FORMAT('IDECF,IDECB,IFILT,IFILTB=')
      READ(8,-) IDECF,IDECB,IFILT,IFILTB
      NS=YEP(25HENTER WVFRM START. POINT=,25,3)
      NS1=NS+1
      LIMIT=YEP(29HDO YOU WISH SCALE ADJUSTMENT?,29,1)
C     * * * * * * * *
C     * * OUTPUT STORAGE DATA
      WRITE(8,888)
888   FORMAT(1X,'OUTPUT STORAGE DATA ')
      CALL RDFLNM(IFILES,IUSERS)
      WRITE(8,8001)
8001  FORMAT(1X,'A(0) OR B(1) ')
      READ(8,-) IABS
C     * * * * *
      NWF=YEP(28HNUMBER OF WVFRMS TO PROCESS=,28,3)
      IDSN=YEP(9HDEASSIGN?,9,1)
      DO 2000 NR=1,NWF
      CALL RWDBFL(TWF,ND,1,0,IFILER,IUSERR,IAB,0,IERR)
      IF((IDECF.EQ.0).AND.(IDECB.EQ.1)) GO TO 333
      IF(NS.EQ.0) GO TO 9006
      DO 9005 I=1,NS
9005  TWF(I)=0.
9006  RR=1.
      IF(NR.GT.1) GO TO 343
      IDC=YEP(11HDC REMOVAL?,11,1)
343   RR=1.
      IF(IDC.EQ.0) GO TO 333
C     * * DC SHIFTING
      SUMM=0.
      DO 1000 I=NS1,ND
1000  SUMM=SUMM+TWF(I)
      SUMM=SUMM/((ND-NS1)+1)
      DO 1001 I=NS1,ND
1001  TWF(I)=TWF(I)-SUMM
333   RR=1
C     * * * * *
      IF(IFILT.EQ.0) GO TO 1999
C     * * FILTERING
      NH1=1
      NH2=20
      NH3=25
      CALL FILT(TWF,SS,FTWF,NH1,NH2,NH3,NS,ND,ND4)
1999  CONTINUE
C     * * * * *
      IF(IDECF.EQ.0)GO TO 14
C     * * POLE EXTRACTION PROCESS
      CALL POLEX(TWF,TWDEC,SR,SM,TB,ND,N,NP,NA,IAMP)
      IF(LIMIT.EQ.0) GO TO 910
C     * *FIND SCALE FACTOR FOR PLOTING(FR)
      FMAX=0.
      DO 909 I=1,ND
      IF(ABS(TWDEC(I)).GT.FMAX) FMAX=ABS(TWDEC(I))
909   IF(ABS(TWF(I)).GT.FMAX) FMAX=ABS(TWF(I))
      WRITE(8,908) FMAX
908   FORMAT(2X,"FMAX=",1PG10.3)
      FR=4./FMAX
      GO TO 13
910   FR=1.
```

```
      GO TO 13
14    RRR=1.
      DO 100 I=1,ND
100   TWDEC(I)=TWF(I)
13    CONTINUE
      IF(NW.GT.1) GO TO 344
      IDCR=YESP('HDC REMOVAL?',1),1)
344   RR=1.
      IF(IDCR.EQ.0) GO TO 334
C     * * DC SHIFTING
      SUMM=0.
      DO 399 I=NS1,ND
399   SUMM=SUMM+TWDEC(I)
      SUMM=SUMM/((ND-NS1)+1)
      DO 499 I=1,ND
499   TWDEC(I)=TWDEC(I)-SUMM
334   RR=1.
C     * * * * *
      IF(IFILTB.EQ.0) GO TO 400
C     * * FILTERING
      CALL FILT(TWDEC,SS,FTWF,NH1,NH2,NH3,NS,ND,ND4)
400   RR=1.
C     * * * * *
CCC   * * RECONSTRUCTION OF EARLY PORTION OF THE
CCC       "FILTERED" WAVEFORM
      IF(IDECB.EQ.0)GO TO 120
      CALL RECONS(TB,TWDEC,TWDECB,KG,NER,NN,ND,NW)
      IF(LIMIT.EQ.0) GO TO 905
C     * * FIND SCALE FACTOR FOR PLOTING(FR)
      BMAX=0.
      DO 904 I=1,ND
      IF(ABS(TWDECB(I)).GT.BMAX) BMAX=ABS(TWDECB(I))
904   IF(ABS(TWF(I)).GT.BMAX) BMAX=ABS(TWF(I))
      WRITE(8,903) BMAX
903   FORMAT(2X,"FMAX=",1PG10.3)
      FR=4./BMAX
      GO TO 120
905   FR=1.
120   RR=1.
C     * * LIMIT MAX OUTPUT TO 4 UNITS(VOLTS)
      IF(LIMIT.EQ.1) GO TO 45
      DO 44 I=1,ND
      IF(TWF(I).GT.4.) TWF(I)=4.
      IF(TWF(I).LT.-4.) TWF(I)=-4.
      IF(TWDEC(I).GT.4.) TWDEC(I)=4.
      IF(TWDEC(I).LT.-4.) TWDEC(I)=-4.
      IF(TWDECB(I).GT.4.) TWDECB(I)=4.
      IF(TWDECB(I).LT.-4.) TWDECB(I)=-4.
44    CONTINUE
45    RR=1.
C     * * * * *
      IDFB=1
      IF((IDECF.EQ.0).AND.(IDECB.EQ.0)) IDFB=0
      IF(IDFB.EQ.0) GO TO 444
C     * * * * *
C     * * STORAGE OF "FILTERED OR RECONSTRUCTED WAVEFORM
      IF(NW.GT.1) GO TO 278
      WRITE(8,555)
555   FORMAT('STORAGE')
      WRITE(8,277)
```

```
      241 277   FORMAT('ENTER FLNM AND DESCR. TEXT')
      242       CALL RTLXT(IFLNM,3)
      243       CALL RTEXT(IDES,14)
      244 278   KK=1.
      245       ICODE(1)=-2
      246       ICODE(2)=ND
      247       ICODE(4)='11111111
      248       IF(IDECF.EQ.1.AND.IDECB.EQ.1)GO TO 222
      249       IF(IDECF.EQ.1)GO TO 222
      250       CALL RWDBFL(TWDEC,ND,IDES,32,IFILES,IUSERS,IABS,1,IERR)
      251       GO TO 223
      252 222   CALL RWDBFL(TWDECB,ND,IDES,32,IFILES,IUSERS,IABS,1,IERR)
      253 223   CONTINUE
      254 C     * * * * *
      255       IF(NR.GT.1) GO TO 2007
      256 C     * * * * *
      257       FKG=KG
      258       FNEN=NEN
      259       NN=N
      260       NNN=NN
      261       DO 443 K=1,NF
      262       SR(K)=SR(K)*(1.E-6)
      263       SM(K)=SM(K)*(1.E-6)
      264 443   KK=1.
      265 444   KK=1.
      266 C     * * * * *
      267 C     * *CONSTRUCTION OF TIME ARRAY
      268       TIME(1)=0.
      269       DO 1111 I=2,ND
      270 1111  TIME(I)=TIME(I-1)+TB
      271 C     * * * * *
      272 C     * * PLOT OF THE ORIGINAL,"FILTERED",AND/OR
      273 C         RECONSTRUCTED WAVEFORM
      274       PAUSE
      275       DFR=2./FR
      276       SFR=-4./FR
      277       DO 24 I=1,ND
      278       TWF(I)=-TWF(I)
      279       TWDEC(I)=-TWDEC(I)
      280       TWDECB(I)=-TWDECB(I)
      281       IF(LIMIT.EQ.1) GO TO 24
      282       IF(TWF(I).GT.4.) TWF(I)=4.
      283       IF(TWF(I).LT.-4.) TWF(I)=-4.
      284       IF(TWDEC(I).GT.4.) TWDEC(I)=4.
      285       IF(TWDEC(I).LT.-4.) TWDEC(I)=-4.
      286       IF(TWDECB(I).GT.4.) TWDECB(I)=4.
      287       IF(TWDECB(I).LT.-4) TWDECB(I)=-4.
      288 24    KK=1.
      289       CALL ASNPLT(100,3)
      290       CALL PLOT(3.6,1.5,-3)
      291       CALL FACTOR(.8)
      292       CALL AXIS(2.,0.,IK ,1.4,180.,SFR,
      293      &DFR,1.,1)
      294       CALL AXIS(0.,0.,11HTIME (MSEC),-11,10.,90.,0.,TWK,
      295      &1.,1)
      296       CALL LINE(TWDEC,0.0,DFR,TIME,0.0,TWK,ND,0,3)
      297       IF((IDECF.EQ.0).AND.(IDECB.EQ.1)) GO TO 21
      298       IF((IDECF.EQ.1).AND.(IDECB.EQ.1)) GO TO 21
      299       CALL STRYP(TWF,0.0,DFR,TIME,0.0,TWK,ND,1,-3)
      300 21    CONTINUE
```

```
      IF(IDECE.EQ.0)GO TO 22
      CALL STRYP(TRDECH,0.0,DFR,TIME,0.0,TMR,ND,1.,-6)
22    CONTINUE
      CALL SYMBOL(2.1,4.8,.11,IFLUX,90.,9)
      CALL SYMBOL(2.1,6.,.11,IDES,90.,30)
      CALL SYMBOL(2.3,6.,.11,IDOR,90.,30)
      IF(IDFB.EQ.1) GO TO 666
      CALL SYMBOL(2.5,6.,.11,IFELT,90.,30)
      GO TO 777
666   CONTINUE
      CALL AXIS(2.5,6.,111.,0.,30,90.,0.,0.,0.,0)
      CALL SYMBOL(2.5,6.,.11,IDOC,90.,30)
      SK=2.7
      IF(IDECF.EQ.0) GO TO 17
      IF((IDECB.EQ.1).AND.(IDECF.EQ.1)) SK=3.5
      CALL SYMBOL(SK,6.,.11,INTH,90.,20)
      CALL NUMBER(SK,8.5,.11,RN,90.,-1)
17    CONTINUE
      IF(IDECB.EQ.0) GO TO 28
      SKK=SK+.2
      IF(SK.EQ.3.5) SKK=2.7
      IF(IDECF.EQ.0) SKK=SK
      CALL SYMBOL(SKK,6.,.11,IDUR,90.,30)
      SKK=SKK+.2
      CALL SYMBOL(SKK,6.,.11,ISTP,90.,30)
      CALL NUMBER(SKK,9.2,.11,FAC,90.,-1)
      SKK=SKK+.2
      CALL SYMBOL(SKK,6.,.11,MENR,90.,30)
      CALL NUMBER(SKK,9.2,.11,FNER,90.,-1)
      SKK=SKK+.2
      CALL SYMBOL(SKK,6.,.11,IREC,90.,20)
      CALL NUMBER(SKK,8.5,.11,RNN,90.,-1)
28    CONTINUE
      IF(IDECF.EQ.0) GO TO 211
      SI=SKK+.4
      IF(IDECE.EQ.0) SI=SK+.2
      CALL SYMBOL(SI,6.,.11,INCNV,90.,33)
      SI=SI+.2
      DO 155 K=1,NP
      CALL NUMBER(SI,8.2,.11,SR(K),90.,2)
      CALL NUMBER(SI,9.2,.11,SM(K),90.,2)
      SI=SI+.2
155   CONTINUE
211   CONTINUE
      DO 212 I=1,NP
      SR(I)=SR(I)*(1.E6)
212   SM(I)=SM(I)*(1.E6)
      CALL PLOT(0.125,-2.3,-3)
777   CONTINUE
C     * * * * *
      IF((IUSR.EQ.1).AND.(MM.EQ.1)) GO TO 2006
      GO TO 2007
2006  RR=1.
      CALL DEASSN
2007  RR=1.
C     * * * * *
C     * *INCREMENT INPUT AND OUTPUT FILE NAMES
      DO 999 I=1,ND
      TMDEC(I)=0.
999   TMDECH(I)=0.
```

```
      IF(NWF.EQ.1) GO TO 2000
      IAB=(IAB+1)/2
      IABS=(IABS+1)/2
      IF(IAB.NE.0) GO TO 2001
      IAB=1
      GO TO 2002
2001  IAB=0
      CALL INCFIL(IFILER,IUSERR)
2002  RR=1
      IF(IABS.NE.0) GO TO 2004
      IABS=1
      GO TO 2600
2004  IABS=0
      CALL INCFIL(IFILES,IUSERS)
2600  CONTINUE
      CALL EXIT
      END
C              ****************
      SUBROUTINE FILT(TWF,SS,FTWF,NH1,NH2,NH3,NS,ND,ND4)
C     * * * THIS SUBROUTINE FILTERS THE SPECTRUM OF A GIVEN
C           WAVEFORM,'TWF',THROUGH A HALF TRAPEZOID, DEFINED
C           BY NH1,NH2,NH3.
C     * * * * * * * * * * * * * * * * * * * * * * * * * * * * * *
C     * * * DESCRIPTION OF PARAMETERS:
C     >>TWF=DISCRETE WAVEFORM TO BE FILTERED
C     >>FTWF=COMPLEX SPECTRUM OF 'TWF'
C     >>NS=STARTING POINT OF THE INPUT  WAVEFORM(TWF);ALL POINTS
C          PREVIOUS TO THIS ARE SET TO ZERO.
C     >>ND=DIMENSION OF THE INPUT WAVEFORM
C     >>ND4=ND/4;DIMENSION OF THE ARRAY 'SS'
C     >>SS=ARRAY TO BE USED BY SUBROUTINE  'FORT'
C     >>NH1=FIRST CORNER OF TRAPESOIDAL FILTER
C     >>NH2=SECOND CORNER OF TRAPESOIDAL FILTER
C     >>NH3=THIRD CORNER OF TRAPESOIDAL FILTER
C     * * * THE OUTPUT IS RETURNED IN 'TWF' * * *
C     * * * * * * * * * * * * * * * * * * * * * * * * * * * * * *
      DIMENSION SS(ND4),TWF(ND)
      COMPLEX FTWF(ND)
      ND2=ND/2
      ND2P=ND2+1
      II=ND
      DO 40 I=1,50
      II=II/2
      N=I
      IF(II.EQ.1) GO TO 41
40    RR=1.
41    RR=1.
      IF(NS.EQ.0) GO TO 39
      DO 1002 I=1,NS
1002  TWF(I)=0.
33    RR=1.
34    RR=1.
      DO 31 I=1,ND
31    FTWF(I)=CMPLX(TWF(I),0.0)
      CALL FORT(FTWF,N,SS,-1,IERR)
      DO 34 I=1,NH1
34    FTWF(I)=CMPLX(0.0,0.0)
      DO 35 I=NH3,ND2
35    FTWF(I)=CMPLX(0.0,0.0)
      IF(NH2.EQ.NH3) GO TO 37
```

```
      DO 36 I=NH2,NH3
36    FTWF(I)=((NH2-I)*FTWF(I))/(NH3-NH2)
37    RRR=1
      FTWF(ND2P)=CMPLX(0.,0.)
      DO 38 I=2,ND2
      J=ND*2-I
38    FTWF(J)=CONJG(FTWF(I))
      CALL FORT(FTWF,N,SS,1,IERR)
      DO 455 I=1,ND
455   TWF(I)=REAL(FTWF(I))
      RETURN
      END
```

APPENDIX C
THE POLE EXTRACTION SUBROUTINE

```
      SUBROUTINE POLEX(TRF,TRDEC,SR,SM,TB,ND,N,NP,MU,IAMP)
C     * * *THIS SUBROUTINE HAS THE CAPABILITY OF EXTRACTING
C          A MAXIMUM OF 3 COMPLEX CONJUGATE POLE PAIRS(6 POLES) OUT
C          OF AN INPUTED DISCRETE WAVEFORM 'TRF'.
C     *   * * * *  * * * * * * * * * * * * * * * * * * * * * * * *
C     >> DESCRIPTION OF PARAMETERS:
C     >> ND=DIMENSION OF INPUT WAVEFORM
C     >> TRF=INPUT WAVEFORM
C     >> TRDEC="FILTERED" WAVEFORM (POLE EXTRACTED)
C     >> NP=NUMBER OF CONJUGATE POLE PAIRS(MAX OF 3)
C     >> N=POLE EXTRACTION INTERVAL
C     >> SR(I)=REAL PART OF ITH POLE PAIR TO BE EXTRACTED IN
C                NEPERS(*E06)
C     >> SM(I)=IMAG PART OF ITH POLE PAIR TO BE EXTRACTED IN
C                MHZ
C     >> TB=WAVEFORM BASIC SAMPLING INTERVAL
C     >> SM2=IMAG PART OF TUNIEL POLE PAIR IN MHZ (USED FOR
C          CORRECTIONS)
C     >> MU=NUMBER OF WAVEFORMS TO PROCESS
C     >> IAMP: IF EQUAL TO '1' AMPLITUDE CORRECTION IS PERFORMED:
C     >>         IF EQUAL TO '0' NO AMPLITUDE CORRECTION
C     * * * * * * * * * * * * * * * * * * * * * * * * * * * * * *
      DIMENSION TRF(ND),TRDEC(ND),SR(3),SM(3)
      DIMENSION COEF(6),ZRL(3),ZMAG(3)
      PI=3.141592
      IF(IAMP.GT.1) GO TO 900
      IAMP=YES(2HAMPLITUDE CORRECTION?,21,1)
      WRITE(6,905)
905   FORMAT('ENTER # OF CONJG. POLE PAIRS TO EXTRACT: NP=')
      READ(5,*) NP
      WRITE(6,905)
      FORMAT('ENTER EXTRACT. INTERVAL,N=')
      READ(5,*) N
      DO 901 I=1,NP
      WRITE(6,902)
902   FORMAT('ENTER POLE PAIR:REAL,IMAG (*E06)=')
      READ(5,*) SR(I),SM(I)
      SR(I)=SR(I)*(1.E06)
      SM(I)=SM(I)*(1.E06)
906   T=N*TB*(1.E-6)
      ZRL(I)=EXP(SR(I)*T)*COS(2*PI*SM(I)*T)
      ZMAG(I)=EXP(2*SM(I)*T)
901   CONTINUE
      NPL=NP+1
      IF(NPL.GT.3) GO TO 401
      DO 400 I=NPL,3
      ZRL(I)=0.
400   ZMAG(I)=0.
401   NN=1.
      COEF(1)=2*(ZRL(1)+ZRL(2)+ZRL(3))
      COEF(2)=ZMAG(1)+ZMAG(2)+ZMAG(3)+4*(ZRL(1)*ZRL(2)
     +ZRL(2)*ZRL(3)+ZRL(3)*ZRL(1))
      COEF(3)=2*(ZMAG(1)*(ZRL(2)+ZRL(3))+ZMAG(2)*(ZRL(1)+ZRL(3))
     +ZMAG(3)*(ZRL(1)+ZRL(2))+4*ZRL(1)*ZRL(2)*ZRL(3))
```

```
      COEF(4)=ZMAG(1)*ZMAG(2)+ZMAG(2)*ZMAG(3)
     &+ZMAG(1)*ZMAG(3)+4*ZMAG(1)*ZRL(2)*ZRL(3)+
     &+4*ZMAG(2)*ZRL(1)*ZRL(3)+4*ZMAG(3)*ZRL(1)*ZRL(2)
      COEF(5)=2*(ZMAG(1)*ZMAG(2)*ZRL(3)+ZMAG(1)*ZMAG(3)*ZRL(2)
     &+ZMAG(2)*ZMAG(3)*ZRL(1))
      COEF(6)=ZMAG(1)*ZMAG(2)*ZMAG(3)
      K=2*NP*N+1
      M=K-1
      SUM=0.
      NB=2*NP
      DO 90 I=1,NB
   90 SUM=SUM+COEF(I)**2
      SUMS=SQRT(1+SUM)
      SUMS=1.
      DO 911 J=1,N
      DO 910 I=K,ND,N
      TWDEC(I)=TWF(I)
      SK=1.
      DO 930 JK=1,NB
      SK=-1*SK
      MM=I-(JK*N)
      TWDEC(I)=TWDEC(I)+SK*COEF(JK)*TWF(MM)
  930 RR=1.
  910 TWDEC(I)=TWDEC(I)/(SUMS)
      K=K+1
  911 CONTINUE
      DO 940 I=1,N
  940 TWDEC(I)=0.
      IF(NM.GT.1) GO TO 947
      WRITE(8,941)
  941 FORMAT('EXTRACTED POLE PAIR#')
      WRITE(8,948)
  948 FORMAT('      REAL          IMAG')
      DO 943 I=1,NP
      WRITE(8,942) SR(I),SM(I)
  942 FORMAT(2F12.1)
  943 CONTINUE
      WRITE(8,944)
  944 FORMAT('COEFFICIENTS#')
      DO 946 I=1,NB
      WRITE(8,945) COEF(I)
  945  FORMAT(F20.6)
  946 RR=1.
  947 RR=1.
C     * * * * *
C     * * CORRECTION
      IF(IAMP.EQ.0) GO TO 5
      WRITE(8,977)
  977 FORMAT('ENTER IMAG(E06) OF TUNNEL POLE PAIR=')
      READ(8,-) SM2
      IF(SM2.EQ.0.) GO TO 6
      SM2=1.E06*SM2
      T=TB*N*1.E-9
    5 RR=1.
C     * * * * *
      DO 6 K=1,NP
CCC   * * AMPLITUDE FACTOR CORRECTION* *
      IF(IAMP.EQ.0) GO TO 7
      FACTR=2*(EXP(SR(K)*T))*(COS(2*PI*SM2*T)-COS(2*PI*SM(K)*T))
      DO 4 I=1,ND
    4 TWDEC(I)=TWDEC(I)/FACTR
    7 RR=1.
CCC   * * PHASE CORRECTION * *
      DO 3 I=1,ND
      IN=I
      II=I+N
```

```
      IF(II.GT.ND) GO TO 18
    5 IWDEC(I)=IWDEC(II)
   18 KK=1.
      DO 19 I=IN,ND
   19 IWDEC(I)=0.
    6 CONTINUE
  111 KK=1.
      RETURN
      END
```

APPENDIX D
THE POLE RECONSTRUCTION SUBROUTINE

```
      SUBROUTINE RECONS(TB,TWDEC,TWDECR,KG,MER,NN,ND)
      DIMENSION TWDEC(ND),TWDECR(ND)
C     * * * THIS SUBROUTINE RECONSTRUCTS THE EARLY PORTION
C           OF A GIVEN DISCRETE WAVEFORM CHARACTERIZED BY
C           A COMPLEX CONJUGATE POLE PAIR BASED ON ITS LATE
C           TIME RESPONSE.
C     >>TWDEC(I)="FILTERED" WVFRM (INPUT)
C     >>TWDECR(I)=RECONSTRUCTED WVFRM USING THE LATE
C     >>PORTION OF THE "FILTERED" WVFRM
C     >>NN=RECONSTRUCTION INTERVAL;MUST SATISFY SHANNON'S THEOREM
C     >>ND=INPUT ARRAY DIMENSION
C     >>KG=RECONSTRUCTION START. POINT, CALCULATED FROM THE END
C     >>OF THE "FILTERED" WVFRM
C     >>SR2=REAL PART OF RECONSTRUCTED POLE PAIR IN MEPERS(XE06)
C     >>SI2=IMAG PART OF   ''          ''  ''  ''  ''  ''
C     >>  THE CALCULATION OF 'KG' IS BASED ON THE BEST MATCH OF THE
C     >>  "FILTERED" AND RECONST. WVFRMS ON A ARBITRARILY SELECTED #
C     >>  OF POINTS,'MER',IMMEDIATELY FOLLOWING THE WINDOW OF THE
C     >>  "FILTERED" WVFRM USED FOR RECONSTRUCTION
C     * * * * * * * * * * * * * * * * * * * * * * * * * * * * * *
      PI=3.141592
      WRITE(6,233)
233   FORMAT('ENTER RECNS. INTERVAL=')
      READ(6,-) NN
      KA=120
      TT=TB*1E
      WRITE(6,139)
139   FORMAT('POLE OF THE "FILTERED" WVFRM')
      WRITE(6,149)
149   FORMAT('REAL(*E06),IMAG(*E06,HZ)=')
      READ(6,-) SR2,SI2
      SR2=SR2*1.E06
      SI2=SI2*1.E06
      ARG2=SR2*TT*1.E-9
      CARG2=SI2*2*PI*TT*1.E-9
      HZD=(-2)*EXP(ARG2)*COS(CARG2)
      SQZD=EXP(2*ARG2)
      COEF3=1/(SQZD)
      COEF4=HZD/(SQZD)
      SUM2=SQRT(1+COEF3**2+COEF4**2)
      WRITE(6,111) COEF3,COEF4
111   FORMAT(2X,'COEF3=',F7.4,2X,'COEF4=',F7.4)
      WRITE(6,112) SR2,SI2
112   FORMAT(2X,'SR2=',F15.3,'SI2=',F15.3)
      CDIF=1.E-3
      NN1=NN-1
      AJ=0
      MER=YES(34HPOINTS TO BE USED IN ERR. CALCUL.=,34,3)
CCC   >>NSS=# OF PTS FROM THE END OF WVFRM
      NSS=YES(17HSEARCH START. PT=,17,3)
      NES=YES(14HSEARCH END PT=,14,3)
      DO 134 KK=NSS,NES
      KZ=KK
```

```
      IF(KK.EQ.NES) MM=KG
      IF(KK.EC.NES) KJ=1
      DO 130 II=1,KK
      JJ=ND+1-II
      TMDECB(JJ)=TMDEC(JJ)
130   CONTINUE
      DO 110 III=1,NN
      DO 115 II=MM,NDM,NN
      JJ=ND-II
      JA=JJ+2*NN
      JB=JJ+NN
      SUM2=1.
115   TMDECB(JJ)=(-COEF3*TMDECB(JA)-COEF4*TMDECB(JB))/(SUM2)
      MM=MM+1
110   CONTINUE
C     * * * * *
C     * * SELECTION OF A GOOD PREDICTOR
      IF(KJ.EC.1)GO TO 137
      JK1=ND-NER-KK
      JK2=JK1+NER-1
      DIFF=0.
      DO 131 I=JK1,JK2
      DIFF=DIFF+((TMDEC(I)-TMDECB(I))**2)
131   KK=1.
      DIFF=DIFF/NER
      IF(DIFF.GT.CDIF)GO TO 135
      CDIF=DIFF
      KG=KK
135   CONTINUE
134   KK=1.
137   KK=1.
      WRITE(8,138) KG
138   FORMAT('GOOD START.POINT=',I4)
120   KK=1.
      RETURN
      END
```

APPENDIX E
THE TRANSMISSION LINE COMPUTER MODEL WITH ADDITIONAL RESULTS

```
1 CCC * * TRANSMISSION LINE MODEL OF AN ANTENNA-TUNNEL
2 CCC                 STRUCTURE
3       OPTIONS 32K
4       INCLUDE ADLDGB,404C
5       INCLUDE FLSBS,404C
6       INCLUDE FORTE,LIB2
7       COMMON GAUSS,SS
8       DIMENSION IER(2),IMR(2),IDISTA(5),IDIST(5),IPOLA(6),
9      &IPOLT(6),ISIGMA(3),INTR(6),IREF(5)
10      DIMENSION  IDES(14),ISET(14),ICODE(4),IFILE(2),IUSER(2)
11      DIMENSION IFUNM(4),TIMEG(512),TWFG(512),IRA(4),IRT(4)
12 CCC   >>DIMENSION OF SS MUST BE NDFREQ/4
13      DIMENSION TWF(256),TIME(256),TWFF(512),SS(2048)
14 CCC   >>COMPLEX VOUT(NFREQ),GAUSS(NDFREQ),ZA(NFREQ), . . .
15      COMPLEX VOUT(4096),GAUSS(8192)
16      COMPLEX CFREQ,GAMAS,ZOARG,GAMA,ZTEQU,ZA,ZAEQU,ZT,
17     &ZO,CTANG,ZIN,CPOLA,CPOLT,POLA,POLT,NUM,DEN
18      COMPLEX ZAO,ZVO,ZTRA,ZRESA,ZREFT,ZDV1
19      EQUIVALENCE(GAUSS(4097),VOUT(1))
20      REAL MR,MU
21      DATA IREF/13HIST ECHO ONLY/
22      DATA INTR/12HINTER. RES.=/
23      DATA IA,IB/1HA,1HB/
24      DATA IER,IMR/3HER=,3HMR=/
25      DATA IDISTA,IDIST/11HANT. DIST.=,12HTARG. DIST.=/
26      DATA IPOLA,IPOLT/15HANT. POLE(MHZ)=,16HTARG. POLE(MHZ)=/
27      DATA ISIGMA/6HSIGMA=/
28      DATA IRA//10HANT. RES.=/
29      DATA IRT/11HTARG. RES.=/
30      CALL ASNDEL(6HOUT112,0,0,2)
31 C     * * * * *
32 C     * * INPUT DATA
33 C     * * * * *
34 C     >>FREQ=EXCITATION FREQUENCY
35 C     >>DIST=TRANSMISSION LINE LENGTH
36 C     >>ER=RELATIVE PERMITIVITY
37 C     >>MR=RELATIVE PERMEABILITY
38 C     >>SIGMA=CONDUCTIVITY
39 C     >>SIGT,SIGA=REAL PART OF TUNNEL&ANTENNA POLES,RESPECTIVLY(E6)
40 C     >>FREQT,FREQA=IMAG PART "   "      "      "      "      "     (MHZ)
41 C     >>RST,RSA=RESIDUES   OF     "      "      "      "
42 C     >>  NOTE:THESE MUST BE LARGE FOR A REAL SYSTEM(E9)
43 C     >>UOH GAUSSIAN PULSE DURATION
44 C     >>VOUT(I)=SYSTEM'S TRANSFER FUNCTION
45 C     >>GAUSS=SPECTRUM OF GAUSSIAN PULSE
46 C     >>TWFG(I)=OUTPUT LONG TIME RESPONSE
47 C     >>TWF(I)=SELECTED WINDOW FROM TWFG OF LENGTH NPNTS POINTS
48 C     >>       FOR TIME EXPANSION
49 C     >>TB=BASIC SAMPING INTERVAL OF TWF IN NSEC
50      WRITE(8,10)
51 10    FORMAT('ENTER DIST.,DISTANT,ER,MR,SIGMA=')
52      READ(8,-) DIST,DISTA,ER,MR,SIGMA
53 CCC   >>TARGET & ANTENNA POLES
54      WRITE(8,20)
```

```
      20    FORMAT('ENTER TARG. & ANT. POLES#')
            WRITE(8,25)
      25    FORMAT('SIGT,FREQT(MHZ),RST,SIGA,FREQA(MHZ),RSA=')
            READ(8,-) SIGT,FREQT,RST,SIGA,FREQA,RSA
            WRITE(8,140)
  140       FORMAT('GAUSSIAN PULSE DURATION(NSEC)=')
            READ(8,-) DURA
            IECHO=YESP(14HIST ECHO ONLY?,14,1)
            DUR=DURA*(1.E-9)
            PI=3.1415927
            FREQT=FREQT*(1.E06)
            FREQA=FREQA*(1.E06)
            SIGT=SIGT*(1.E06)
            SIGA=SIGA*(1.E06)
            MU=AMU*(4PU.*PI*1.E-9)
            EPS=EPR*((1/(36*PI))*1.E-9)
            WRITE(8,119) MU,EPS
  119       FORMAT(1P2G20.6)
            OMEGAA=2*PI*FREQA
            OMEGAT=2*PI*FREQT
C           >>TW=TOTAL TIME WINDOW DESIRED (NSEC)
CCC         >>NFREQ=NUMBER OF FREQ. POINTS IN THE TRANSFER FUNCTION
CCC         >>DF=FREQUENCY INCREMENT LEVEL
            NPNTS=256
            NPS=512
            N2P=13
            NFREQ=4096
            TW=3200.
C           * * * * *
C           * * DETERMINATION OF TIME AND FREQUENCY INTERVAL
C           * * * * *
            NDFREQ=2*NFREQ
            N4=NDFREQ/4
            TWD=TW/10.
            DF=(1/TWD)*1.E03
            TS=TW/(NPS-1.)
            FMAX=(NFREQ/TW)*1.E09
            OMEGA=2*PI*DF*1.E06
            WAD=OMEGA
C           >>RA=ANTENNA SHUNT RESISTOR
C           >>RT=TARGET SHUNT RESISTOR
            IF(SIGA.EQ.0.) GO TO 84
            RA=ABS(RSA/(2*SIGA))
   84       RR=1.
            IF(SIGT.EQ.0.) GO TO 83
            RT=ABS(RST/(2*SIGT))
   83       RR=1.
            RS=SIGMA*(MU/EPS)
C           * * * * *
C           * * CALCULATION OF ARRAY VOUT
C           * * * * *
            DO 100 I=2,NFREQ
C           * *DETERMINE ANTENA & TARGET IMPEDANCE(ZA & ZT)
            CFREQ=CMPLX(0.,OMEGA)
            POLA=CMPLX(SIGA,OMEGAA)
            CPOLA=CONJG(POLA)
            ZA=(RSA*CFREQ)/((CFREQ-POLA)*(CFREQ-CPOLA))
            POLT=CMPLX(SIGT,OMEGAT)
            CPOLT=CONJG(POLT)
            ZT=(RST*CFREQ)/((CFREQ-POLT)*(CFREQ-CPOLT))
C           * * TARGET IMPEDANCE AT INPUT  TERMINALS(ZTEQU)
C           >>Z0=LINE CHARACTERISTIC IMPEDANCE
C           >>GAMA=PROPAGATION COSTANT
            ZARG=OMEGA*MU
            ZARGD=OMEGA*EPS
            ZWARG=CMPLX(RS,ZARG)/CMPLX(SIGMA,ZARGD)
```

```
      ZD=CSQRT(ZDARG)
      GAMA=CMPLX(RS,ZARG)/ZM
      RGAMA=REAL(GAMA)
      GGAMA=AIMAG(GAMA)
C     * * FIRST ECHO CALCULATION ONLY FROM REFLECTION &
C           TRANSMISSION COEFFICIENTS
      IF(IECHO.EQ.0) GO TO 6
      RES=377.
      ZAD=(ZA*ZD)/(ZA+ZD)
      ZVD=ZAD/(ZAD+RES)
      ZRESA=(ZA*RES)/(ZA+RES)
      ZTRA=(2*ZRESA)/(ZRESA+ZD)
      ZREFT=(ZT-ZD)/(ZT+ZD)
      VOUT(I)=1.-(((ZTRA*ZVD*ZREFT))*CEXP(-2*GAMA*DIST))
      GO TO 5
6     RR=1.
C     * * * * *
      TANA=TANH(RGAMA*DIST)
      TANB=TAN(GGAMA*DIST)
      TANAB=TANA*TANB
      CTANG=CMPLX(TANA,TANB)/CMPLX(1.,TANAB)
      ZTEQU=(ZD*(ZT+ZD*CTANG))/(ZD+ZT*CTANG)
C     * *IMPEDANCE SEEN BY THE SOURCE (ZIN)
      ZIN=(ZTEQU*ZA)/(ZTEQU+ZA)
C     >>SET  INTERNAL RESISTANCE EQUAL
C      TO THE LINE'S CHARACTERISTIC IMPEDANCE
      RES=377.
      IF(I.GT.2) GO TO 105
      WRITE(8,104) RES,ZD
104   FORMAT('RES=',1P1G12.4,'ZD=',1P2G12.4)
105   RR=1.
C     * * TRANSFER FUNCTION
      VOUT(I)=(RES)/(ZIN+RES)
5     RR=1.
      OMEGA=2*PI*(DF*I)*1.E06
100   CONTINUE
C     * * * * *
C     >>SET DC TERM EQUAL TO ZERO
      VOUT(1)=CMPLX(0.,0.)
C     * * * * *
CC    * *MANIPULATION OF VOUT FOR STORAGE SAVING
C     * * * * *
      WRITE(2) VOUT
      CLOSE 2
143   RR=1.
      CALL VGAUSS(GAUSS,SS,NOFREQ,DUR,FMAX,N2P,N4)
      READ(2) VOUT
      CLOSE 2
      CALL ASNDEL(6HOUT!!2,0.0,2)
202   RR=1.
C     * * * * *
C     * * MULTIPLY EXCITATION BY TRANSFER FUNCTION
C     * * * * *
      DO 200 I=1,NFREQ
200   GAUSS(I)=GAUSS(I)*VOUT(I)
C     * * * * *
C     * *TIME INVERSION OF OUTPUT VOLTAGE GAUSS(I)
C     * * * * *
C     >>SET UP CONJUGATES FOR FFT
      GAUSS(NFREQ+1)=CMPLX(0.,0.)
```

```
161         DO 220 I=2,NFREQ
162         J=NOFREQ+2-I
163         GAUSS(J)=CONJG(GAUSS(I))
164 220     AA=1.
165         CALL FCNT(GAUSS,M2P,SS,1,IERR)
166         AA=1
167         INC=NOFREQ/NPS
168         DO 240 I=1,NOFREQ,INC
169         BB=BB+1
170 240     TWFG(II)=2PI.*(REAL(GAUSS(I)))
171 C       >>TWFG IS NOW THE LONG TIME SYSTEM RESPONSE
172         DO 599 I=1,NPS
173         IF(TWFG(I).LT.-4.) TWFG(I)=-4.
174 599     IF(TWFG(I).GT.4.) TWFG(I)=4.
175 C       * * * * *
176 C       * * WAVEFORM SHIFTING
177 C       * * * * *
178         WRITE(6,301)
179 301     FORMAT('# OF PNTS TO BE SHIFTED=')
180         READ(6,-) NSHFT
181         DO 302 I=1,NSHFT
182         TWFF(I)=TWFG(NPS)
183         DO 303 II=2,NPS
184         JJ=II-1
185         TWFF(II)=TWFG(JJ)
186 303     AA=1.
187         DO 305 IJ=1,NPS
188 305     TWFG(IJ)=TWFF(IJ)
189 302     AA=1
190 304     AA=1.
191 C       * * * * *
192 C       * *SELECTION OF A TIME WINDOW OUT OF THE TOTAL RESPONSE TWFG
193 C       * * * * *
194         TBG=0./(NOFREQ-1)
195         TWB=((NPNTS-1.)/10.)*TBG
196         WRITE(6,222) TBG
197 222     FORMAT('TBG=',1P1G12.4)
198         RTIM=6.*DIST*SQRT(ER)
199         NSTART=RTIM/TBG
200         NEND=NSTART+NPNTS
201         AA=0
202         DO 695 N=NSTART,NEND
203         AA=1+AA
204         TWF(II)=2PI*(REAL(GAUSS(N)))
205         IF(TWF(II).GT.4.) TWF(II)=4.
206         IF(TWF(II).LT.-4.) TWF(II)=-4.
207 695     AA=1.
208 C       * * * * *
209 696     AA=1.
210         ZAR=SIGA*1.E-6
211         ZAI=FREGA*1.E-6
212         ZTR=SIGT*1.E-6
213         ZTI=FREQT*1.E-6
214 C       * * * * *
215 C       * *STORAGE OF PARAMETERS AND OUTPUT TIME VOLTAGE
216 C       * * * * *
217         GO TO 271
218         WRITE(2,122) DIST,ER,MR,RST,MSA
219 122     FORMAT(5X,'DISTANCE=',F4.2,2X,'ER=',F6.2,'MR=',F6.2,
220        1/,'TARGET RESIDUE=',1P1G10.2,'ANT. RESIDUE=',1P1G10.2)
```

```
      WRITE(2,123) SIGMA,SIGT,FREQT,SIGA,FREQA
123   FORMAT(/,5X,'SIGMA=',1P1G12.4,'TARGET POLE=',
     &1P2G12.4,'ANTEN. POLE=',1P2G12.4)
      WRITE(2,124) RES,DURA,TW
124   FORMAT(/,'RESIS.=',2F10.4,'PULSE WIDTH=',F4.1,/,'TIME WIND.=',
     &F5.5,'(USEC)')
      WRITE(2,129) NPNTS
129   FORMAT('NUMBER OF PTS IN TIME DVERN=',I4)
      WRITE(2,131)
131   FORMAT(5X,'REAL',8X,'IMAG',8X,'REAL',
     &8X,'IMAG',8X,'REAL',8X,'IMAG',8X,'REAL',
     &10X,'IMAG')
      WRITE(2,200)
200   FORMAT(30X,'GAUSSIAN TIME RESPONSE')
      WRITE(2,270) TRF
270   FORMAT(1P8G12.4)
271   KK=1.
C     * * * * *
C     * *CONSTRUCTION OF TIME ARRAYS TO BE USED FOR PLOTING
C     * * * * *
      TIME(1)=0.
      DO 250 I=2,NPNTS
250   TIME(I)=TIME(I-1)+TBO
      TIMEG(1)=0.
      DO 251 I=2,NPS
251   TIMEG(I)=TIMEG(I-1)+TB
C     * * * * *
C     * * STORAGE OF THE SELECTED OUTPUT TIME WINDOW
C         IN A FORM COMPATIBLE FOR FURTHUR PROCESSING
C     * * * * *
      WRITE(8,555)
555   FORMAT('STORAGE')
8888  CALL RDFLUN(IFILE,IUSER)
      WRITE(8,8001)
8001  FORMAT(1X,'A(0) OR B(1)= ')
      READ(8,*) IAB
      IF((IAB.EQ.0).OR.(IAB.EQ.1)) GO TO 8004
      WRITE(8,8002)
8002  FORMAT(1X,'?')
      GO TO 8888
8004  CONTINUE
      ICODE(1)=-2
      ICODE(2)=NPNTS
      ICODE(4)='11111111
      CALL RTEXT(IDES,14)
      CALL RWDBFL(TRF,NPNTS,IDES,32,IFILE,IUSER,IAB,1,IERR)
      WRITE(8,611)
611   FORMAT('ENTER FILE NAME:')
      CALL RTEXT(IFLUN,10)
C     * * * * *
C     * *PLOTING OF THE LONG TIME RRESPOSE (TYPE) AND
C        THE SELECTED EXPANDED WINDOW (TPF)
C     * * * * *
      PAUSE
      DO 214 I=1,NPNTS
214   TRF(I)=-TRF(I)
      DO 215 I=1,NFS
215   TRFG(I)=-TRFG(I)
      CALL ASKPLT(100,3)
      CALL FACTOR(.8)
```

```
      DO 1000 I=1,2
      CALL PLOT(4.5,1.875,-3)
      CALL AXIS(2.,0.,10HFREQUENCY,1,4.,180.,-4.,
     &2.,1.,0)
      IF(I.EQ.2) GO TO 212
      CALL AXIS(0.,0.,11HTIME (MSEC),-11,10.,90.,0.,TMP,
     &1.,0)
      CALL LINE(TMP0,0.,2.,TIMEG,0.,TMP,NPS,0,0)
      GO TO 213
  212 HR=1.
      CALL AXIS(0.,0.,11HTIME (MSEC),-11,10.,90.,RTIM,TMP,
     &1.,0)
      CALL LINE(TPF,0.0,2.,TIME,0.0,TMP,NPNTS,0,0)
  213 CONTINUE
      IF(IECHO.EQ.0) GO TO 216
      CALL SYMBOL(1.8,6.,.11,IREF,90.,15)
  216 HR=1.
      CALL SYMBOL(2.,4.,.11,IFLIM,90.,10)
      CALL SYMBOL(2.,4.9,.11,IPOLA,90.,18)
      CALL NUMBER(2.,6.8,.11,ZAR,90.,2)
      CALL NUMBER(2.,7.8,.11,ZAI,90.,2)
      CALL SYMBOL(2.2,4.9,.11,IPOLT,90.,15)
      CALL NUMBER(2.2,6.8,.11,ZTR,90.,2)
      CALL NUMBER(2.2,7.8,.11,ZTI,90.,2)
      CALL SYMBOL(2.4,4.9,.11,IER,90.,5)
      CALL NUMBER(2.4,5.25,.11,ER,90.,1)
      CALL SYMBOL(2.4,6.35,.11,IMR,90.,5)
      CALL NUMBER(2.4,6.65,.11,MR,90.,1)
      CALL SYMBOL(2.6,4.9,.11,ISIGMA,90.,8)
      CALL NUMBER(2.6,5.7,.11,SIGMA,90.,102)
      CALL SYMBOL(2.8,4.9,.11,IDISTA,90.,15)
      CALL NUMBER(2.8,6.4,.11,DISTA,90.,2)
      CALL SYMBOL(3.,4.9,.11,IDIST,90.,15)
      CALL NUMBER(3.,6.4,.11,DIST,90.,2)
      CALL SYMBOL(3.2,4.9,.11,IWTR,90.,15)
      CALL NUMBER(3.2,6.4,.11,RES,90.,2)
      CALL SYMBOL(3.4,4.9,.11,IRA,90.,11)
      CALL NUMBER(3.4,6.4,.11,RA,90.,2)
      CALL SYMBOL(3.4,7.8,.11,IRT,90.,12)
      CALL NUMBER(3.4,9.3,.11,RT,90.,2)
      CALL PLOT(6.125,-2.4,-3)
 1000 HR=1.
      END
C     * * * * *
      SUBROUTINE VGAUSS(DATA,SS,N,DUR,FMAX,IRP,N4)
C        'VGAUSS' RETURNS THE SPECTRUM OF A GAUSSIAN TIME
C     DOMAIN PULSE IN THE FIRST (N/2+1) ELEMENTS OF 'DATA'.
C        DATA(1) IS THE D.C. TERM.
C
C     N=   NUMBER OF TIME DOMAIN POINTS (MUST BE POWER OF 2)
C     DUR= DESIRED PULSE WIDTH OF GAUSSIAN PULSE IN SECONDS.
C     FMAX=HIGHEST FREQUENCY DESIRED. RESULT FOR FMAX IS
C          RETURNED IN DATA(N/2+1).
C
      DIMENSION SS(N4)
      COMPLEX DATA(N)
C     * * * * *
C     * * GENERATE INPUT SIGNAL
C     * * * * *
      DELF=FMAX/(N/2.)
```

```
C     'N' IS THE NUMBER OF TIME DOMAIN POINTS.
C     IT SHOULD BE A POWER OF 2.
      N2P1=N/2+1
      N2=N/2
      N3=N2+1
      DT=.5/FMAX
      T=N*DT
C     PULSE AMPLITUDE NORMALIZED TO UNITY.
      VOLTP=1.
      XTP=2*(2*FMAX*DUR)
      TP=DUR
      WRITE(6,999)XTP
999   FORMAT(' PULSE HAS ',E13.6,' TIME POINTS')
320   CONTINUE
      DO 9 I=1,N
9     DATA(I)=(0.,0.)
C     * * * * *
C     * *GENERATE GAUSSIAN INPUT VOLTAGE PULSE
C     * *GAUSSIAN PULSE
C     * * * * *
      TI=1.5/3.*TP
      TTIS=2.*TI**2
      DATA(1)=CMPLX(VOLTP,0.)
      TM=2.**6
      DO 41 I=2,N2
      TT=(I-1)*DT
      TT=-TT**2/TTIS
      IF(ABS(TT).GT.TM)GO TO 42
      DATA(I)=VOLTP*CMPLX(EXP(TT),0.)
      J=N+2-I
41    DATA(J)=DATA(I)
42    CONTINUE
C     'DATA' NOW HAS TIME DOMAIN GAUSSIAN PULSE
C     IN ITS REAL PART.
C     * * * * *
C     * *OBTAIN SPECTRUM AND STORE IN 'DATA'
C     * * * * *
      CALL FFT(DATA,N,-1)
      DO 30 I=1,N
30    DATA(I)=DATA(I)/N
      DATA(N2P1)=CONJG(DATA(N2P1))
      RETURN
      END
C     * * * * *
      SUBROUTINE FFT(DATA,NN,ISIGN)
C     FFT=FAST FOURIER TRANSFORM
C     DATA=ARRAY TO BE TRANSFORMED
C     NN=# OF POINTS IN 'DATA'
C     ISIGN=IF '=-1','DATA' IS TRANSFORMED FROM TIME TO
C     FREQUENCY=IF '=1','DATA' IS TRANSFORMED FROM FREQUENCY
C     TO TIME
       DIMENSION DATA(1)
       N=2*NN
       J=1
       DO 5 I=1,N,2
       IF(I-J)1,2,2
1      TEMPR=DATA(J)
       TEMPI=DATA(J+1)
       DATA(J)=DATA(I)
       DATA(J+1)=DATA(I+1)
```

```
421           DATA(I)=TEMPR
422           DATA(I+1)=TEMPI
423 2         J=N/2
424 3         IF(J-M)5,5,4
425 4         J=J-M
426           M=M/2
427           IF(M-2)5,3,3
428 5         J=J+1
429           MMAX=2
430 6         IF(MMAX-N)7,10,10
431 7         ISTEP=2*MMAX
432           THETA=6.28318530717/FLOAT(ISIGN*MMAX)
433           SINTH=SIN(THETA/2.)
434           WSTPR=-2.*SINTH*SINTH
435           WSTPI=SIN(THETA)
436           WR=1.
437           WI=0.
438           DO 9 M=1,MMAX,2
439           DO 8 I=M,N,ISTEP
440           J=I+MMAX
441           TEMPR=WR*DATA(J)-WI*DATA(J+1)
442           TEMPI=WR*DATA(J+1)+WI*DATA(J)
443           DATA(J)=DATA(I)-TEMPR
444           DATA(J+1)=DATA(I+1)-TEMPI
445           DATA(I)=DATA(I)+TEMPR
446 8         DATA(I+1)=DATA(I+1)+TEMPI
447           TEMPR=WR
448           WR=WR*WSTPR-WI*WSTPI+WR
449 9         WI=WI*WSTPR+TEMPR*WSTPI+WI
450           MMAX=ISTEP
451           GO TO 6
452 10        RETURN
453           END
454
```

Additional Results on the Transmission Line Model

We present here the results of five more sets of parameters used in the transmission line model for calculating the target (tunnel) pole pair and its depth. The first echo responses are given in Figures E1, E3, E5, E7, E9 and their respective filtered waveforms (double antenna pole pair extracted) and reconstructed target responses in Figures E2, E4, E6, E8 and E10. Attention should be given to the first set of parameters. In this case Equation (61) is not satisfied for the target response. Thus, the imaginary part of the calculated target pole (Table E1) deviates from the actual one (Table 2). This situation becomes more cirtical as the target resistance increases with respect to Z_o. The same is also true for the antenna pole pair. Under such conditions we can still calculate the target's depth, but not its structure. It should be noted, though, that given the transmission line parameters (Z_o and R_s) we could finally calculate the proper target resonances to determine the target's structure. All sets have the following common parameters:

Conductivity of $\sigma = 5.\times10^{-6}$ ℧/m.

Line characteristic impedance of $Z_o = 377.+j0.$

Generator internal resistance of $R_s = 377.\Omega$

Relative permitivity of $\epsilon_r = 1.$

Relative permeability of $\mu_r = 1.$

Line length (target depth) of $d = 30$ m.

Table E1
MODEL PARAMETERS

WVFRM	TARGET* POLE($\times10^6$)	ANTENNA* POLE($\times10^6$)	R_A (ohms)	R_T (ohms)	T_B (nsec)	GAUSSIAN PULSE WIDTH
Fig. 1E	$-50\pm j40$	$-50\pm j50$	100	600	.39064	6 nsec
Fig. 2E	$-30\pm j60$	$-40\pm j70$	312	416.67	.61043	6 nsec
Fig. 4E	$-60\pm j80$	$-50\pm j90$	250	208.33	.61043	6 nsec
Fig. 6E	$-40\pm j80$	$-90\pm j100$	277.78	625.0	.73251	6 nsec
Fig. 8E	$-80\pm j100$	$-100\pm j120$	250	312.5	.48834	3 nsec

* The real and imaginary parts of the poles are in Nepers/sec and Hz, respectively.

Table E2
RESULTS

PRONY RESULTS; MIN. SQUARE ERROR CASE							
WVFRMS	IBS[1]	ITS[2]	POLES($\times 10^6$)[3] REAL	POLES($\times 10^6$)[3] IMAG	RESIDUES($\times 10^{-2}$V) REAL	RESIDUES($\times 10^{-2}$V) IMAG	CALCULATED DEPTH (see Eq. (71))
Figure 1E	$5T_B$	70	- 80.52708 - 72.82090 -130.9758	± 48.37224 ± 49.72958 ± 35.39557	- 5.707915 - 5.48269 - .4447925	± 5.97173 ∓ 5.297205 ∓ .6985125	29.33 meters (T_o=201.5 nsec)
Figures 2E and 3E	$5T_B$	49	-115.8673 - 96.12898 - 63.55564	± 69.43538 ± 67.36128 ± 59.20473	.1827605 1.200883 2.621827	±20.83578 ±26.09179 ± 4.576278	29.8 meters (T_o=204.8 nsec)
Figures 4E and 5E	$5T_B$	43	-112.4678 - 94.92625 -113.6392	± 79.43148 ± 83.47676 ± 91.97491	-12.65175 11.12528 .8954798	± 2.153908 ±10.88101 ± 9.228865	29.8 meters (T_o=204.8 nsec)
Figures 6E and 7E	$5T_B$	51	-232.3181 -213.4742 -106.3283	± 92.84101 ± 95.88572 ± 78.45726	51.26945 -53.20845 .6760264	±10.99064 ± 3.064266 ± 6.854331	29.6 meters (T_o=203.5 nsec)
Figures 8E and 9E	$5T_B$		-263.2653 -210.3741 -144.8997	±116.1694 ±115.2889 ± 98.08942	23.35237 -26.0449 1.520388	± 4.361558 ± 9.528409 ± 5.611749	29.9 meters (T_o=202.3 nsec)

[1] IBS = Interval between samples used by Prony's method for calculating the poles.

[2] ITS = Starting point of the window used by Prony's method for calculating the poles.

[3] The real and imaginary parts of the poles are given in Nepers/sec and Hz, respectively. The first two pole pairs correspond to the double antenna pole pair, and the third to the target.

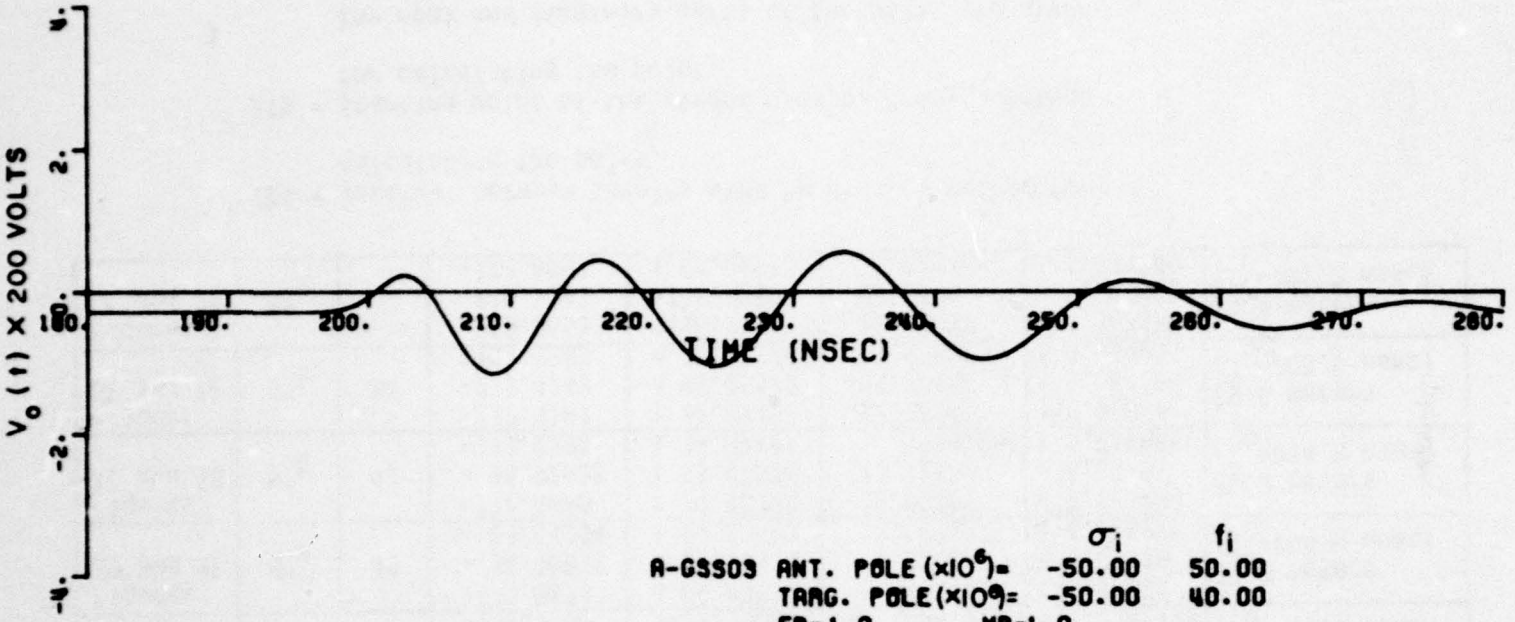

122

		σ_i	f_i		
A-GSSO3	ANT. POLE ($\times 10^6$)=	-50.00	50.00		
	TARG. POLE ($\times 10^9$)=	-50.00	40.00		
	ER=1.0	MR=1.0			
	SIGMA= 5.00 $\times 10^{-6}$ ℧/m				
	ANT. DIST.=	0.00 m			
	TARG. DIST.=	30.00 m			
	INTER. RES.=	377.00 Ω			
	ANT. RES.=	100.00 Ω		TARG. RES.=	600.00 Ω

Figure E1. First echo response.

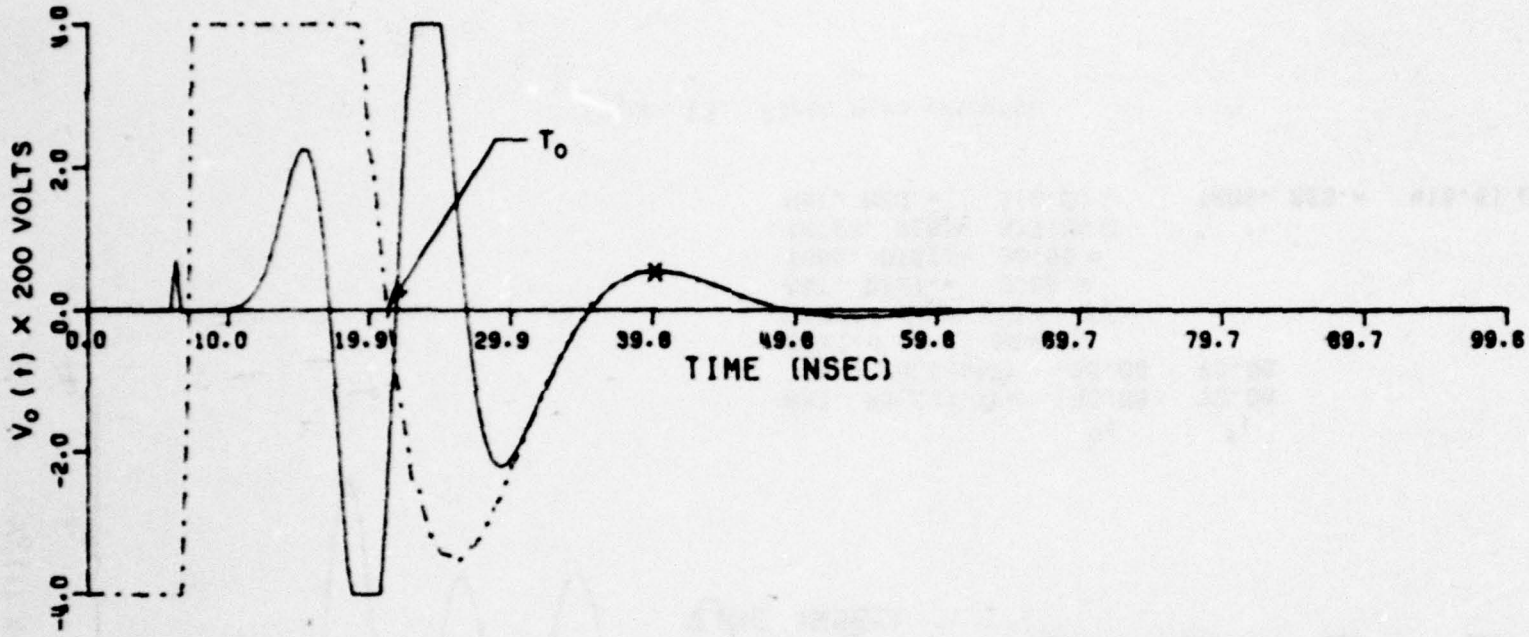

— FILTERED WVFRM
-·- RECONSTRUCTED WVFRM
* RECONSTRUCTION START. POINT
POINTS USED FOR ERR CALCUL.= 10
RECNS. INTERVAL= δT_s
EXTRACTION INTERVAL= δT_s

EXTRACT. POLE ($\times 10^6$):	σ_i	f_i
	-80.53	46.37
	-72.62	49.73

Figure E2. Extraction of antenna double pole pair and reconstruction of target response of the signal in Figure E1.

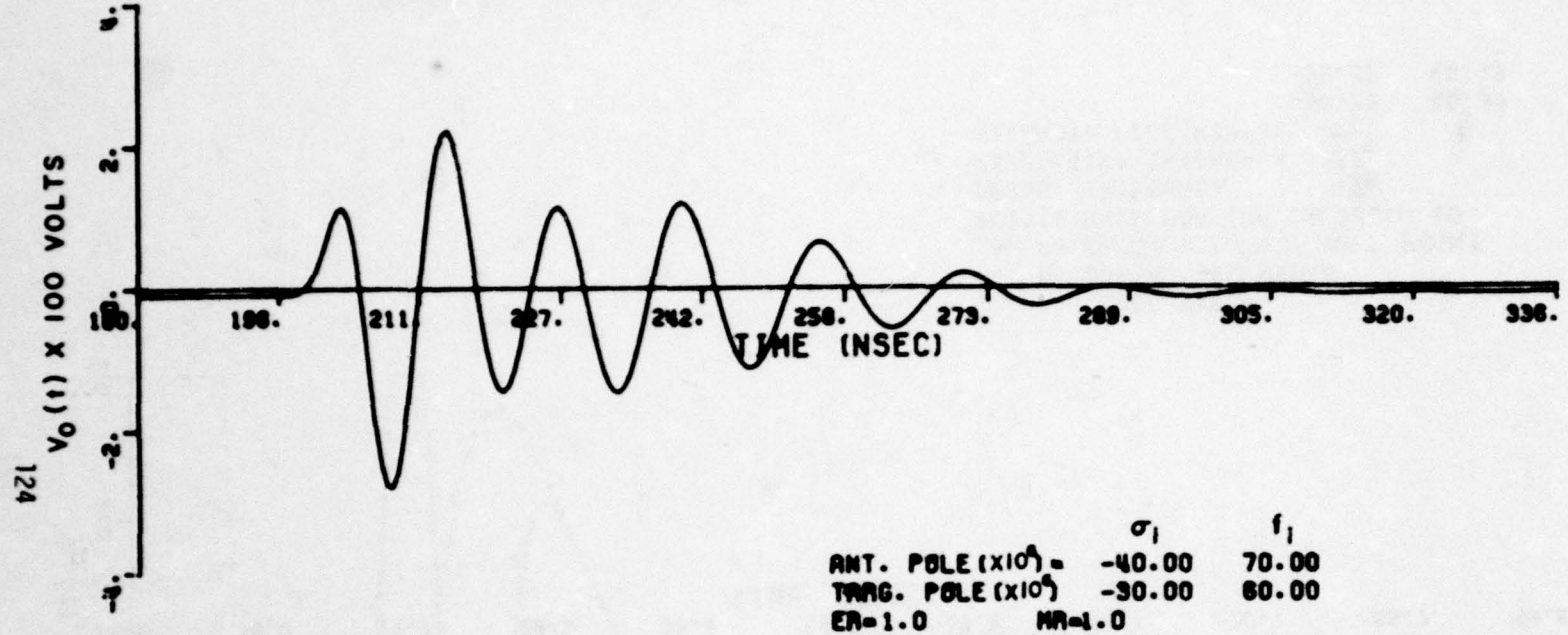

	σ_i	f_i	
ANT. POLE ($\times 10^6$) =	-40.00	70.00	
TARG. POLE ($\times 10^6$)	-30.00	60.00	
ER=1.0	MR=1.0		
SIGMA= 5.00 $\times 10^{-6}$ $\mho$/m			
ANT. DIST.=	0.00 m.		
TARG. DIST.=	30.00 m.		
INTER. RES.=	377.00 Ω		
ANT. RES.=	312.50 Ω	TARG. RES.=	416.67 Ω

Figure E3. First echo response.

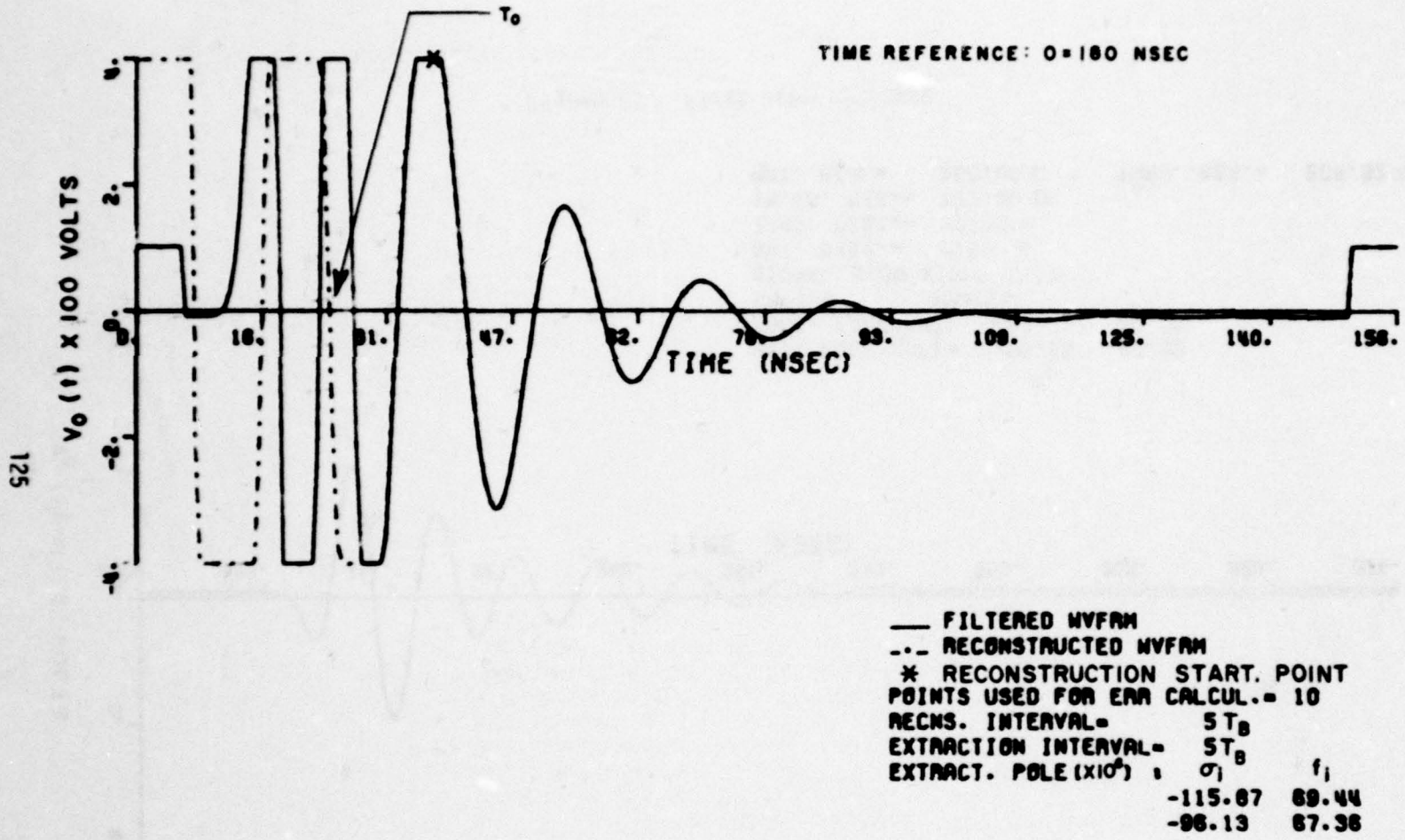

Figure E4. Extraction of antenna double pole pair and reconstruction of target response of the signal in Figure E3.

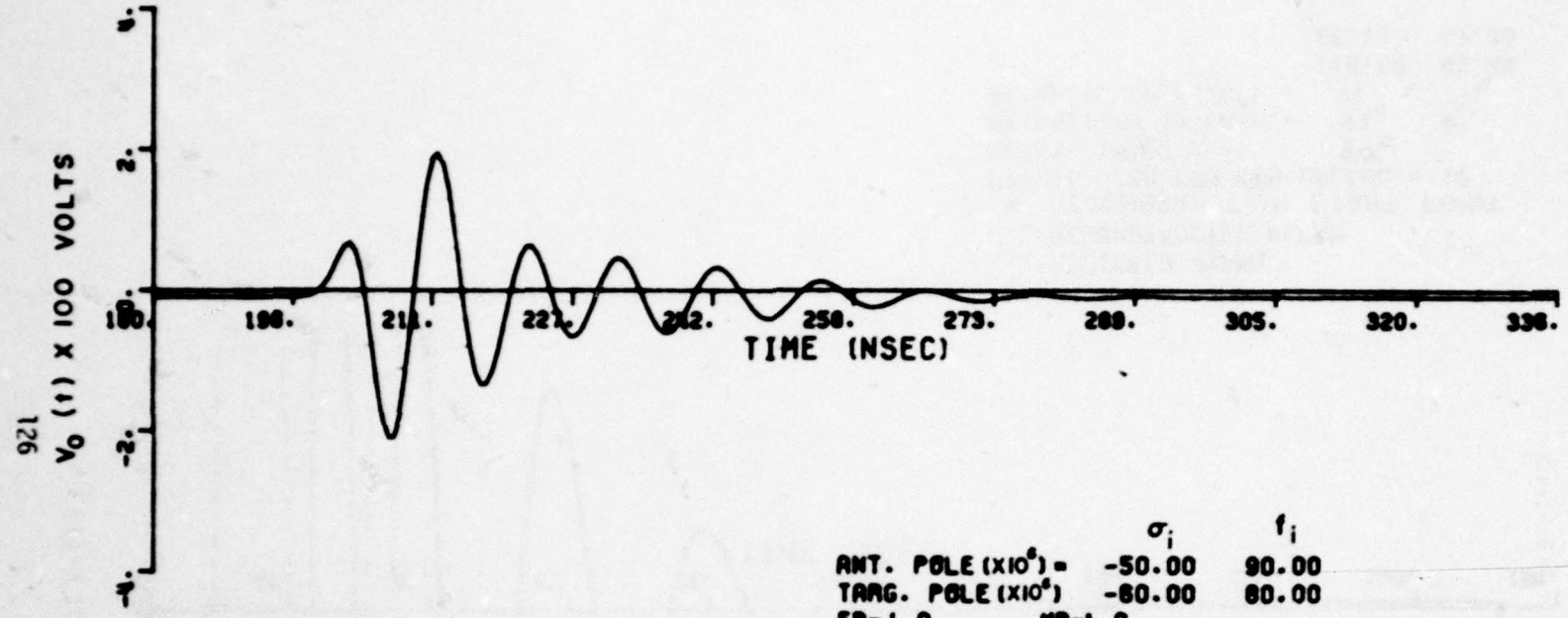

	σ_i	f_i
ANT. POLE ($\times 10^6$) =	-50.00	90.00
TARG. POLE ($\times 10^6$)	-60.00	60.00

ER= 1.0 MR=1.0
SIGMA= 5.00 $\times 10^{-6}$ $\mho$ / m
ANT. DIST.= 0.00 m.
TARG. DIST.= 30.00 m.
INTER. RES.= 377.00 Ω
ANT. RES.= 250.00 Ω TARG. RES.= 208.33 Ω

Figure E5. First echo response.

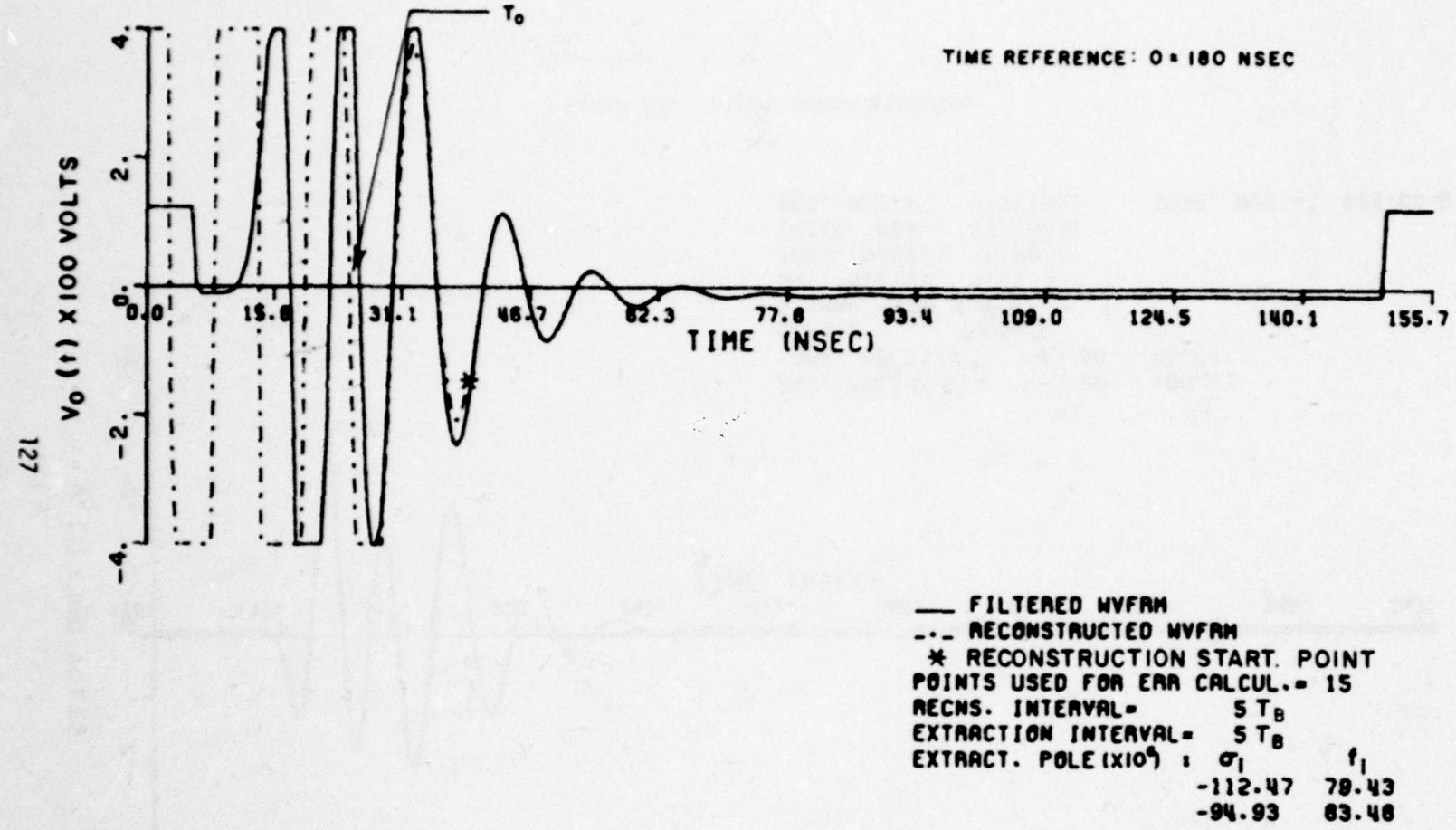

Figure E6. Extraction of antenna double pole pair and reconstruction of target response of the signal in Figure E5.

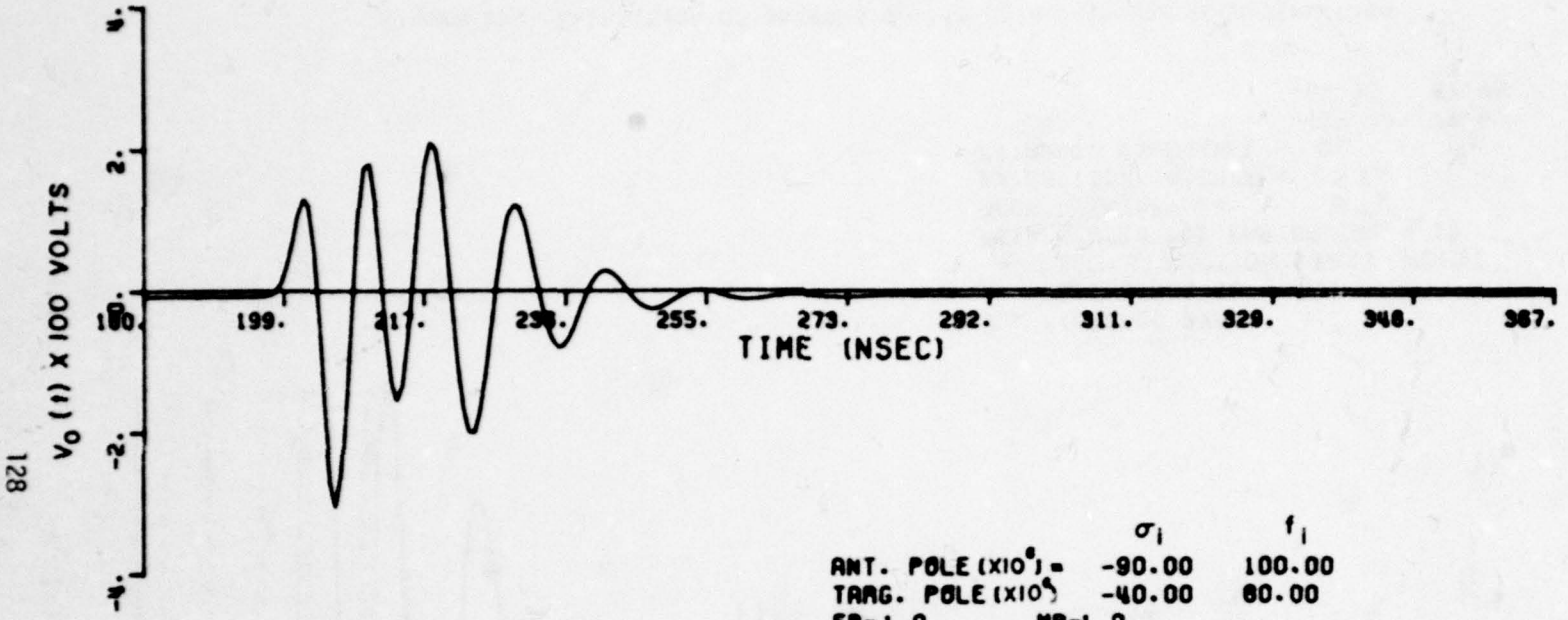

	σ_i	f_i	
ANT. POLE ($X10^6$) =	-90.00	100.00	
TARG. POLE ($X10^6$)	-40.00	60.00	
ER=1.0	MR=1.0		
SIGMA= 5.00 $X10^{-6}$ ℧/m			
ANT. DIST.=	0.00 m.		
TARG. DIST.=	30.00 m.		
INTER. RES.=	377.00 Ω		
ANT. RES.=	277.78 Ω	TARG. RES.=	625.00 Ω

Figure E7. First echo response.

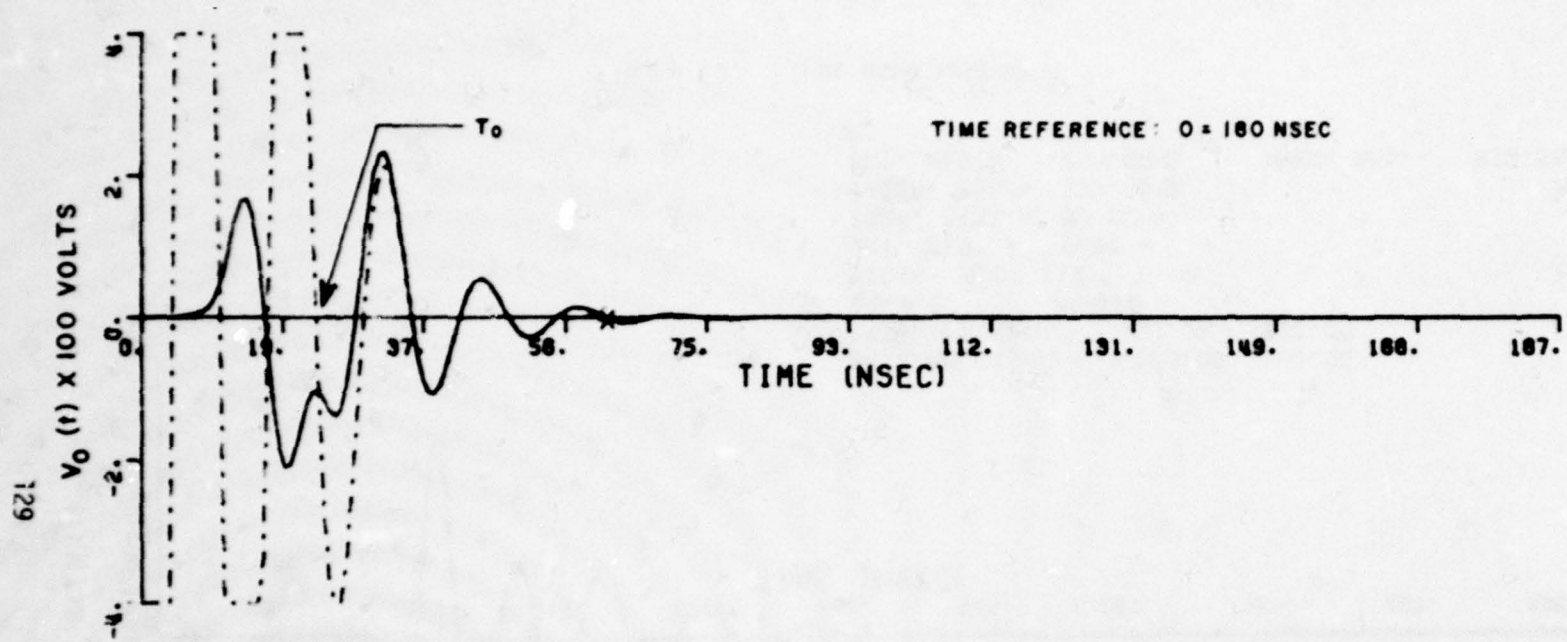

Figure E8. Extraction of antenna double pole pair and reconstruction of target response of the signal in Figure E7.

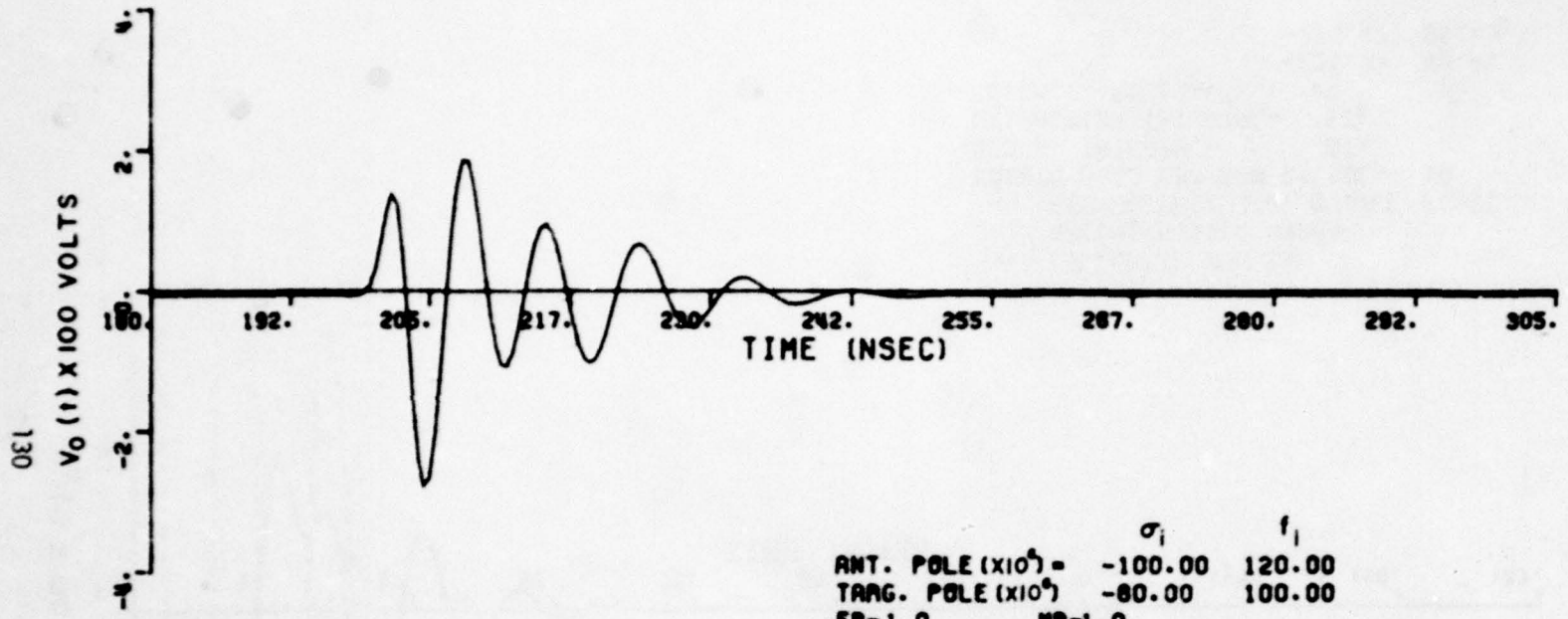

	σ_i	f_i		
ANT. POLE ($\times 10^6$) =	-100.00	120.00		
TARG. POLE ($\times 10^6$)	-80.00	100.00		
ER=1.0	MR=1.0			
SIGMA= 5.00 $\times 10^{-6}$ $\mho$/m				
ANT. DIST.=	0.00 m.			
TARG. DIST.=	30.00 m.			
INTER. RES.=	377.00 Ω			
ANT. RES.=	250.00 Ω		TARG. RES.=	312.50 Ω

Figure E9. First echo response.

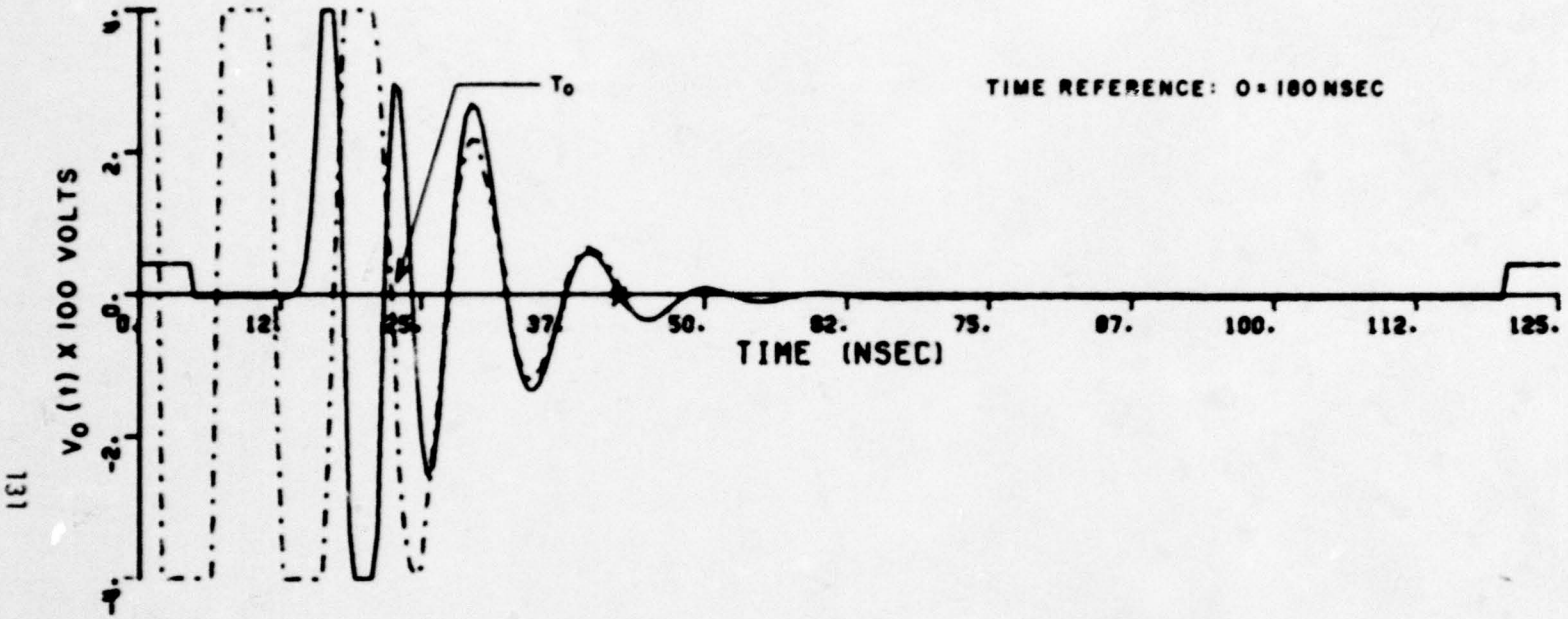

Figure E10. Extraction of antenna double pole pair and reconstruction of target response of the signal in Figure E9.